博士論文

A Study on Tactile Presentation Using Edge Stimulation Method
(境界刺激法による触覚提示の研究)

櫻井　達馬

境界刺激法による触覚提示の研究

本研究では触覚を用いて線形状を提示する触覚技術，および触覚ディスプレイの開発を行った．本研究の目的は，局所的に生じる振動触覚を用いて線形状を生成し，その組み合わせから仮想物体の場所，領域，形状といった空間的な情報を，直観的にヒトに伝達することである．

著者らは新しい振動触覚提示法，境界刺激法を開発した．境界刺激法は局所的で鮮明，強烈な振動感覚を，数ミクロン程度の微小振幅で実現するものである．本手法により省パワーで小型の振動子，例えば剛性の高いピエゾ素子などを，触覚ディスプレイに使用し易くする．さらに，触覚ディスプレイ表面を凹凸の無い平面に製作することが可能であり，映像の投影や，デバイスの平面部分への埋め込み等，様々なアプリケーションに応用できる。

本手法を確立するために，1. 基礎的な特徴と 2. メカニズムを調査した．1. では心理物理実験を用いて，感覚強度と触覚像の広がりをいくつかの機械的パラメータに対して調査した．結果から，振動子を隙間なく密に配置し，5-50 Hz 程度，振動面同士は逆位相の振動を用いた場合に最も振動知覚閾値が降下し，強烈な振動感が得られることが明らかとなった．また線を提示する際の，二線弁別域は 4.2 mm であった．2. では有限要素変形解析を用いて，境界刺激条件下でのヒト皮膚内部のひずみの時空間的な分布を調査した．ヒト皮膚内部では振動面のエッジ付近で応力集中が発生し，単一の振動子を用いる刺激法と比較してひずみピークが増大，さらに振動面と振動面の境界で入力周波数の倍周波数のひずみ変化が観測された．ヒトの振動に対する周波数感度曲線から，周波数が倍程度になると 5-50 Hz 付近では 10dB 程感度が上昇するため，この倍波成分が強烈な振動感に関与していると考えられる．また，ひずみの広がりを調査した結果，単一の振動子を用いる刺激法と比較してひずみが振動面の境界に集中して発生しており，局所的な触覚像に寄与していることが分かった．得られた知見を用いて，3×3 の振動子アレイ型触覚ディスプレイを開発し，境界刺激による線形状の提示を行った．結果，95% の高い弁別率が得られ，境界刺激法を用いた線形状提示の有効性が明らかとなった．

Abstract

This thesis addresses the techniques and the development of haptic displays that produce intuitive tactile lines. Our consistent concept is to present tactile edges, areas and shapes (as a combination of them) with highly localized vibrotactile lines that overcomes the barrier against haptic spatial recognition.

We developed novel vibrotactile stimulation methods and tactile displays using the vibrotactile method. The developed edge stimulation method presents sharp and distinct tactile edge sensations using considerably small amplitude of vibrations (several microns). This technology achieves low power and strong intensity vibrotactile stimulation and is able to be fabricated in flat surfaces, and these characteristics are suitable for actual applications. To establish the edge stimulation technology, we investigated the 1. fundamental characteristics of edge stimulation method and the 2. mechanism of enhancement on tactile intensity. For the former, we conducted psychophysical experiments to investigate the performance on tactile intensity and tactile spatial sharpness for several mechanical parameters. The experimental results indicated that edge stimulation method is efficient when the vibrations are in close proximity, the vibration frequencies are low and the gap distance of the vibrators are close to be zero. Also it is demonstrated that edge stimulation method produces more localized vibrotactile sensation compared to a single pin vibrator, pin-array vibrator and flat vibrator. For the latter, the mechanism for these characteristics was investigated by observing spatio-temporal deformation of skin using deformation analysis on finite element finger model. It was revealed that not only strain peak due to strain concentration, but also strain frequency were increased. It is known that the increase in frequency has much larger effect on human vibrotactile sensitivity at lower frequencies than increase in amplitude and the generation of higher frequency in localized spot is a key effect of edge stimulation method. The measurement of the high frequency strain with finger model sensor was also conducted (section 4). Our idea for applications of edge stimulation method was to utilize the characteristics of sharp and localized vibrotactile sensations for tactile line presentation. We developed

1.5 cm×1.5 cm size 3×3 vibrator-array edge stimulation device with piezo-vibrators to present several tactile line patterns. Although we succeeded in rendering 8 tactile shape patterns with the combination of the tactile lines, the further variations of the patterns were limited due to the generation of unexpected lines. To solve this, we have developed selective tactile line control method by phase shift of vibrations. We demonstrated the combinations of tactile patterns of alphabets theoretically.

Contents

List of Figures

viii

List of Tables

Chapter 1

Introduction

1.1 Background

Through our research, we aim to open up new possibilities for haptic communication by transmitting haptic shape information. Human communication is an essential element for people to understand and empathize with each other, and is done in every sensory modality. Communication is clarified into typically of two types: verbal communication (VC) and non-verbal communication (NVC).

NVC involves sending and receiving linguistic information consciously/unconsciously without any exchange of words. Instead, information is exchanged using the senses: facial expressions, complexion, eye motions, gestures, appearance, and distance (proxemics) for vision; breathing, voice tone/color, and music for audioception; smell; taste; and touch [1, 2, 3]. Studies have extensively focused on non-verbal information transmission using haptics with several modalities such as thermal sense and sense of touch. For example, [57] developed TECHTILE Toolkit that presents vibrotactile feelings encountered in daily life. A microphone can obtain vibrations produced by certain events, i.e., moving balls in a cup, and a voice coil speaker attached to an empty cup can then apply the obtained vibrations to the user grasping the empty cup. A thermal drawing by [94] contains an array of Peltier element that obtain the spatial distribution of temperature which mechanical concept is smiler to the work by [10]. Teh developed unique pressure display, Haggy Pajama and a pressure sensor equipped stuffed bear[4]. A user wears a pajama with embedded air pads that expand when another user hugs the stuffed bear to provide the sensation of an embrace on the entire body.

VC involves conveying information through the exchange of ideas, feelings, intentions, attitudes, expectations, perceptions, or commands by speech and writing. It mainly uses the visual and auditory senses[5]. The development of communication device elements
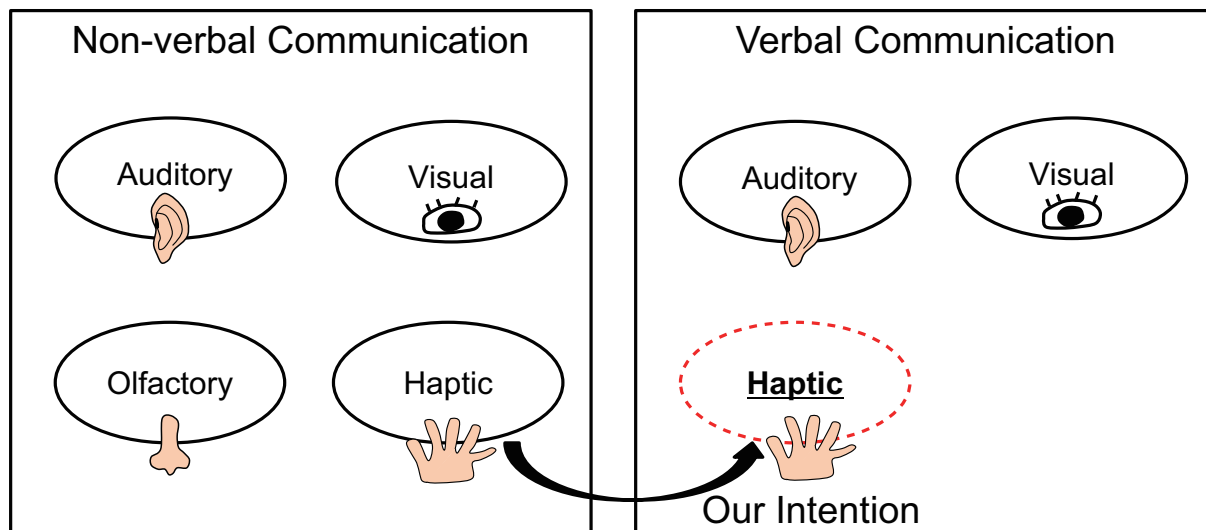
Fig. 1.1: Schematic of our research concept. Major organs used in non-verbal and verbal communication. Utilization of haptics for verbal communication is our research focus.

such as speaker/display and microphone/camera enable us to interact with distant and mobile devices, thus making communication more ubiquitous. In daily life, we mainly obtain considerable verbal information via visual and auditory senses, but little information is obtained through haptic senses. In some settings, Braille displays and related devices (described in detail in chapter 2) may be available for presenting haptic sensations; however, these devices take a few years to master and currently find limited use. Fig. 1.1 shows our research concept that explores the possibility of using haptics for verbal communication, especially as a channel for "character information". Our aim is to realize display-level haptic communication (Fig. 1.2) and focus on new approaches for presenting sensations of intuitive haptic characters (alphabets). In this thesis, we define "verbal" as linguistic symbols including Braille and Morse signals but not for speech; "character information" as the alphabet of a language because they are widely used; and "haptic communication" as verbal information interactions between people using haptic sensations.

1.2 Peculiarity of Haptics and Significance of Haptic Communication

Haptic communication can be used in situations where visual and auditory communication is unsuitable. For example, we can communicate through a haptic device in a pocket
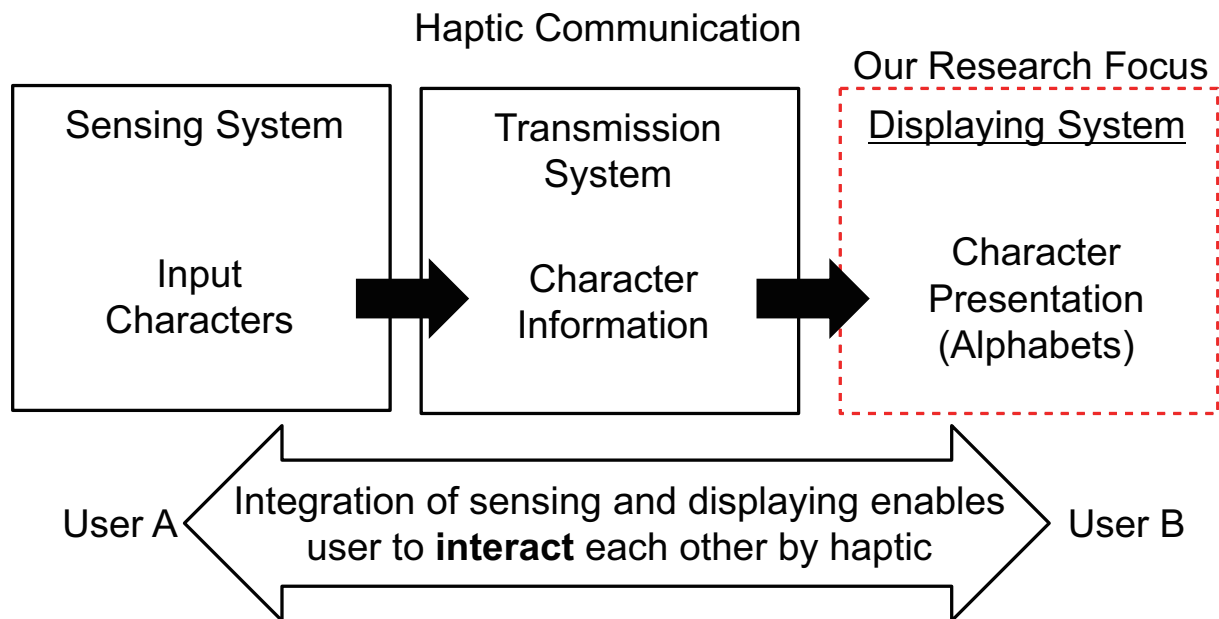
Fig. 1.2: The schematic of haptic verbal communication. It includes three stages, sensing system, transmission system, displaying system. Our research focuses on displaying character information using haptics.
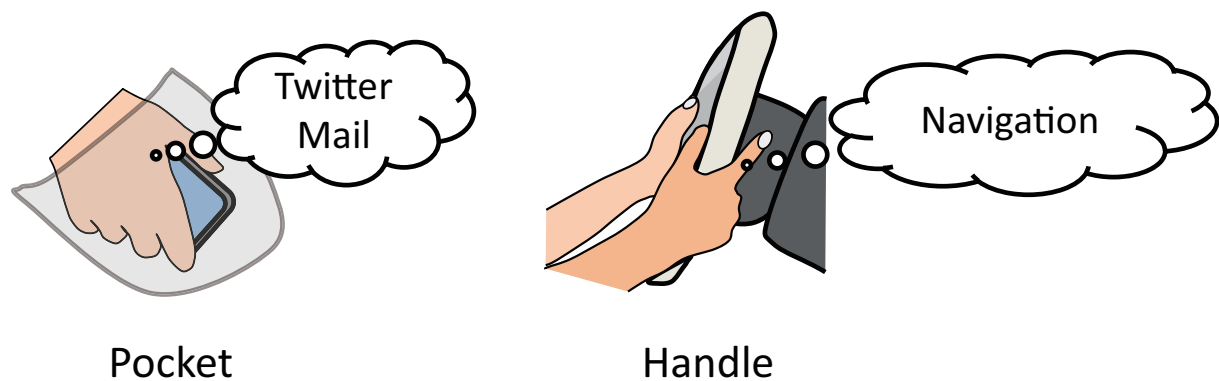
Fig. 1.3: Future applications of haptic verbal communications. User can input and read texts in pocket and other visually/auditory unmanageable situations.
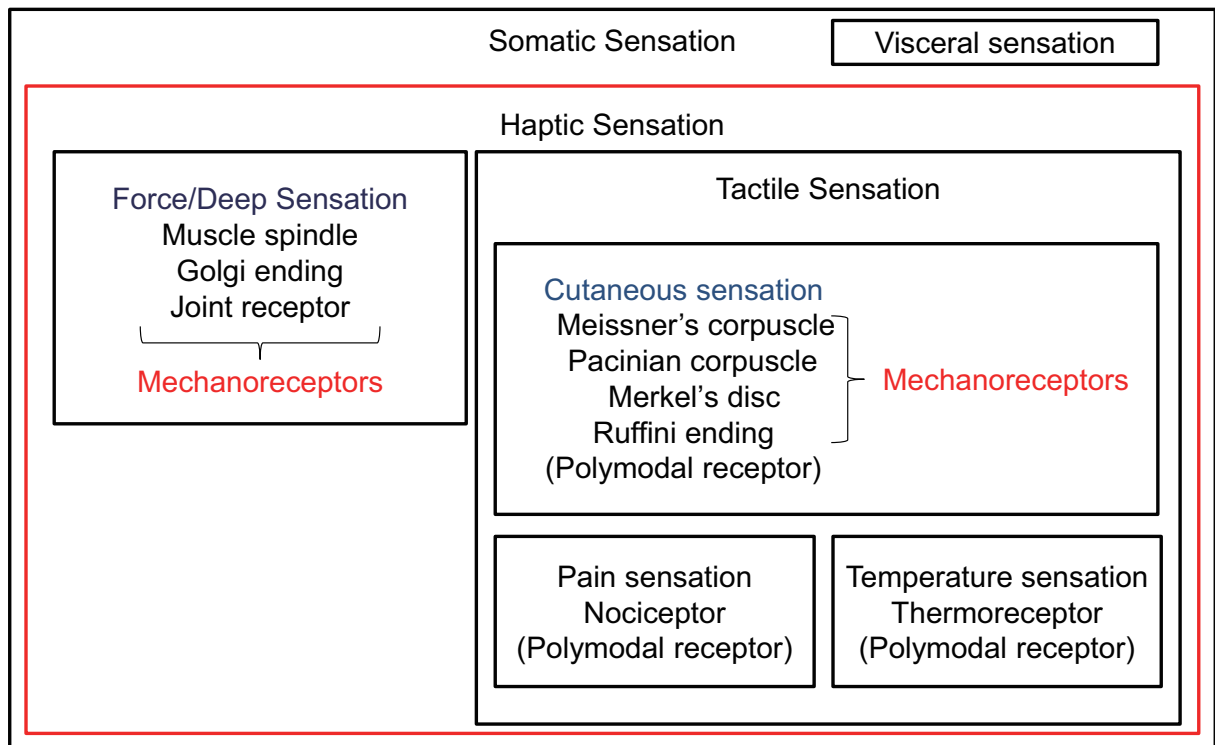
Fig. 1.4: Charts of the clarifications of somatic sensation. Cutaneous and force sensations are being on our focus.

regardless of the environment (Fig. 1.3). Similarly, in quiet environments such as in a meeting, we can send mail or tweets through a haptic device without even glancing at it. As another example, we can "read" a haptic display behind the handle of a car.

Haptics provides confidentiality, and this improves privacy because nobody can "peep" without touching the display. Outputs as well as inputs cannot be perceived through the visual and auditory senses (hand movements may be seen but would be quite difficult to recognize); in contrast, the gesture and voice inputs used with the visual and auditory senses can both be intercepted easily.

Moreover, haptic can be used to add modalities to verbal information to create new content such as a warm "hello" or soft "good night" in a manner similar to a bright yellow "Hello" for the visual sense and a soft "Hello" in a velvety voice for the auditory sense.

1.3 Physical and Psychophysical Aspects of Target Mechanoreceptors

Haptic sensations have several modalities, each of which has corresponding receptors inside the skin. Fig. 1.4 shows human sensations and the corresponding receptors. The somatic sensation is derived from body tissues different from those for the other senses. It includes haptic and visceral sensations. Haptic sensations can be classified as force and tactile sensations. We specifically focus on force and cutaneous sensations obtained by mechanoreceptors. Mechanoreceptors are a type of receptor that produce afferent impulses in response to mechanical stimuli.

Cutaneous Mechanoreceptors

Cutaneous mechanoreceptors are embedded in the skin tissue as shown in Fig. 1.5. They can be of four types depending on their characteristics in response to stimuli and perceptive field areas. They are FA I (Fast Adapting type I), FA II (Fast Adapting type II), SA I (Slowly Adapting type II) and SA II (Slowly Adapting type II) as shown in Fig 1.6. The adaptation time indicates the time for which a neural activity pulse is not generated upon inducing the static displacement of the skin surface. The receptive field indicates the spatial area in which a neural activity pulse is generated upon inducing the static displacement of the skin surface. The corresponding mechanoreceptors are FA I: Meissner's corpuscle (0.7 mm from surface), SA I: Merkel's disk (0.9 mm from surface), FA II: Pacinian corpuscle (2.0 mm from surface), and SA II: Ruffini ending (2.0 mm from surface) in Fig. 1.5 [8]. The spatial density and resolutions of each cutaneous mechanoreceptor are shown in Fig. 1.7. In particular, FA I is concentrated in the fingertip and makes the spatial distributions of stimuli highly recognizable. This is why Braille and other tactile displays are designed to be explored by the fingertip. Fig. 1.8 shows details about each mechanoreceptive fields. Most fields are circular or oval and have a diameter of 2-8 mm [8]. SA I and FA I are suitable for sensing spatially distributed information.

Fig. 1.9 shows the detection thresholds of each cutaneous mechanoreceptors for vibratory stimuli under two prove conditions. Each cutaneous mechanoreceptor has certain characteristic: for example, for vibratory stimuli, SA I is sensitive to a frequency of 5 Hz; FA I, 30 Hz; and FA II, 300 Hz. Accordingly, each cutaneous mechanoreceptor can be selectively triggered using its most sensitive frequency and with certain detection

threshold level amplitudes; this approach is called selective stimulation (temporal) [12]. The selective stimulation of SA I, FA I, and FA II presents a sense of pressure [12, 11], flutter, and vibration, respectively. Selectively innervating SA II does not cause subjective sensations. Furthermore, it should be noted that the Ruffini ending (SA II) has not been observed in certain apes [13], and its existence is still debated.

Cutaneous mechanoreceptors can also be selectively stimulated by specially arranged mechanical stimuli, as shown in Fig. 1.10. Air pressure stimulates the receptors in the shallow layer (SA I and FA I), whereas the overall vibration stimulates receptors in both shallow and deep layers. This is because of the skin's spatial low-pass characteristics; stimulation over a tiny area is attenuated as it goes through the skin tissue to the deeper layer [15].

Deep Mechanoreceptors

To perceive proprioception, humans use the muscle spindle and Golgi 's tendon organ. Fig. 1.11 shows the Ib afferent fiber responses of the Golgi 's tendon organ against muscle conditions [89]. Ib fibers are innervated when the muscle is stretched or constricted [16]. The muscle and tendon consist of two types of stretch receptors that respond to the muscle activity or status. The spindle has two types of afferent fibers: Ia and II group fibers. Ia group fibers are innervated actively and statically. Fig. 1.12 shows their response against the muscle length [89]. In particular, Ia fibers show strong responses to the dynamic stretch of the muscle, including vibratory stimuli [17]. II group fibers statically detect the muscle length.

1.4 Difficulties in Displaying Haptic Shape Information

Our approach to present characters and shapes using haptic sensations, specifically, by individually presenting tactile or force sensations, is challenging because both of these sensations involve certain difficulties. Here, we describe previous methods for displaying haptic shape information and the difficulties faced in them.

Presentation Using Tactile Sensations

Presentation using tactile sensations is commonly in 2-D, since tactile stimulation is displayed on the skin surface. Braille, finger spelling (finger alphabet), and handwritten
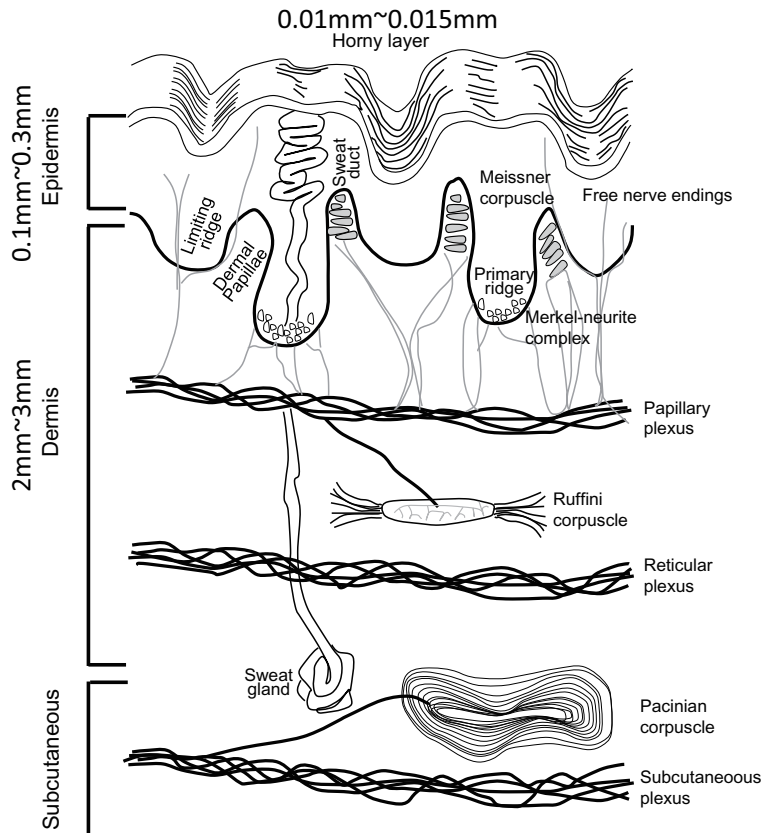
Fig. 1.5: Schematic of the structure of skin and cutaneous mechanoreceptors. [6] modified.

Fig. 1.6: Types of tactile afferent units in the glabrous skin of the human hand and some of their distinguishing properties. Lower trace shows the impulse discharge and upper trace shows the perpendicular ramp indentation. [8] modified.
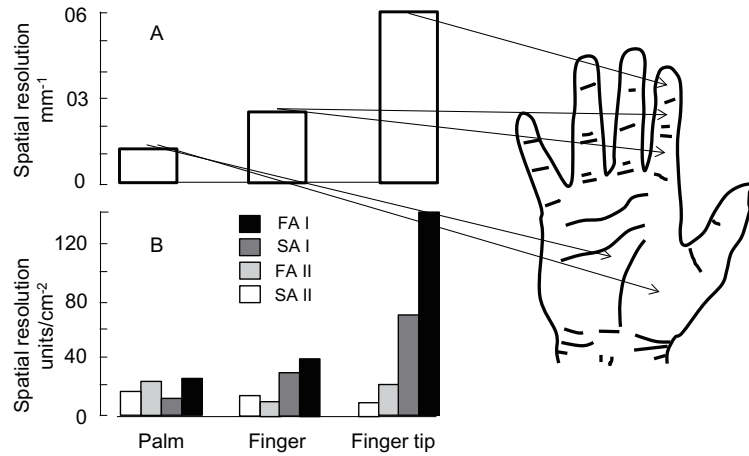
Fig. 1.7: A. Spatial resolution of two-point discrimination. The height of the columns show the inverse of the two-point threshold in units. B. Histogram showing the density of innervation of the four types of mechanoreceptive units in different regions of the glabrous skin area of the human hand. [9] modified.
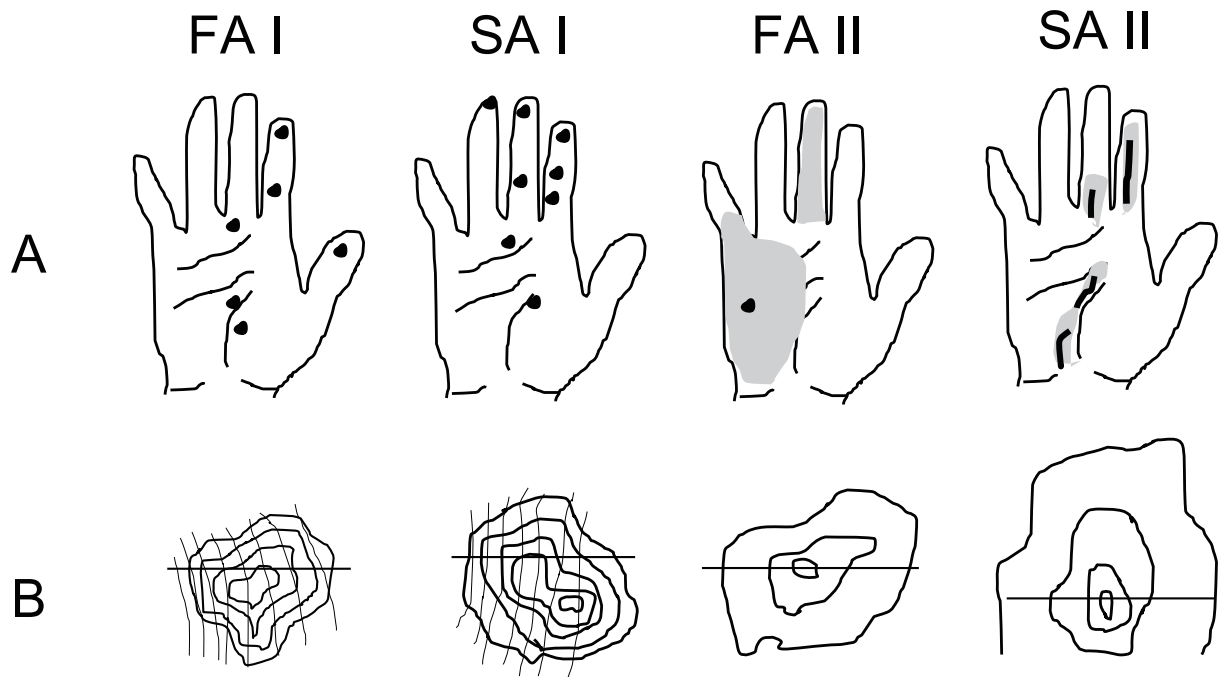
Fig. 1.8: Characteristics of mechanoreceptive units for receptive field size and its structures. A. Receptive field size. The black patches of the drawing of the hands indicate receptive fields of 15 units as measured with von Frey hairs providing a force of 4-5 times the threshold force of the individual unit. B. Microstructure of receptive fields. Sensitivity maps of single mechanoreceptive fields. [8] modified.

8
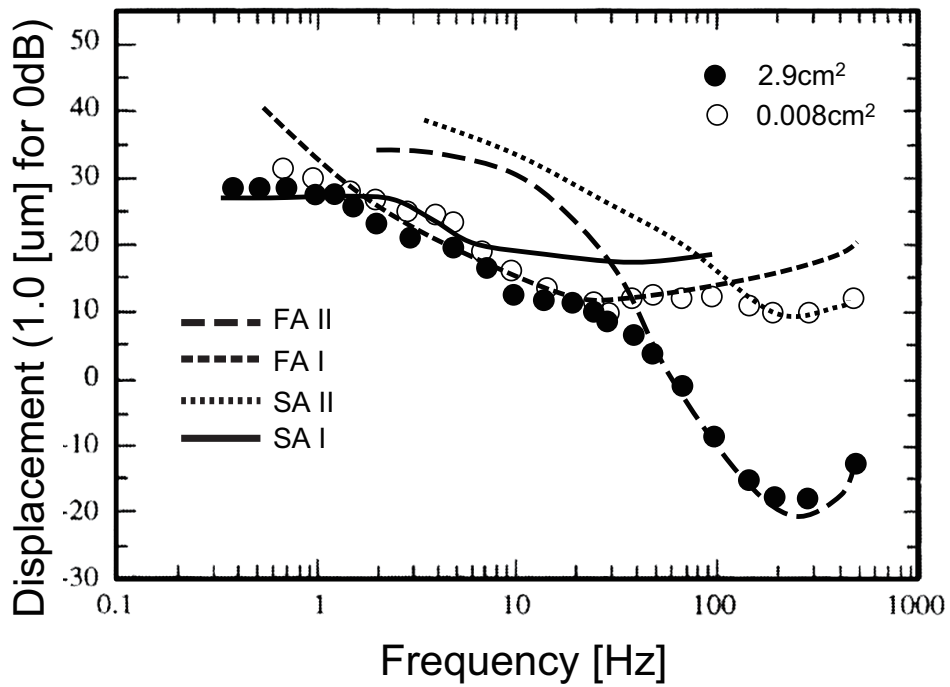
Fig. 1.9: Threshold-frequency plots of the cutaneous mechanoreceptors. Black and white circulars indicate the prove diameter. [8] modified.
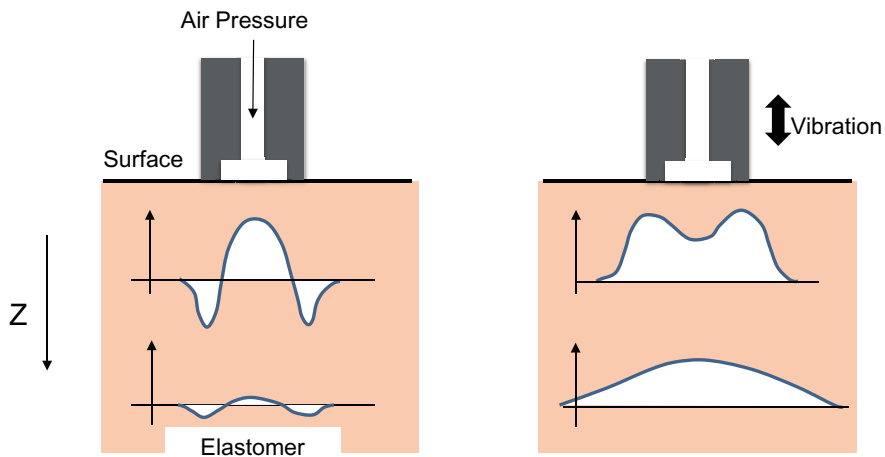
Fig. 1.10: Two kinds of stimulation in cross-section. The graphs illustrate the stress distributions at a shallow level and a deep level. The air pressure stimulates shallow receptors due to skin's spatial low-pass filter effect. The vibratory stimulus reach to deeper layer where FA II exist [14].
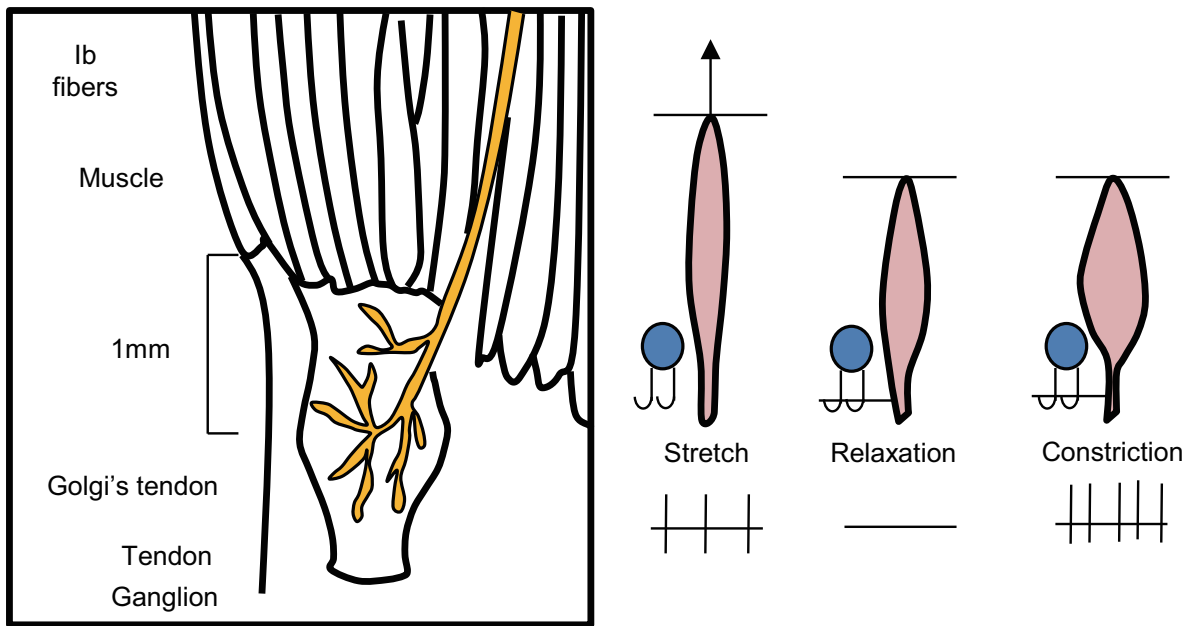
Fig. 1.11: Responses of Ib of Golgi's tendon organ against muscle conditions. [89] modified.
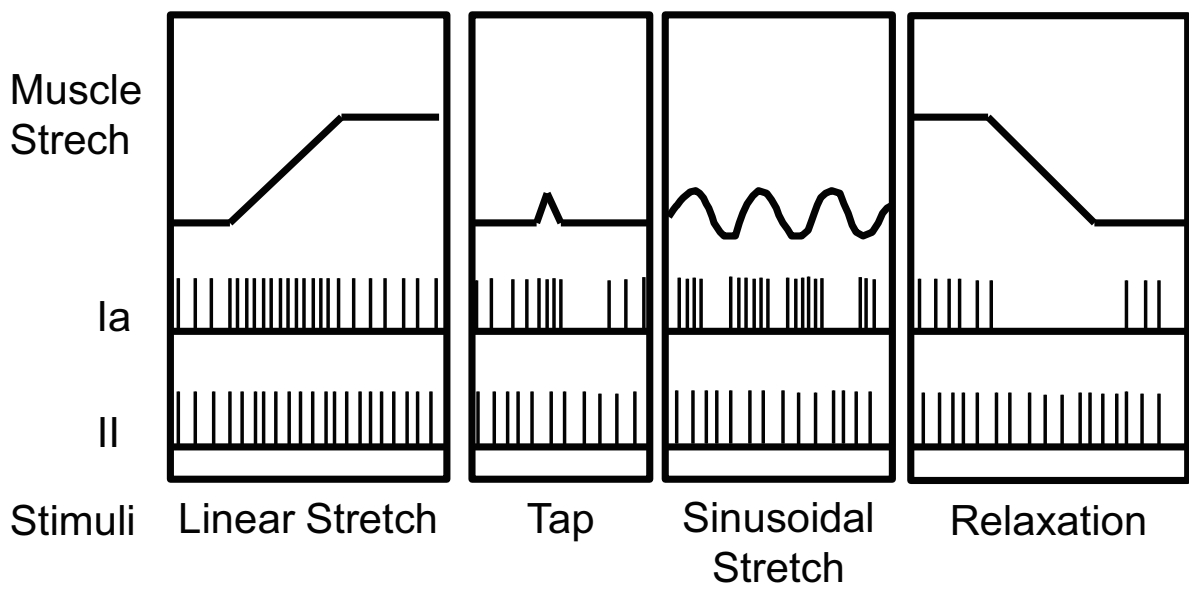
Fig. 1.12: Responses of Ia and II against muscle length that stimuli produce. [89] modified.

characters are few of the methods used by visually impaired people for transmitting verbal information. These methods are considered to integrate symbolic/verbal information into haptic spatial information; furthermore, tactile Morse code delivers them with time information.

The need for practice to recognize these forms of communication mean that sighted people cannot utilize them casually. Braille involves two main difficulties. First, one must recognize the dot combination precisely; this takes considerable practice. Second, one must be able to convert the obtained dot combination into an alphabet using the correspondence table; this chart can take a few years to memorize [91]. These difficulties mean that, for example, of all visually impaired people in Japan [92], only 20 % can read Braille, and few new users learn how to use this approach. Tactile Morse code and finger spelling also involve difficulties in translating the tactile perceptions into alphabets. Handwritten characters suffer from problems related to the transferring speed. One must write all characters on the reader's hand, and the spatial resolution of the palm compels writers to write characters one-by-one, making it difficult to distinguish the end of the word.

Moreover, the tactile characteristics of humans make it difficult to engineer effective tactile devices. For the presentation of alphabets, if the shapes are shown by static displacements, the actuators need large amplitudes (more than 100 μm) and force against the indentation finger force. Consequently, the device size increases considerably. For using vibratory stimuli at 200-300 Hz, according to Fig. 1.9, a low amplitude is required; nonetheless, the tactile sensation is blurry because FA II has a large receptive field, as shown in Fig. 1.8.

Presentation Using Force Sensations

Presentation using force sensations is displayed in both 2-D and 3-D. PHANToM (Sensable Technology [18]) and SPIDER [90] are the most widely used devices for presenting force feedback. Studies using these devices mainly focus on the teaching/training system for handwriting [19] and the medical techniques [20] and shape presentations for interaction with a virtual object [18]. However, thus far, studies have not directly focused on achieving the presentation of alphabets using force sensations.

1.5   Our Approach

We especially focus on the tactile shape information delivery, since the tactile displays demand smaller strokes compared to the force ones and displays become miniature. As described above, the effective tactile shape presentation to achieve characters have not been accomplished, not even presenting a single continuous line (previously dots combination) which is a primitive of 2-D line drawing. Our approach is to establish a new vibrotactile stimulation method to present high resolution tactile lines, and shapes as a combination of the lines. The potential of high resolution tactile lines for application are presenting virtual edges, areas, and shapes. Such high resolution information helps the user with faster and more accurate handling, and enables transmission of additional symbolic information.

1.6   Organization of the Thesis

This thesis is composed of five chapters. Chapter 1 is the introduction of this thesis. Chapter 2 is the proposal of a new tactile stimulation method and the investigation on it's performance, including section 2.1, 2.2, and 2.3. Chapter 3 describes the advanced version of the developed stimulation method dedicated for a tactile shape presentation, including section 3.1, 3.2, and 3.3. Chapter 4 treats a tactile shape presentation using developed tactile device, including section 4.1 and 4.2. Chapter 5 is the concluding part.

Chapter 2

Sharp Line Sensation by Edge Stimulation Method

2.1 Fine Tactile Stimulation Method

Haptic stimulation is classified into two parts according to the modality it focuses; force stimulation and tactile stimulation. Force stimulation is mainly perceived by Golgi tendon organ and muscle spindle causing a kinesthetic sensation (proprioceptive sensation). In contrast, tactile stimulation fires cutaneous mechanoreceptors such as FAI, FAII, SAI and SAII triggering a tactile sensation, sense of touch.

In this section, the explanation of a new tactile stimulation method for presenting sharp and easy recognizable tactile image is described.

2.1.1 Tactile Stimulation Method and Reviews on Related Works

In order to stimulate the cutaneous mechanoreceptors described above, three types of tactile stimulation methods have been developed so far. Here, the description about the stimulation methods and the related works in the view of shape presentation are denoted.

Static tactile stimulation: Static tactile display is common for past few years that shows static displacement of actuators arranged in matrix array. User explore the surface of the display with their palms/fingers and obtain tactile information by tracing the difference in dents and bumps. The shape information including figures, symbols, characters, numbers and most popularly Braille dots are presented by combination of the dents and bumps that are generated by the stroke difference of the actuators. Tactile displays using static tactile stimulation method is called static refreshable device and numerous numbers of them have been developed. Fernando have classified those previous works [41] of static refreshment devices, Table. 2.1

13

shows the characteristics of each devices concerning the parameters of refreshing time, resolution, size and stroke. [45] equips an image sensor and the display translate the obtained image into tactile shapes. [46] has large array to rub over the display surface. A tactile image generated by these static tactile stimulation tends to elusive and demands user to practice to a certain extent for accurate and fast recognition of whole shapes.

Electro-tactile stimulation: Considering to the afferent nerve system, replacing nerve impulses to electro stimuli injection from skin surface is a natural approach to present tactile images. A pile of woks has been conducted in electro-tactile stimulation method [58, 59, 60], Kajimoto's recent work[54] for presenting spatio-temporal electro-tactile patterns to represent the afferent nerve impulses reaching to brain achieved the generation of a more realistic friction sensation. Superficial electrodes generate the electro-tactile stimuli while measuring and adjusting the electrical impedance between skin and the display surface. They have achieved that the display be manufactured very small, thin, durable, energy efficient and free from mechanical resonance. However, in the course of inducing electrical stimuli to skin, there emerges a pain sensation since nociceptors are also stimulated. Because the sense of pain is stronger than any other tactile modality, once it is triggered, human cannot distinguish the shapes (spatial patterns) of the stimuli. It seems to be needed a little more challenge to overcome the pain and be able to utilize electro-tactile stimulation method in shape presentation.

Vibrotactile stimulation: A vibrotaction triggers the cutaneous mechanoreceptors by inducing moving actuators to human skin. This method is widely used in mobile phones for a tactile alert. The vibrotactile sensation produced by the vibration differs in accordance with the single vibration's frequency and amplitude. In addition, the vibrotactile sensation changes with multi-vibration's spectral combinations. Asamura reported that by stimulating each cutaneous mechanoreceptors individually, the tactile sensation transforms as the combination of stimulated receptors[14]. Kajimoto called each sensation bring about by each cutaneous mechanoreceptors as 'tactile primary colors'[54].

In dairy life, the most frequent vibratory phenomena on skin are caused by contact friction. For instance, when grasping an object, human perceive slippage between target object and fingers unconsciously and adjust our grasping force. Konyo rep-

resented the slipping area and vibratory parameters on fingers by ICPF actuators and succeeded in inducing grasping force reflex[55]. Tsuchiya succeeded in presenting friction sensation with a single motor by representing vibration when rubbing an object[56]. Minamizawa developed 'TECHTILE Toolkit' which produces vibrotactile sensation with voice coil motor; the wave patterns are recorded by a microphone[57]. These works certificate how an intuitive and natural way it is to present tactile sensation by the method of vibrotactile stimulation. Moreover, vibrotactile stimulation is suitable for both active and passive touch. Users realize the changes in spatio-temporal patterns in passive ways while keeping still touching the surface.

When it comes to shape presentation, the related works' devices using vibrotactile stimulation employ tactors in array similar to the conditions of the static refreshment devices. Table. 2.2 [41] shows the characteristics of each devices. According to the table, devices employing piezo actuators tends to use high frequency except for VirTouch Mouse. Due to the characteristics of piezo electric device, the stroke is small, less than 1 mm. SMA type is superior in high stroke though the tactile device become large. Electromacnetic and suction type are very bulky, not suitable for portable/handy devices. Motor type has difficulty in its integration, and as a consequence, the possible tactile spatial patterns decreases. Summarizing the above, piezo vibrators are suitable for its capability of high-density integration and presentation of wide variety of tactile patterns, while the sensational intensity is relatively small since the stroke is small. In this study, vibrotactile stimulation method using piezo electric device is in focus since static type has difficulty in its vague sensation and electro type has difficulty in its pain.

Table. 2.1: Static Refreshment Devices [41] modified

Device	refreshing times	resolution	size	stroke	actuator
[42] DMD-12060METEC	10s	3.08mm	27.2cm × 18.6cm 7200 taxels	0.7mm	solenoids
[43] KGS & NASDA	less1s	3mm	19cm × 14cm 3072 taxels	0.7mm	piezo
[44]	less1s	2.4mm	1536 taxels	0.7mm	piezo
[45] TIM, ABTIM	1/24s	2.5mm	4cm × 4cm, 256 taxels	0.8mm	piezo
[46] NIST & NFB	ND	2.54mm	17.8cm × 12.7cm 3600 taxels	ND	ND
[47]	ND	2.54mm	48 × 12.7cm 32 taxels	2mm	ND
[48]	15s	3mm	64 × 64 taxels	0-10mm	3D-SM motors
[49]	ND	10mm	16 × 16 taxels	0-6mm	3D-SM motors
[50]	0.66s	2.6mm	8 × 8 taxels	1.4mm	SMA
[51]	0.3s	2.5mm	2.5cm × 2.5cm 10 × 10 taxels	2mm	SMA
[52]	ND	13mm	5 × 5 taxels	ND	ELF

3D-SM:3dimension stepper motor, SMA:shape-memory alloy, ELF:electrorheological fluid

Table. 2.2: Dynamic Devices[41] modified

Device	resolution	stroke	forces	bandwidth	size	actuator
[61] Optacon	1.27mm rows 2.54mm columns	10μm	6mN	250Hz	12.7mm×29.1mm 24×6 taxels	piezo
[62]	2mm	57μm	ND	250Hz	5×10 taxels	piezo
[63]	1mm	50μm	ND	25-400Hz	10×10 taxels	piezo
[64]	1.8mm	0-0.7mm	0.06N	0-500Hz	6×5 taxels	piezo
[65] VirTouch Mouse	1.5mm	0-1mm	0.1N	10Hz	8×4 ×3displays	piezo 3D
[66] VirTouch Mouse	2.45mm	0.7mm	0.15N	50Hz	6×8 taxels 43mm×16mm	piezo
[67]	1mm	ND	ND	700Hz	10×10 taxels	piezo lateral stimulation
[68, 69] HAPTAC	3mm	ND	0.2N	170ms rise time	5×6 taxels	SMA
	2.5mm	ND	0.6N	50ms rise time	3×3 taxels	SMA
[70]	3.6mm	3.2mm	0.7N	500ms rise time	64 taxels	SMA
[71]	2.2mm	3mm	1.2N	1500ms rise time	3×3 taxels	SMA
[72]	2mm	3mm	1.5N	40Hz	10 taxels	SMA
[73]	3.5mm	5mm	2N	5Hz	4×4 taxels 15mm×15mm	pneumatic
[74]	2.5mm	0.6mm	180mN	5Hz	5×5 taxels 12mm×12mm	pneumatic
[75]	5mm	NA	NA	50ms time constant	19 taxels	suction pressure
[76] TACTACT	3mm	1.6mm	4.5N	100Hz	6×6 taxels	electromagnetic bulky
[77]	0.5mm	2.5mm	0.3N/mm	less40Hz	20×20 taxels 1cm×1cm	electromagnetic bulky
[78]	5mm	±100μm	ND	800Hz	8×8 taxels	microcoils
[79]	2mm	2mm	ND	25Hz	6×6 taxels	RC servomotors
[80]	2.7mm	3mm	1.7N	2Hz	4×8 taxels	micro brushless motors
[81]	2mm	2.5mm	3N	less15Hz	4×4 taxels	DC motors

2.1.1.1 Edge Stimulation (ES) Method for Fine Shape Presentation

Previous vibrotactile displays generally use high-frequency vibrations (100-500 Hz) due to the vibrotactile sensitivity of humans to frequency. Since piezo actuators are inferior in their amplitude, previous works employed high frequency. However, mechanoreceptors that are sensitive to high frequencies (fast adopting type Ⅱ unit: Pacinian corpuscle) have large receptive fields and are essentially unsuitable for obtaining the spatial distribution of vibrations. In contrast, low-frequency vibrations (5-30 Hz) are sensed by mechanoreceptors such as Merkel's disks (slowly adopting type I unit) and Meissner's corpuscles (fast adopting type I unit), which have a high spatial resolution for tactile stimuli. Thus, using low-frequency vibrations to present tactile shapes is a natural approach, although large amplitudes are required for those low frequencies to be perceptible (about 30 μm); thus, actuators are large.

We have proposed a vibrotactile stimulation method that uses a low-frequency and small-amplitude vibration while reducing the detection threshold. The method selectively stimulates high spatial resolution mechanoreceptors such as Merkel's disks and Meissner's corpuscles in the shallow layer by locating two surfaces in close proximity and vibrate one of them while suppressing the spread of vibration on the skin. The tactile image emerges along the boundary edge of the surfaces, and the sensation is sharp localized, and clear. This method is termed edge stimulation (ES) method and the mechanical condition of ES method called ES condition. The use and the mechanism of ES method are the main topic for this chapter. Fig. 2.1 shows a schematic of ES method. The ES method allows the tactile display surface to be fabricated as a flat plane in contrast to the previous pin-array displays discussed above; we can mount the ES tactile display on the flat surface of any device and project images on the display surface. Moreover, the low-frequency and small-amplitude vibration of the ES method allows for low-power actuation. Main idea of this study is to utilize ES method for presenting sharp and distinct shapes. Fig. 2.2 shows the schematic of shape presentation display using ES method. Instead of dots sensation of previous pin-array display, by locating square shape vibrator array, continuous lines emerge on the display surface. A concept of continuous line shaped vibrotactile sensation is completely new idea that will lead to more intuitive and recognizable shape presentation.
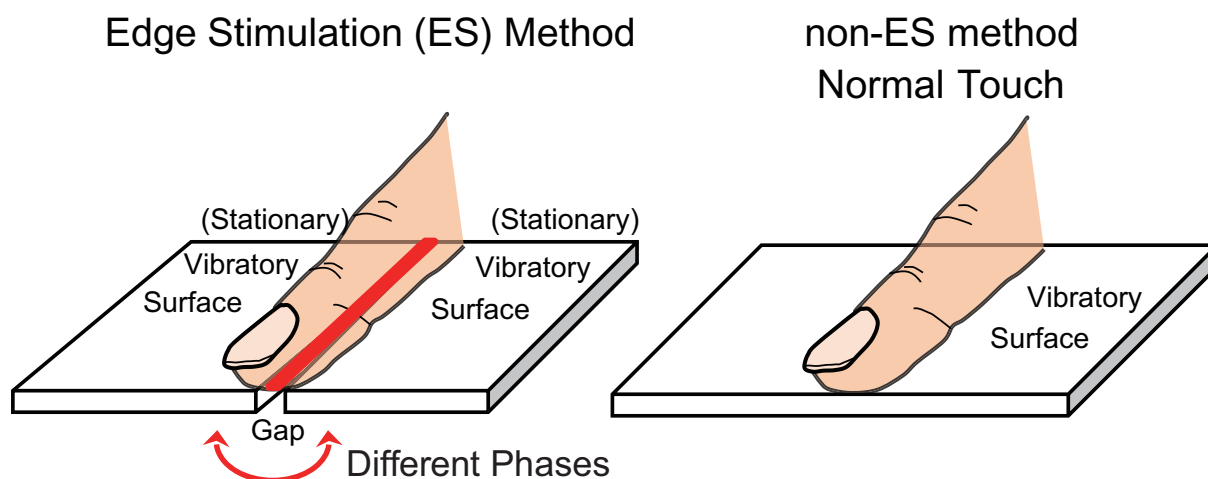
Fig. 2.1: Schematic of vibrotactile stimulation methods. Left. ES method. Simultaneous contact with a vibratory surface and a stationary surface enhances human vibrotactile sensitivity; humans perceive strong tactile sensations at the boundary between the two surfaces. Right. Non-ES method. Vibrations need to be of larger amplitudes to be perceived by humans through a simple touch of the vibrating surface.

2.1.2   Related Works of ES Method

Enhancement of human vibrotactile sensitivity

The enhancement of human vibrotactile sensitivity is an effective approach to improve the efficiency of vibrotactile stimulation to support the lack of amplitudes of piezo vibrators. ES method also achieves in falling the detection threshold and enables users to perceive with a few amplitudes. In this subsection, the previous works concerning an enhancement of human vibrotactile sensitivity are explained.

When inducing vibrotactile stimuli to skin, human vibrotactile sensitivity alters under the effect of the shapes of the contactor, the contacting area, the curvature of the contactor, the boundary conditions between the skin and the contactor and so on[25, 83, 28, 27]. Further, the effect of an edge has one out of the most controlling affection on the detection threshold. The work of Johansson revealed that not only in central nervous system due to lateral inhibitory mechanisms in [87] but also at the level of the cutaneous mechanoreceptors such as FA I and SA I, enhancement of spatial contrast occurs[7].

Several studies have been conducted to evaluate several active methods for enhancing human sensitivity to vibrotactile stimulations. Liu et al. investigated the changes in the vibrotactile sensitivity of older people, stroke patients, and patients with diabetic neuropathy to 30 Hz vibrations containing mechanical noise[23].They reported that the detection threshold of the fingertip for a vibratory stimulus of 30 Hz containing me-
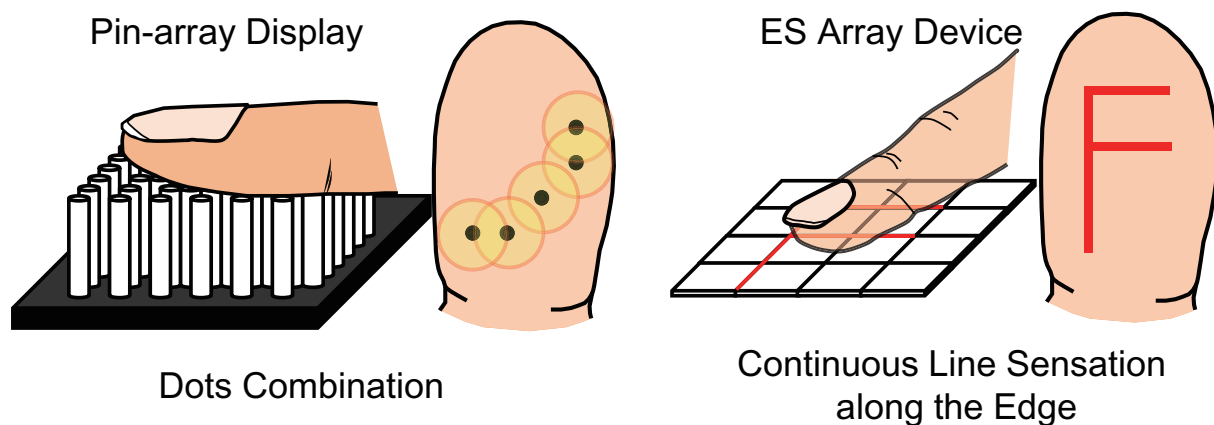
Fig. 2.2: Schematic of shape presentation. Left. Previous tactile display with pin-vibrators. The shape is represented by a combination of dots. Right. ES array device. The shape is represented by continuous line sensation.

chanical noise was significantly lower than that without mechanical noise. Jeong et al. found that the addition of a tangential vibration stimulus to a vertical vibration enhances vibrotactile sensitivity[22]. They investigated the changes in vibration sensitivity at frequencies of 8, 10, and 25 Hz when tangential vibration was added to the stimulation of the surface of human skin. They modified various mechanical parameters to enhance human sensitivity to vibrotactile stimuli. Neel et al. reported that the superposition of electrical noise enhances the detection threshold for an indentation force[24].They applied electrical noise to a human foot and investigated the correlation between the magnitude of the electric noise and the human detection threshold for an indentation force. These conventional methods, however, require space for another actuator and/or extra power. These are critical factors for haptic devices, which have limited space for actuators and are challenged by power conservation.

Simultaneous contacts with vibratory and stationary surfaces in close proximity, ES method can reduce the detection threshold. This phenomenon was first reported by Verrillo [25] as stationary surface enhanced sensitivity. His vibrotactile stimulation apparatus included a rigid ring (stationary surface in our study) around a circular vibrating probe. The original purpose of the rigid ring was the suppression of running waves over the human skin around the contactor, and the restriction of the stimulation area[25]. Verrillo investigated the effects of the rigid surrounding on human vibrotactile sensitivity when the probe and the ring were simultaneously touched — a mechanical situation similar to ES condition. He reported that the presence of the rigid surrounding enhanced human vibrotactile sensitivity at low frequencies and that the gap between the probe and the

surrounding was positively correlated to the human detection thresholds for vibratory stimuli; the wider the gap, the greater was the detection threshold. He suggested that this might be due to the pattern of the surface waves as they moved across the gap to the perimeter of the hole. If the gap is equal to half of the wavelength, the displacement of the tissue over the gap could be expected to be maximum. He plotted his data using the ratio of the wavelength to the gap, but no systematic relationship could be determined, and he concluded that there was no explanation for the results.

In [82, 83, 84, 85, 86], the mechanical situation in the apparatus of Verrillo was reproduced, and the psychophysical effects of the rigid surrounding on human temporal and spatial perception of vibratory stimuli were investigated. All these studies concluded that the presence of the rigid surrounding affected both sensitivity and the shape of the temporal tuning curve for low frequencies. Lamore particularly concluded that the effects of a rigid surrounding were tuned at low frequencies and the detection threshold was significantly lower at 18 Hz under the conditions of his mechanical apparatus, in which the contactor size was 1.5 cm^2 and the gap between the contactor and the circular aperture in the table was always 1 mm. He determined and extensively discussed the effects of the surroundings on human vibrotactile sensitivity under various structural conditions of the mechanical apparatus and various human conditions such as age, application area, and hairiness. He, however, did not clearly explain the mechanism of how the presence of a stationary surface enhances human vibrotactile sensitivity. Our study, in the course of the investigation on the mechanism of ES's enhancement in the later section, will argue about the stationary surface enhanced sensitivity in detail.

2.2 Performance of ES method

In this section, while changing several mechanical parameters, human vibrotactile detection thresholds are investigated under ES condition. The detection threshold indicates the effectiveness for presenting vibrotactile stimulation. At an amplitude of detection threshold level, for example $A_{D.L.}$ mm, one feels just noticeable intensity of vibrotactile sensation. If the detection threshold becomes low, one perceives stronger vibrotactile sensation at the amplitude of $A_{D.L.}$ mm.

2.2.1 Determination of ES Characteristics as a Function of Several Parameters

2.2.1.1 Psychophysical Experiments

Three psychophysical experiments were conducted to assess the performance of ES method. Experiment 1 was designed to investigate the effects of the vibration frequency on the detection threshold under ES condition. The detection thresholds for three frequencies were examined here. For comparison and to evaluate the effectiveness of ES method, the detection thresholds for the same frequencies under non-ES conditions (Fig. 2.1) were also examined.

Experiment 2 was designed to investigate the effects of the gap distance between the vibratory and stationary surfaces on the detection threshold. The gap distance was gradually increased while other mechanical parameters were kept constant.

Experiment 3 was designed to investigate the effects of the height deviation between the vibratory and stationary surfaces on the detection threshold. The height was gradually increased while other mechanical parameters were kept constant. This experiment was conducted for the requirement of ES device development, so the condition set was smaller (only at 30 Hz) than experiments 1 and 2 (see the Experimental Procedure).

2.2.1.2 Apparatus

The experimental setup is shown in Fig. 2.3. A mechanical stage of a precision of 0.1 mm was placed on a base of sufficient area and weight. A piezoelectric actuator (Tokin, AHB850C851FPOL-1F bimorph type) was also rigidly placed on the base. The actuator could generate vibrations of amplitude greater than 85 μm and responses higher than 400 Hz. For a frequency 5 Hz, the amplitude of the generated vibration was not sufficient to make it perceptible by some subjects. We therefore used another large-amplitude vibrator (Emic Corporation, Vibration Generator 511-A), on which the same contactor was placed. Rectangular aluminum contactors were placed on the edge of the mechanical stage and on top of the piezoelectric vibrator to even the size, shape, and material of the two contact areas. The area of each contactor was 20 mm, which made them sufficiently larger than the finger tip. Pressure sensors (Flexi Force A-201) were embedded at the center of the contactors to observe the indentation force applied by the finger of the subject. The contactors on the stage and the vibrator respectively functioned as the stationary and vibrating surfaces of an ES situation. The gap between the two surfaces was measured by the mechanical stage, which could be easily adjusted by sliding along
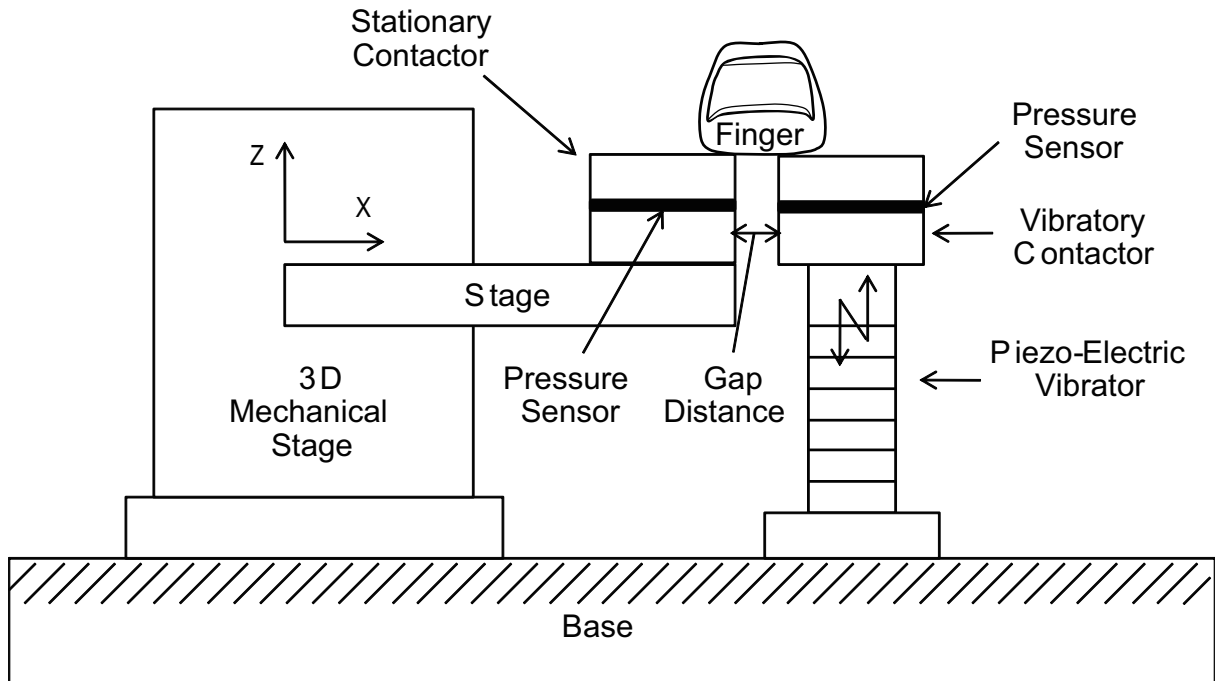
Fig. 2.3: Apparatus schema for psychophysical experiment.

the x-axis using a jog dial.

2.2.1.3 Apparatus Originality

The ES condition of our study and our approach are different from those of previous works mentioned above [25, 82, 83, 84, 85, 86]. The specific differences in apparatus are as follows: In previous works, it was difficult to change the gap between the vibrator and the rigid surrounding, which made the experiments more cumbersome. The rigid ring had to be continually changed to vary the diameter; otherwise, the vibrating contactor was changed to another one of a different diameter. This inevitably changed the stimulation area. We used a simpler method to vary the conditions of the boundary between the vibrating and stationary surfaces. We simply located the stationary surface close to the vibrating surface so that we could focus on the typical effects of the stationary surface. The stimulation area was thus constant for different gaps. Moreover, the structure made changing the gap easy.

2.2.1.4 Methods

Vibratory Stimuli

The vibratory stimuli that were used in this study were generated by the following equation:

$$y(t) = A(\sin(2\pi f t) + 1) \tag{2.1}$$

where $y(t)$ is the displacement of the vibrator [μm], A is the amplitude [μm], and f is the frequency [Hz].

The sinusoidal stimuli were generated with LEPRACAUN-CPU (general robotics SH4 board, real time art-linux os) and were amped by amplifier (Syou-Ei systems, SPD-410).

Vibratory Frequency Choice

5, 30, and 300 Hz are mainly used in our study and the reason for this choice is as follows.

Tactile receptors of mechanical stimuli differ in their temporal frequency characteristics. The SA I receptor (known as Merkel's disk) is most sensitive to vibrations at approximately 5 Hz; the FA I receptor (Meissner's corpuscle) is most sensitive at about 30 Hz; and the FA II receptor (Pacinian corpuscle) is most sensitive at approximately 300 Hz [28, 87]. Each type of tactile receptor can therefore be selectively stimulated by the application of a vibratory stimulus that has a detection threshold amplitude and frequency that the receptor is most sensitive to [12]; this is known as selective stimulation. Hence, when threshold amplitudes are applied, only the tactile receptors with corresponding detection threshold frequencies are triggered. Therefore, we can discuss the mechanism of the ES enhancement regarding to the tactile receptors' characteristics.

Experimental Procedures

Experiment 1: Detection Threshold as a Function of the Frequency

Firstly, the detection thresholds under non-ES conditions were determined as a reference. The stationary contactor was removed from the mechanical stage so that the subjects only touched the vibrating surface. To standardize the relative locations of the finger and the contactor surface, each subject was required to position the root of his/her nail on the edge of the contactor.

This experiment examined the conditions of three frequencies, namely, 5, 30, and 300 Hz. As previously described, these frequencies were selected to stimulate the different types of tactile receptors: SA I, FA I, and FA II, respectively. While each subject was

24

touching the vibrating contactor with his/her index finger and adjusting the indentation force to 1 N, the input voltage of the piezoelectric actuator was progressively increased by 1 V to vary the vibration amplitude between 0 μm and 85 μm. After each increase, the subject was asked whether he/she could perceive any vibratory stimulus. The threshold amplitude at which the subject first perceived vibration was recorded. The input voltage was then decreased in steps of 1 V from a well-defined source, and the threshold amplitude at which the subject could no longer perceive the vibratory stimulus was recorded. The detection threshold was thereafter calculated by the method of limits, which was generally used in previous studies [87]. The process was repeated 3 times for each frequency; i.e., a total of 9 times for each subject. Each step was repeated as many times as was necessary for the subject to satisfactorily judge his/her perception of the vibratory stimulus.

Secondly, the detection thresholds under ES conditions were determined. Each subject simultaneously touched the vibrating and stationary contactors, using one index finger to apply an indentation force of 1 N. The positioning of the finger was the same as in the first experiment, and the gap was set to 0.1 mm. Nine tests were performed for each subject as described above, and the detection threshold was similarly calculated for each frequency by the method of limits.

Experiment 2: Detection Threshold as a Function of the Gap Distance

In this experiment, the gap between the vibrating and stationary surfaces was increased in steps of 0.5 mm. Precisely, the gap was sequentially set to 0.1, 0.5, 1.0, 1.5, 2.0, 2.5, and 3.0 mm. The applied vibration frequencies were 5 Hz and 30 Hz. 300 Hz was left out because ES method has no significant effect on vibrotactile sensitivity to a vibratory stimulus of the frequency, as noted in the experimental results below. Each subject simultaneously touched the vibrating and stationary contactors, using one index finger to apply an indentation force of 1 N. For each frequency, each subject underwent three trials for each value of the gap; that is, each subject underwent a total of 21 trials. The method of limits was once again used to calculate the detection thresholds.

Experiment 3: Detection Threshold as a Function of the Height Deviation

The height of the stationary surface was increased in steps of 0.1 mm from -1.0 mm to 1.0 mm (21 conditions) and the process above was repeated 21 times per subject. The gap distance was kept to be 0.5 mm. The applied vibration frequencies was 30 Hz. This experimental result is utilized in the ES device development in the later chapter.
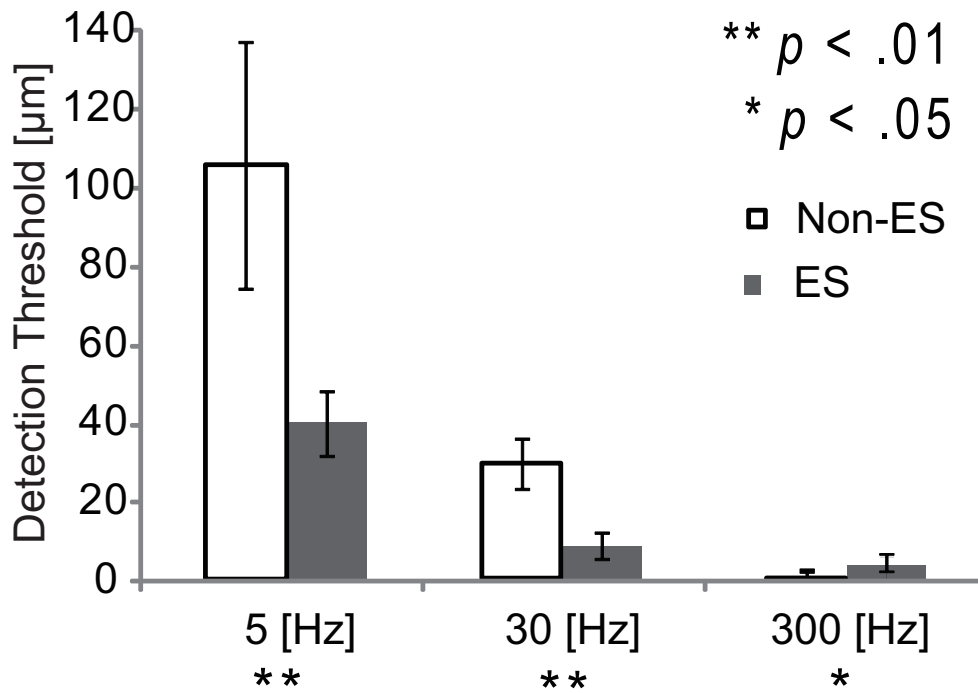
Fig. 2.4: Results of psychophysical experiments 1. Average detection thresholds of all subjects for each frequency under ES and non-ES conditions. Error bars indicate standard deviation.

In experiments 1, 2, and 3, the subjects wore headphones that delivered white noise to mask environmental changes. In experiments 1 and 2, the seven subjects were right-handed males aged between 21 and 25 years. In experiment 3, the five subjects were right-handed males aged between 21 and 25 years. None suffered from a medical disorder that affected his tactile sense.

2.2.1.5 Results

Experiment 1

Fig. 2.4 compares the average detection thresholds of the subjects under ES and non-ES conditions. The average detection thresholds under non-ES conditions were 105.65, 29.43, and 1.02 μm for frequencies of 5, 30, and 300 Hz, respectively. When the vibratory and stationary contactors were simultaneously touched (ES conditions), the average detection thresholds were 40.47, 9.17, and 3.58 μm for 5, 30, and 300 Hz, respectively.

When the subjects simultaneously touched the vibratory and stationary contactors, the detection thresholds for frequencies of 5 and 30 Hz were about one-third of those when only the vibrating contactor was touched. However, the detection threshold for a frequency of 300 Hz had the opposite tendency; it increased when the subjects simulta-
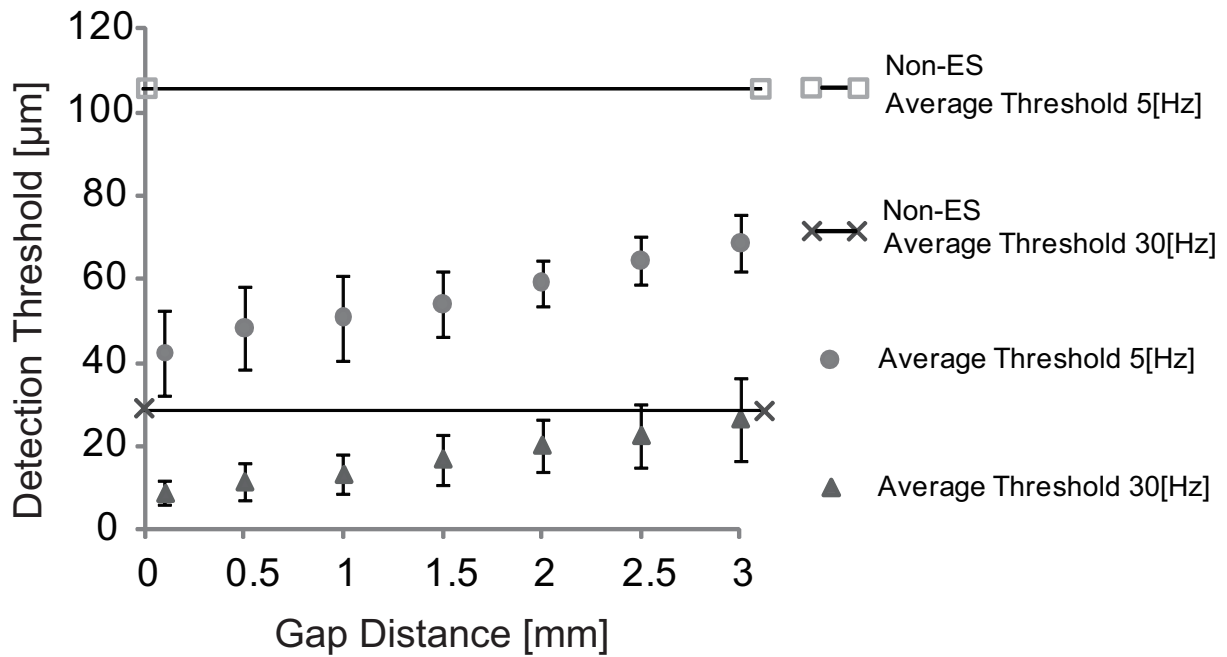
Fig. 2.5: Results of psychophysical experiment 2. 5 Hz and 30 Hz average detection thresholds of the subjects for different gaps under ES conditions. Detection thresholds under non-ES conditions (black lines) are added for comparison. Error bars indicate standard deviation.

neously touched the vibrating and stationary contactors ($p < 0.02$). This showed that ES method was not effective and unsuited for vibrotactile stimulation for a vibration frequency of 300 Hz.

Experiment 2

Fig. 2.5 shows the average detection thresholds of the subjects for 5 and 30 Hz as the gap was gradually increased. The values are compared with those for the non-ES conditions in experiment 1. As can be seen, the detection threshold increased with the gap for both frequencies. This shows that ES method is more effective when the gap is small.

Experiment 3

Fig. 2.6 shows the relation between the height gap and the detection threshold. The detection threshold and the absolute value of the height were positively correlated and the curve was almost linear. There was no significant change between a higher stationary surface and a lower stationary surface.
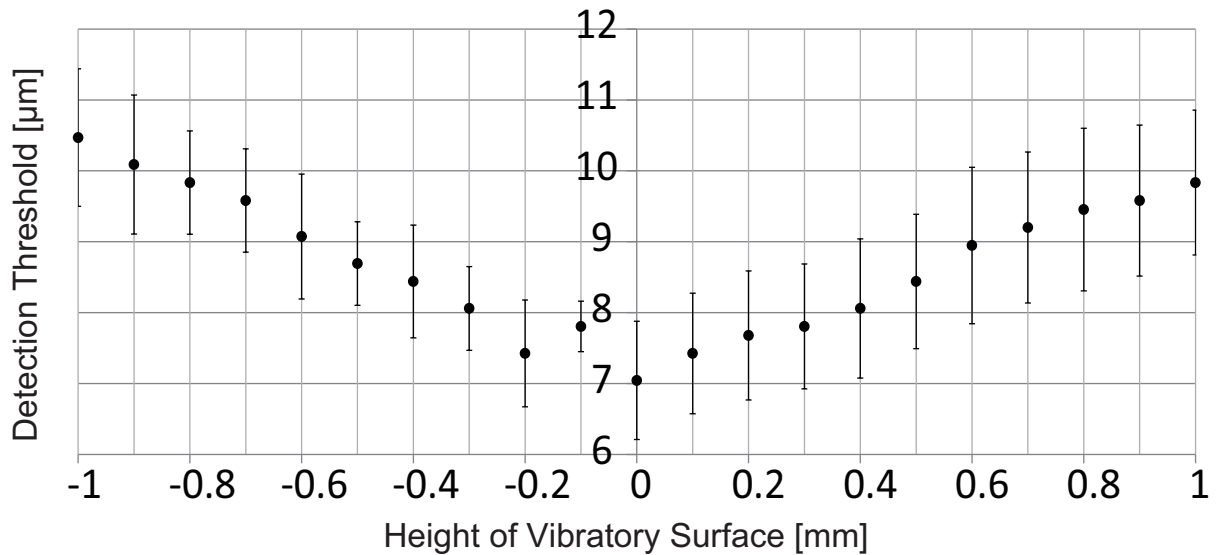
Fig. 2.6: Results of psychophysical experiment 3. Average detection thresholds of all subjects for each height gap under ES conditions. Error bars indicate standard deviation.

2.2.1.6 Discussion

In the studies of Verrillo and others [25, 82, 83, 84, 85, 86] who investigated the detection threshold as a function of a rigid surrounding (the stationary surface in this study), an adjustment ring was placed around the circular contactor to set the gap to 0.5 mm. This created a mechanical setting similar to that of this study. In experiment 1 of our study, when the gap was set to 0.1 mm and the boundary condition was linear shape (circular in previous works), the detection threshold under the ES condition was almost the same as that reported by Verrillo. We found that the ES enhancement was effective at lower frequencies and that the variation of the detection threshold with the vibration frequency was the same as in previous reports. The ES condition can thus be considered as part of the mechanical factors that affect stationary surface enhancement.

In contrast to the behavior of the ES method at lower frequencies, the detection thresholds for high-frequency vibratory stimuli under the ES condition are higher than those under the non-ES condition. The reason why the ES method is not effective for a vibration frequency of 300 Hz could be the same as that reported by Goble [86], who attributed the effect of the surroundings on high-frequency vibratory stimuli to spatial summation in the Pacinian system. To investigate and further understand the reason why ES method is less effective for high-frequency stimuli, we carried out a deformation analysis of the finger model under ES condition using vibratory stimuli at higher frequency in later chapter 3 section 2. This analysis involved an examination of the deeper

skin layer in which the Pacinian corpuscle is located.

Based on the graph of the effect of the gap between the vibrating and stationary surfaces (Fig. 2.5), the approximate equation of the detection threshold for 5 Hz is

$$A = 8.67d/100 + 42.33 \tag{2.2}$$

where A is the detection threshold amplitude [μm] and d is the gap [mm]. The approximate curve of the relationship between the gap and the detection threshold is almost linear. The curve crosses the detection threshold for a single contactor at a gap greater than 7.30 mm. Thus, the ES effect almost disappears when the gap is greater than 7.30 mm for a frequency of 5 Hz.

Similarly, the approximate equation for a frequency of 30 Hz is

$$A = 5.93d/100 + 8.13 \tag{2.3}$$

It can be seen from the approximate curve that the ES effect almost disappears when the gap is greater than 3.4 mm. Comparing the approximate curves for 5 and 30 Hz, it can be observed that the gradient of the former is greater than that of the latter, which indicates that ES method is stronger at 5 Hz.

For the experiment 3, the gradient of the curve was small, that is, the detection threshold is still low compared to the one in which the vibratory surface was simply touched and the ES method is sufficiently effective with the height gap of 1.0 mm.

2.3   Analysis on ES method

To investigate the mechanism of the ES enhancement, we conducted a series of finite element (FE) analyses of the deformation of the finger using a simple model comprising four skin layers, and simulated vibrotactile stimulation under the ES conditions. This chapter contains static and dynamic analyses to observe the strain energy density (SED) behavior inside the finger model.

Note that section 2.2 and 2.3 are preliminary steps for further and detail analyses on ES method with multiple vibration in chapter 3 section 2, the following deformation analysis and psychophysical experiments are elementary estimation of a phenomenon occurring under the ES.

2.3.1 Analysis of Skin Deformation under the ES Conditions

2.3.1.1 Strain Energy Density for an Index of Vibrotacitle Perception

The stress and strain energies are positively correlated and previous studies have also reported a correlation between the SED and vibrotactile sensation. For example, Srinivasan [32] analyzed the mechanism of human perception of a cylindrical model containing rectangular indentations. In his study, the maximum compressive strain and SED at typical receptor locations emerged as two strain measures that were directly related to the electrophysiologically recorded response rate of SA I mechanoreceptors. He concluded that the SED was a better candidate for the relevant stimulus of SA I receptors because it is a scalar quantity and invariant to the orientation of the receptor, and also a direct measure of the distortion of the receptor caused by the loads imposed on the skin. In addition, Maeno et al. constructed an FE model of the human finger by determining its geometry and the material properties of its tissue [33]. They concluded that there was a linear relationship between the SED of the tactile receptors and the firing frequency of the nerve impulse. Makino also investigated the spatial distribution of the SED inside an FE model of a finger [75]. They suggested that similar SED distributions inside the finger produced the same tactile sensation. For example, the static suction sensation generated by a small cylindrical hole was the same as the sensation produced when a pin of the same size as the hole is pressed against the skin. Considering the foregoing, we used the SED as an index of the effect of vibration on the deformation of the skin model in this subsection. The better index for FA I and FA Ⅱ are still controversial, considering the Fig. 1.6 in section 1.3, FA I and FA Ⅱ respectively respond to the velocity and acceleration of the stimulation that translated into a skin strain, and the skin strain is correlated with SED. Thus, we particularly focused on the spatial distributions of the SED peaks and the SED frequencies inside the model. The SED peak is related to the amplitude of the deformation caused by the vibration, whereas the SED frequency is correlated to the frequency of the deformation. Hence, by observing the spatio-temporal behaviors of SED, we can estimate why human perceive strong vibrotactile sensation with small amplitudes under the ES conditions.

2.3.1.2 Method: FE Analysis

Fig. 2.7 shows the finger model used for the simulation of this study. In this sub-subsection, the Marc and Marc Mentat was used for the analysis solver and the model builder. Because our focus was to determine the tendency of the spatial distribution

30

of the SED, the developed FE model of this study had a simple 2-D rectangular shape (More realistic model was analyzed in Part Ⅲ). The absolute value of the SED that was obtained was therefore not precisely that of an actual finger. The largest mesh size was 2.0 mm^2, which was used around the top of the finger model. The smallest was 10.0 μm^2 and was used around the bottom of the model. The height of the model (the average distance from the surface of the human skin to the peripheral bone) was 8.0 mm, and the width was 51.2 mm. These dimensions were large enough to make the sides free from the boundary effects. The first layer of the model (0.0-0.05 mm deep) represented the horny layer; the second layer (0.05-0.3 mm) represented the epidermis; the third layer (0.3-0.6 mm) represented the dermis; and the last layer (0.6-8.0 mm) represented the subcutis. Table 1 lists the parameters of the finger model, namely, the Young—s modulus, Poisson—s ratio, and density of each layer, which were obtained from the work of Maeno et al.[33].

There were two rigid surfaces at the bottom of the contacting finger model, as shown in Fig. 2.7. The left side was the stationary surface and the right side was the vibrating surface. Both surfaces were in frictional contact with the finger model and the skin was able to peel off from them. The top of the finger model, which represented the bone inside the finger, was fixed by zero displacement.

Static Analysis

Static analyses were carried out to determine the spatial distributions of the SED under the ES and non-ES conditions. The gap was varied to observe the variation of the SED with it. If ES phenomenon is a linear phenomenon, the input vibration frequency will not change inside the skin of the finger, and the skin will move with the same frequency (assuming the skin behavior is linear for sufficiently low frequencies and small amplitudes). Hence, the detection threshold tendencies during the psychophysical experiment can be explained by comparing the SED peaks. During the static analyses, we expected stress concentrations at the edges under the ES conditions to result in a significant increase in the SED peak. In other words, the SED peak was not expected to decrease when the gap was increased, as was observed during the psychophysical experiment.

The vibratory surface was moved by a fixed displacement of 10.0 μm, was determined from the experimental results to correspond to the average detection threshold for a vibratory stimulus of 30 Hz. The top of the finger model also moved down by a fixed displacement of 2 mm which represents an indentation force. First, under the ES con-

Table. 2.3: Parameters of finger model

Depth from Surface [mm]	Young's Modulus [MPa]	Poisson's Ratio -	Density [kg/mm ^{3}]
0.0-0.05	0.680	0.48	1.1e-6
0.05-0.3	0.136	0.48	1.1e-6
0.3-0.6	0.085	0.48	1.1e-6
0.6-8.0	0.034	0.48	9.6e-7

ditions, one surface was raised by 10.0 μm, and the spatial distribution of the SED was investigated. Additionally, under the non-ES conditions, the bottom of the finger model was used to touch and raise one flat vibrating surface of width 60 mm by 10.0 μm, and the SED distribution was investigated.

Secondly, the gap was sequentially set to 0.1, 1.0, and 3.0 mm under the ES condition, and the SED distributions and SED peaks were similarly analyzed.

Dynamic Analysis

Dynamic analysis was conducted to observe skin deformations that could not be observed by the static analysis, such as the impact effects of the skin on the surfaces and skin resonance and so on. We considered not only the SED peak, but also the SED frequency. If ES phenomenon is a nonlinear, the deformation frequency of the skin could be changed compared to the input frequency. In this analysis, we expected the frequency of the skin deformation to rise under the ES conditions, and/or the absolute value of the SED to alternately rise and fall as the gap was increased. This would make the variation the same as that of the psychophysical experiment.

The vibrating surface was vibrated at a frequency of 30 Hz and amplitude of 10.0 μm. The top of the finger model also moved down by a fixed displacement of 2 mm which represents an indentation force. The gap was then sequentially set to 0.1, 1.0, and 3.0 mm, and the variations of the SED were observed. Increments of 500 were used and the total analysis time was 0.5 s.

2.3.1.3   Results
Static Analysis

Fig. 2.8 shows the spatial distribution of the SED inside the finger model. It should be noted that the initial SEDs (after application of the initial pressure) were different for
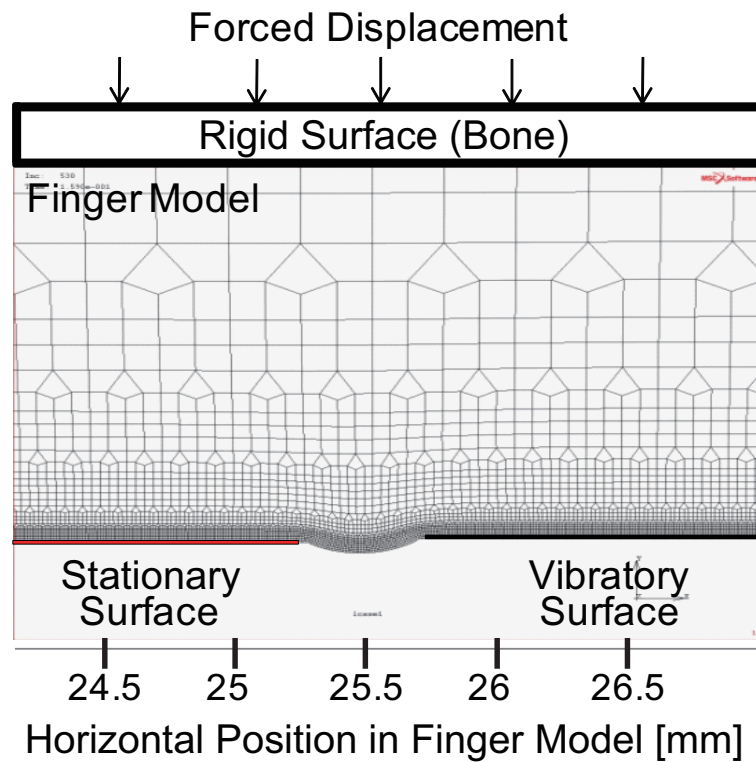
Fig. 2.7: Finger model for deformation analyses.

the different conditions (i.e. gap 3.0 mm had the maximum initial SED due to stress concentration at edge), and each initial SED was subtracted from those in the graphs. Therefore, the SEDs in the graph indicate the differences due to the displacement of the vibrating surface. There was an increase in the SED above the raised edge of the vibrating surface, and the significant differences between the SED peaks under the ES and non-ES conditions were observed. The sample points in the finger model layer were between 0 and 1.0 mm, where the FA I and SA I receptors were located. The SED peaks under all ES conditions were greater than those under the non-ES conditions, which did not contradict the results of the psychophysical experiment of section 2.2. The SED increased as the gap was increased, and a maximum value was observed for a gap of 3.0 mm. This observation contradicted the results of the psychophysical experiment against the gap parameters of section 2.2. Although we expected an increase of the gap to reduce the SED, the opposite was observed.

We have observed the generation of large SEDs at the gap's edge under the ES condition for the gaps of 0.1, 1.0, and 3.0mm which are larger than those of under the non-ES condition as we expected, however the effects of the gap under the ES conditions could not be explained by this static analysis.
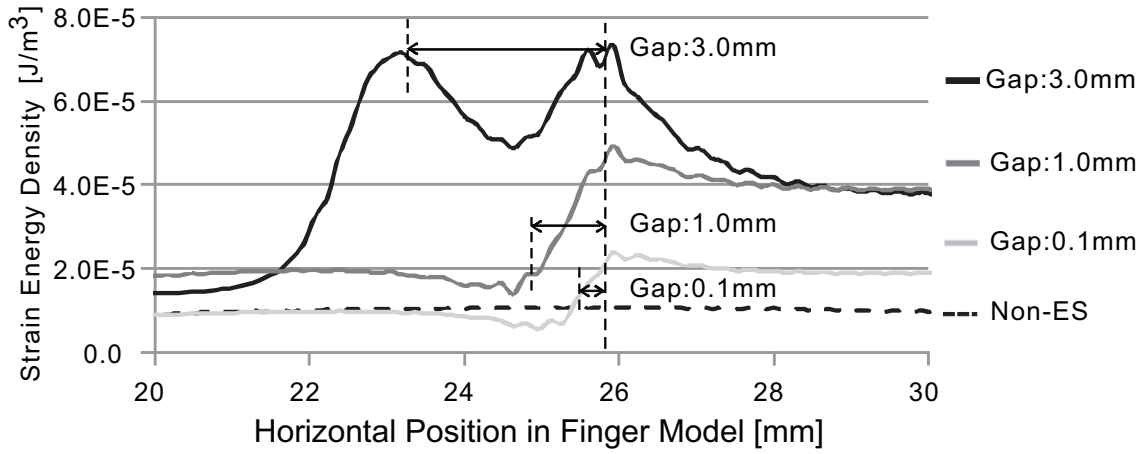
Fig. 2.8: Static analysis results. The gap was varied between 0.1 and 3.0 mm under the ES conditions (continuous lines). Data for non-ES conditions are added for comparison (dashed lines).

Dynamic Analysis

Fig. 2.9 shows the spatial SED distribution at some representative nodes inside the finger model under the ES conditions for gaps of 0.1 and 3.0 mm, and under the non-ES conditions in the time domain. It should be noted that each initial SED was subtracted from the SEDs in the graphs, as in the static analysis. The figures on the left respectively show the SED (solid lines) at points A, B, C, D, and E for a gap of 0.1 mm. The vibrator displacement (dashed lines) has been added for frequency reference. The figures on the right show the SED at points A, B, and C for a gap of 3.0 mm. The figure at the bottom right shows the SED at the center of the finger model under the non-ES conditions. Point A is at the edge of the stationary surface; point B is at the middle of the gap; point C is at the edge of the vibrating surface; point D is 10 mm to the left of point A; and point E is 10 mm to the right of point C. Give in Table. 2.4 are the SED peak values, the values of the maximum SED minus the minimum SED (SED amplitude), and the SED frequencies at the different points. For both gaps of 0.1 and 3.0 mm, the maximum SED peak and maximum SED amplitude occurred at the edge of the vibrating surface. This was due to the stress concentration inside the finger model at the edge of the vibrating surface. The maximum SED peaks and SED amplitudes under the ES conditions were greater than those under the non-ES conditions. This observation was the same as that of the static analysis.

Under both ES (gap 3.0 mm) and non-ES conditions, the SED curves for every sample point followed the vibrator displacement for a frequency of 30 Hz. In contrast, for a gap
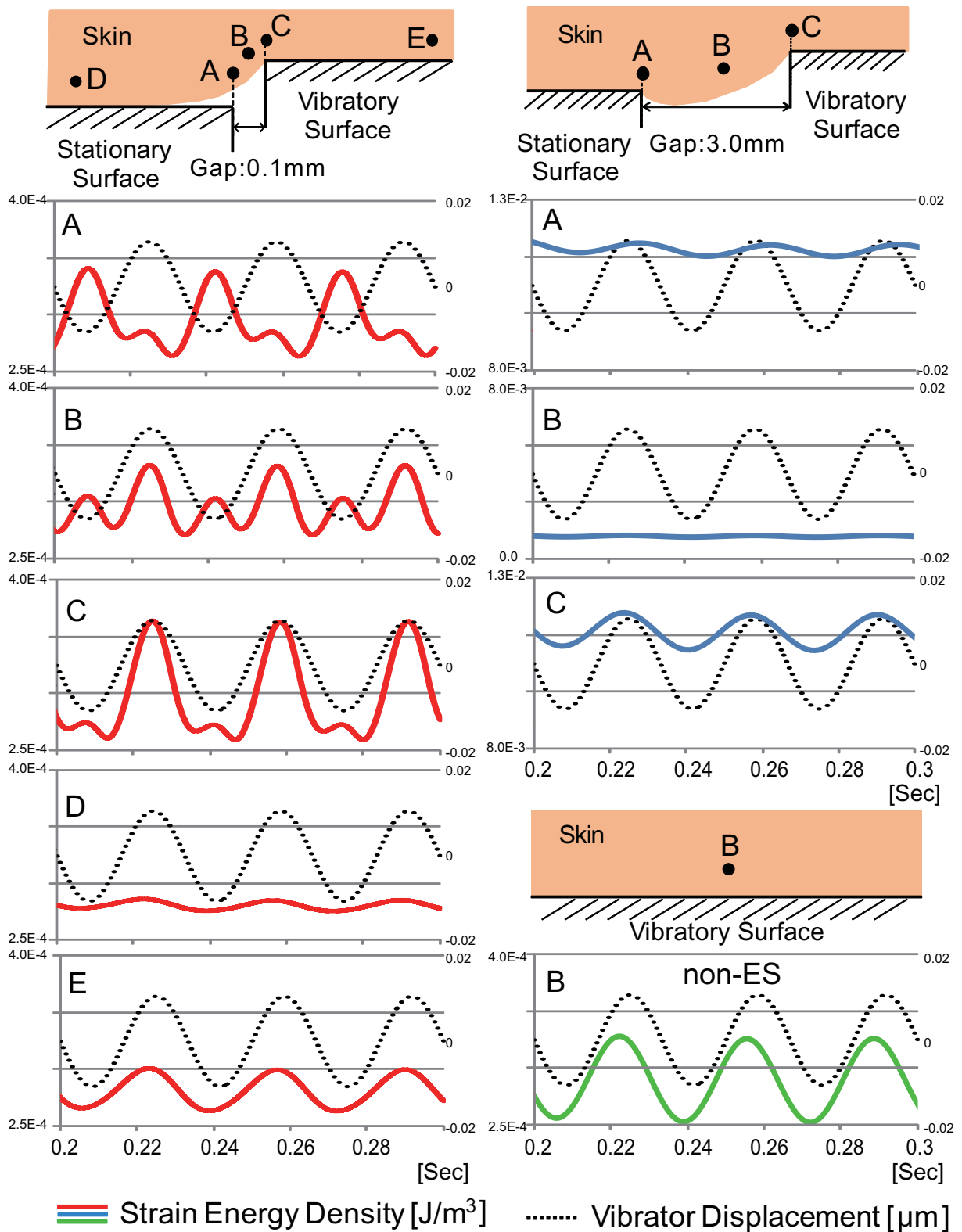
Fig. 2.9: Results of the dynamic analysis. The continuous lines represent the spatial distributions of the SED at the different points under the ES (gaps 0.1 and 3.0 mm) and non-ES conditions. The vibrator displacements (dashed lines) are added for frequency and phase reference.

Table. 2.4: Results of dynamic analysis

Position	A	B	C	D	E
SED peak Gap 0.1mm	3.42e-4	3.34e-4	**3.67e-4**	2.85e-4	3.03e-4
SED peak Gap 3.0mm	1.17e-2	1.26e-3	**1.20e-2**	-	-
SED peak non-ES	-	**3.13e-4**	-	-	-
SED amplitude (SED Max-Min) Gap 0.1mm	7.90e-5	6.37e-5	**2.08e-4**	9.46e-6	4.04e-5
SED amplitude (SED Max-Min) Gap 3.0mm	3.30e-4	7.24e-5	**1.04e-3**	-	-
SED amplitude (SED Max-Min) non-ES	-	**6.21e-5**	-	-	-
SED frequency Gap 0.1mm	non-Linear	non-Linear	non-Linear	Linear	Linear
SED frequency Gap 3.0mm	Linear	Linear	Linear	-	-
SED frequency non-ES	Linear	Linear	Linear	Linear	Linear

of 0.1 mm, the SED curves for points A, B, and C included nonlinear components when compared with the input frequency components. At A particularly, the SED phase change was opposite to the movement of the vibrating surface. Hence, the SED frequency at point B increased to almost 60 Hz.

Under conditions of 3.0 mm gap ES and non-ES, the SED curves moved along the vibrator displacement at 30 Hz in every sample point. In contrast, under condition of 0.1 mm at position A, B and C, SED curves included non-linear components compared to the input frequency component. Especially in position A, the SED was changing in opposite phase against the vibratory surface movement. Hence in position B, the SED frequency was increased (almost 60 Hz).

2.3.2   Discussion

2.3.2.1   Nonlinear Filtering Effect of the ES Structure

The static analysis showed that the ES conditions increased the SED peak and made it higher than that under the non-ES conditions. However, the variation of the vibrotactile sensitivity with the gap under the ES conditions cannot be used as an index of the SED peak. During the dynamic deformation analyses, the variation of the gap could not be explained by the behavior of the SED peak. Hence, we focused on the frequencies of the SED curves. Fig. 2.9 and table. 2.4 indicate a nonlinear variation of the SED at points A, B, and C under the ES conditions for a gap of 0.1 mm.

At skin, the contacted object's information transmitted before reaching to the cutaneous mechanoreceptors through several non-linear translations such as non-linearity of material, geometrical non-linearity and non-linearity of contact [95]. The behavior of nonlinear variation of the SED is mainly due to the non-linearity of the contact conditions between the skin and the stationary and vibrating surfaces. For example, Fig.2.10 shows the schismatic of non-linearity of time variant contact condition between the skin and an object. If the contacted surface vibrated in sinusoidal waves, the skin responds to the indented (pushing) direction while not for pulling. Then, the resultant skin deformation becomes half-wave, non-linear response due to this non-linearity of contact. This phenomenon is also reported in [34], they observed the mismatch between probe sinusoidal motion and skin motion.

Fig. 2.11 (a) is a schematic of the skin deformation and the contact conditions. On the left of Fig. 2.11 (a), the SED increased at the edge of the vibrating surface when it was raised, and at the contact boundary between the skin and the edge of the vibrating surface, as was observed during the static analysis. The same occurred on the right of Fig. 2.11 (a) when the vibrator was lowered; the contact of the skin with the stationary edge increased the SED. Owing to the coupling effect, the skin surface peeled off the vibrating surface when the gap was small. The forced sinusoidal displacement input of the vibrating surface was transformed into nonlinear strain of the skin owing to the variation of the contact in Fig. 2.11 (a) with time. The conditions of the mechanical structure of the ES can be considered as having a filtering effect that rectifies the half-wave at the edge of the stationary surface when the gap is sufficiently small. For such a small gap, the inputted sinusoidal stimulation is transformed into a half-wave at point A (see Fig. 2.11 (a)). The
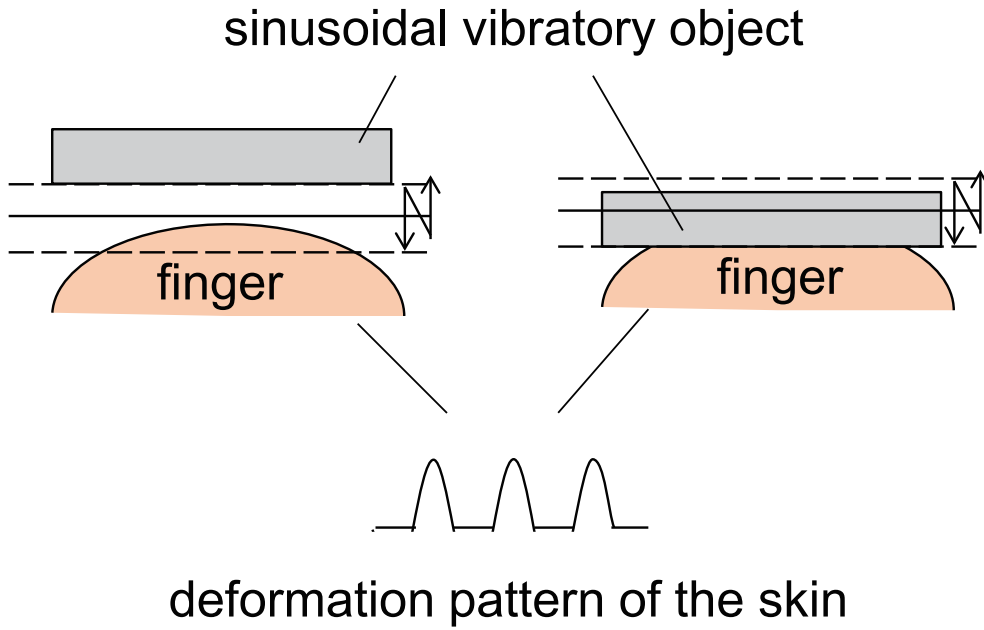
Fig. 2.10: Schematic of the non-linearity of contact between the skin and an object.
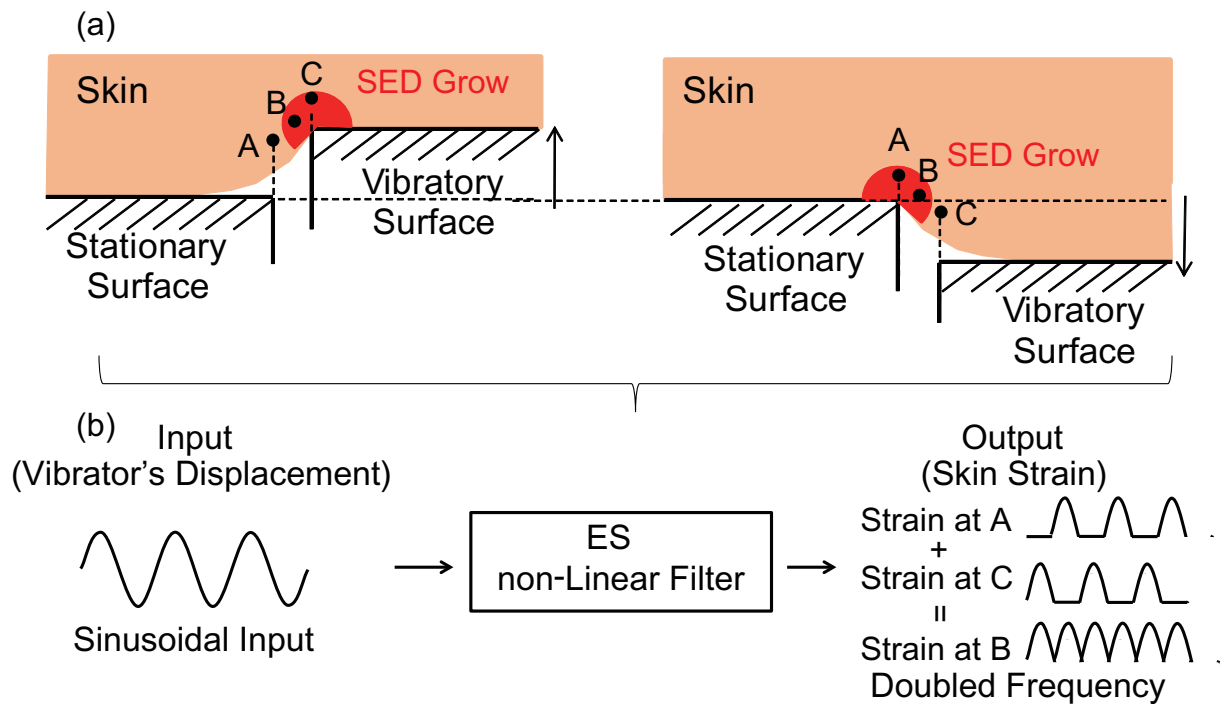
Fig. 2.11: (a) Schematic of the ES nonlinear filter. The sinusoidal input is transformed into a half-wave at points A and B, and a doubled frequency component of the skin strain is generated at points B. (b) ES nonlinear relationship between input stimulation and skin deformation.

outputted skin strain at point A is therefore described by the following equation:

$$input : x(t) = A\sin(2\pi ft) + B \tag{2.4}$$

$$output : \sigma_A(t)/E = \begin{cases} A\sin(2\pi ft + \pi) + B & y \geq B \\ B & y < B \end{cases} \tag{2.5}$$

where A is the amplitude [μm], f is the frequency [Hz], B is the initial forced displacement (offset) [μm], $\sigma(t)$ is the skin strain [N/m^2], and E is the Young's modulus [N/m^2]. Similarly, the skin strain at point C is described by the following equation:

$$\sigma_B(t)/E = \begin{cases} A\sin(2\pi ft) + B & y \geq B \\ B & y < B \end{cases} \tag{2.6}$$

Based on the results of the dynamic analyses, the behavior of the SED at point B can be explained by the linear combination of the half-waves at points A and C. When the gap is large, the nonlinear effect of the ES structure disappears. Fig. 2.11 (b) shows the flow chart of the nonlinear relationship between the displacement of the vibrating surface and the skin strain described above.

It should be noted that the SED is the square root of the strain that would double the frequency component. However, the spectral power density of the SED obtained by this mathematical procedure is small. For example, assuming a simple uniform elastic body, the strain energy (SE) is given by the following equation:

$$SE = \frac{1}{2}E\epsilon^2 \tag{2.7}$$

$$= \frac{1}{2}E(A\sin(\omega t) + B)^2 \tag{2.8}$$

$$= \frac{1}{2}E(2AB\sin(\omega t) - \frac{A^2\cos(2\omega t)}{2} + \frac{A^2}{2} + B^2) \tag{2.9}$$

$$\simeq \frac{1}{2}E(2AB\sin(\omega t) + B^2)(\because B \gg A) \tag{2.10}$$

where E is the Young's modulus [N/m^2], and ϵ is the strain [μm]. The offset B is much greater than the amplitude A, and the doubled frequency component 2ω can be assumed to be zero. For example in our analysis, amplitude A was 10 μm and initial offset B was 2 mm.

2.3.2.2 Frequency-rising Hypothesis

We assume that human may perceive higher frequencies under the ES Conditions. We focused on the frequency of the SED and assumed that the generation of a high-frequency SED at the gap increases the perceived frequency of a vibratory stimulus under the ES

conditions. We termed this as frequency-rising hypothesis. In general, with a combination of SA I, FA I, and FA II sensitivity, the resultant human sensitivity to vibratory stimuli increases with increasing amplitude and/or frequency of the vibration [28, 87]. If the perceived frequency is higher under the ES conditions, it might explain the reduction of the detection threshold. A comparison of the SED frequency at point B in Fig. 2.9 under the ES conditions for a gap of 0.1 mm with that at the same point under the non-ES conditions for a gap of 3.0 mm shows that the former is about twice the latter. If the frequency doubles from 30 Hz to 60 Hz, the detection thresholds fall to about one-third the original values as shown in Fig. 1.9 in chapter 1. This effect could reverse the SED peak tendency toward the gap distance which contradicted to the psychophysical experiments result.

2.3.3 Verification Tests

Two psychophysical experiments were conducted to verify the frequency-rising hypothesis.

2.3.3.1 Experiment 1: Verifying whether perceived frequency is actually higher under the ES conditions

This experiment was designed to verify the hypothesis that humans perceive higher vibration frequency under the ES conditions than under the non-ES conditions. We examined whether the increase in the SED frequency contributed to the perception of a higher frequency. In doing this, the subjects compared the frequencies perceived under the ES conditions with those under the non-ES conditions. We expected the subjects to report higher frequencies under the ES conditions.

Method

Fig. 2.12 shows the contactor conditions. Condition 1 corresponds to non-ES, and Condition 2 corresponds to ES. Each subject simultaneously assessed both conditions using the right index finger and the left index finger, and vice versa. Both vibrators were vibrating at 30 Hz and amplitudes were set to double of a previously determined detection threshold amplitude. The subjects were allowed to adjust the frequency of the non-ES vibrator so that they could perceive the same sensations under the ES and non-ES conditions. To accomplish the adjustment, the subjects first touched both contactors for 3 s. They then adjusted the frequency of Condition 1 (non-ES) by a jog dial of a function generator (NF Corporation, WF1973), which enabled a 0.01 Hz change. This process was
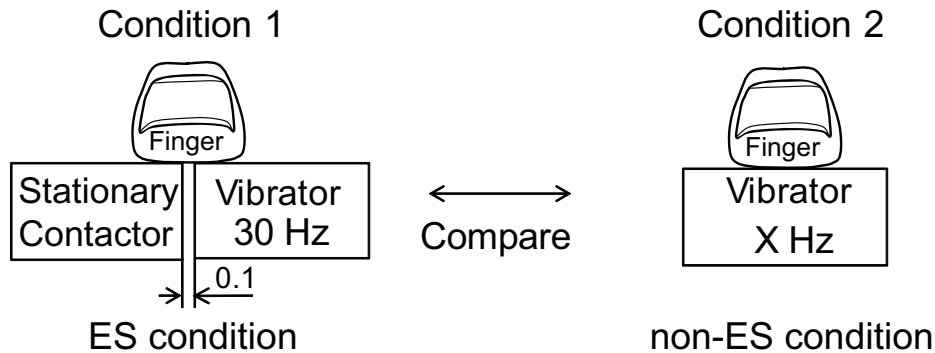
Fig. 2.12: Psychophysical experiment to investigate the perceived change in frequency under the ES conditions. The subjects compared the vibrotactile frequency sensations under the ES conditions (left) with those under the non-ES conditions (right).

repeated as many times as was necessary for the subject to satisfactorily complete the frequency adjustment. Each subject executed three trials and the mean frequency was calculated. It should be noted that humans can clearly perceive a frequency difference of 2 Hz in vibrations of about 30 Hz [35, 36, 37, 38].

Result

Fig. 2.13 shows the results of the perceived frequencies under the ES conditions for the seven subjects. As can be seen, all the subjects felt higher frequencies (average of 51.7 Hz) under the ES conditions. This showed that the high-frequency SED generated at the gap contributed to the perceived higher frequency of the vibration.

2.3.3.2 Experiment 2: Verifying whether threshold under the ES conditions is the same as that for doubled frequency under the non-ES conditions

Based on the results of Experiment 1, humans perceive almost twice the actual frequency under the ES conditions. In this experiment, we investigated and compared the detection threshold for a vibration of 60 Hz under the non-ES conditions and that for a vibration of 30 Hz under the ES conditions. We were interested in determining whether ES performance for a given frequency was the same or more effective than that of non-ES for twice as high frequency.
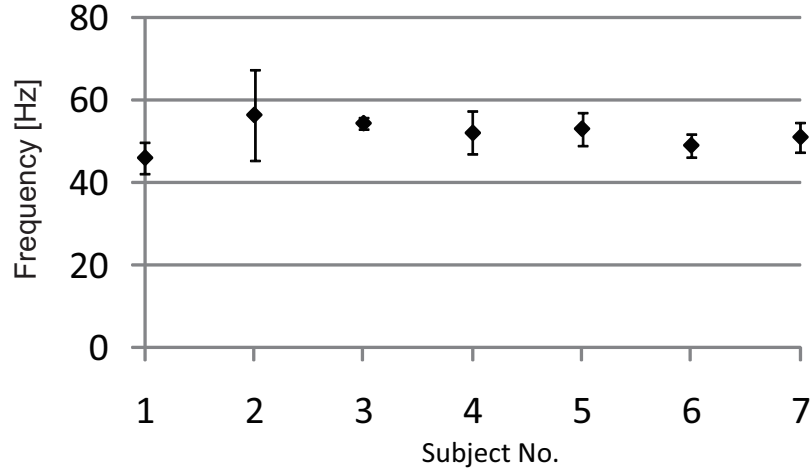
Fig. 2.13: Results of psychophysical experiment. Higher frequencies (average of 51.7 Hz) were perceived when a vibration of frequency 30 Hz was applied under the ES conditions.

Method

The experimental setup is shown in Fig.2.3. The mechanical setup was the same as previous experiment. The vibratory stimuli were generated using the following equation:

$$y(t) = A(sin(2\pi ft) + 1) \tag{2.11}$$

where $y(t)$ is the displacement of vibrators [μm], A is the amplitude [μm], and f is the frequency [Hz]. Detection thresholds were investigated with the same method in section 2.2. We used 60 Hz vibratory stimuli under the non-ES conditions and 30 Hz vibratory stimuli under the ES conditions. The six subjects were all right-handed males.

Results

Fig. 2.14 shows the detection threshold for each condition. The detection threshold for 30 Hz vibration under the ES conditions was lower than that for 60 Hz vibration under the non-ES conditions. As can be seen, the ES effect on the detection threshold was greater than that of simply doubling the frequency under the non-ES conditions.

2.3.3.3 Discussion

In experiment 1, under the ES conditions, the subjects perceived almost twice the actual frequency, which supported the frequency-rising hypothesis. In experiment 2, we doubled the frequency under the non-ES conditions to determine whether the effect would be the same as that of ES enhancement. The detection threshold was, however, still lower under the ES conditions. This suggests that ES enhancement has the combined effect of
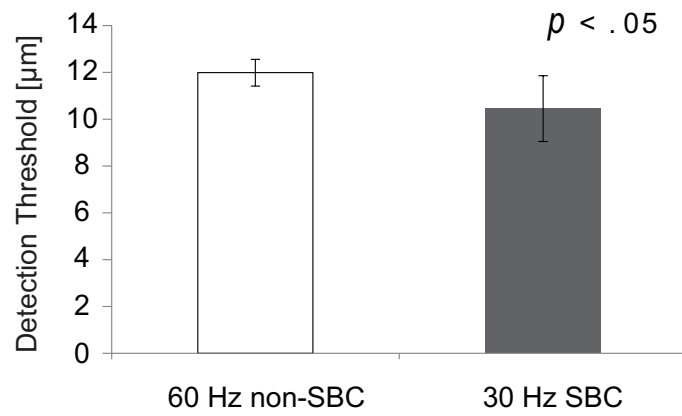
Fig. 2.14: Results of psychophysical experiment. ES enhancement was more effective than simply doubling the vibration frequency under the non-ES conditions.

increasing the perceived frequency and intensity of the stimulus by increasing both the SED frequency and the SED peak.

Chapter 3

Advanced Techniques of Edge Stimulation Method: Edge Stimulation Method Using Multi-vibrations

3.1 Performance of the ES method with multiple vibrations

When applying the ES method to the shape presentation on a vibrator-array type tactile device, it is essential for presenting supposed tactile sensations to consider the situation such like vibrators in close proximity vibrates simultaneously in different phases, amplitudes and frequencies. The phenomenon occurring behind the ES method with stationary surface described in chapter 2 will also happen in ES method with multiple vibrations; several analyses and psychophysical experiments verified this in the following sections. Especially in this section, we conduct several psychophysical tests to investigate the sharpness of tactile image by ES method with a view of applying ES device in chapter 5.

3.1.1 Determination of ES Characteristics as a Function of Several Parameters

3.1.1.1 Psychophysical Experiments

Three experiments were conducted in this section to examine the effects on detection thresholds for 'frequency', 'gap distance' and 'phase deviation' under the ES condition with two vibratory surfaces.
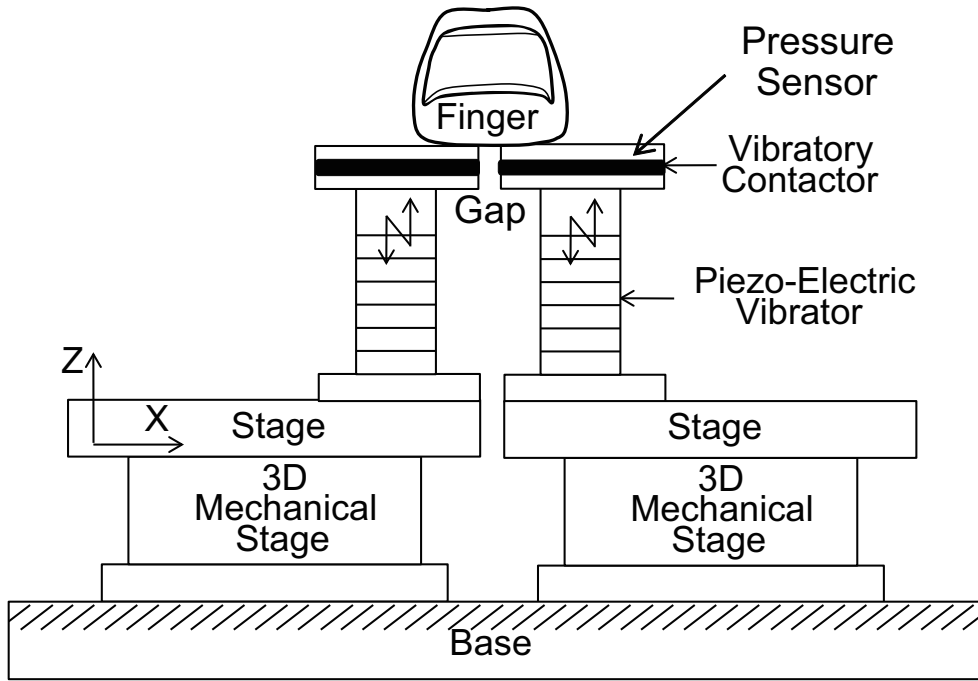
Fig. 3.1: Experimental setup. Two vibrators vibrate in opposite phases, and the gap between them can easily be changed by tuning the jog of the mechanical stage.

3.1.1.2 Apparatus

Fig. 3.1 shows the experimental setup. A mechanical stage with a precision of 0.1 mm and a rigid stage were located on a base with sufficient area and weight. Two sets of piezoelectric actuators, same ones as previous apparatus, were placed on these stages. Contactors with pressure sensors were located on the vibrators to regulate the size and shape of the contact area. By tuning the jog of the mechanical stage, the gap distance can be easily changed.

3.1.1.3 Methods

Vibratory Stimuli

Each vibrations are generated according to the following equation:

$$A : Y_A(t) = A\sin(2\pi ft) \tag{3.1}$$

$$B : Y_B(t) = A\sin(2\pi ft + \phi) \tag{3.2}$$

Here $Y_A(t), Y_B(t)$ are the displacement [μm], A is the amplitude [μm], f is the frequency [Hz] and ϕ is the phase deviation.

The digital signals were generated by Arduino Mega 2560, passed through 1st order

analog low-pass filter (RC parallel circuit, cut off 800 Hz), and were amped by amplifier same as previous experiment.

Experimental Procedures

Experiment 1: Detection Threshold as a Function of the Frequency

Firstly, the detection thresholds under the non-ES conditions were determined as a reference. One contactor was removed from the mechanical stage so that the subjects only touched the vibrating surface. To standardize the relative locations of the finger and the contactor surface, each subject was required to position the root of his/her nail on the edge of the contactor.

This experiment examined the conditions of frequencies, namely, 5, 10, 20, 30, 40, 50, 60, 70, 80, 90, 100, 150, and 200 Hz. While each subject was touching the vibrating contactor with his/her index finger and adjusting the indentation force to 1 N, the input voltage of the piezoelectric actuator was progressively increased by 1 V to vary the vibration amplitude between 0 μm and 85 μm. After each increase, the subject was asked whether he/she could perceive any vibratory stimulus. The threshold amplitude at which the subject first perceived vibration was recorded. The input voltage was then decreased in steps of 1 V from a well-defined source, and the threshold amplitude at which the subject could no longer perceive the vibratory stimulus was recorded. The detection threshold was thereafter calculated by the method of limits, which was used in previous studies[87]. The process was repeated 3 times for each frequency; i.e., a total of 36 times for each subject. Each step was repeated as many times as was necessary for the subject to satisfactorily judge his/her perception of the vibratory stimulus.

Secondly, the detection thresholds under the ES conditions were determined. Each subject simultaneously touched the vibratory contactors covering the gap between them, using one index finger to apply an indentation force of 1 N. The positioning of the finger was the same as in the first experiment, and the gap was set to 0.1 mm. 36 tests were performed for each subject as described above, and the detection threshold was similarly calculated for each frequency by the method of limits.

Experiment 2: Detection Threshold as a Function of the Phase Deviation of two vibrations

The detection thresholds for overlapped vibrations at each phase deviation were investigated by the method of limits. The subjects touch both vibratory contactors with an indentation force of 1 N. The phase deviation between the two vibrators is changed from

0 to π at 15° intervals divided into 12 trials and presented randomly. Note that the stimuli were presented as many times as the subject satisfactorily estimated the vibration presence. Each trial was repeated thrice and the detection thresholds were averaged for a total of 36 times for each individual. The eight subjects were all right-handed males of ages 21-25.

Experiment 3: Detection Threshold as a Function of the Gap Distance

Subjects touched both vibratory contactors with their first finger to cover the gap with an indentation force of 1 N. The detection threshold was then calculated by the method of limits. Under these conditions, the gap between the surfaces was increased by 0.5 mm for each trial. The gap distances used in this study were 0.01, 0.5, 1.0, 1.5, 2.0, 2.5, 3.0, 3.5, 4.0, 4.5, and 5.0 mm at 30 Hz. At 5 Hz, they were 0.01, 0.5, 1.0, 1.5, 2.0, and 2.5 mm, because vibrators were not able to provide sufficient amplitude for some subjects for the gap more than 2.5 mm. The vibration stimuli followed eqs. 1 and 2. The frequencies were set to 5 and 30 Hz. Note that the stimuli were presented as the number of times the subject satisfactorily judged the presence of vibrations. Each trial was repeated twice, and the detection thresholds for five individuals were averaged. The five subjects were all right-handed males aged 21-28 years.

For all experiments, subjects wore headphones that played white noise and also wore an eye mask so that they would not perceive any environmental changes. None of the subjects had any known medical condition or disorders affecting their tactile sense.

3.1.1.4   Results
Experiment 1

Fig. 3.2 shows the average detection thresholds for each frequencies. Black line is non-ES condition and gray line is ES condition. As frequency got higher, detection thresholds became lower for each conditions. For frequency lower than 50 Hz, the detection threshold of ES condition was lower than that of non-ES condition. Detection thresholds for 60-200 Hz, there were no significant difference between two conditions. Therefore the ES method is effective for frequencies lower than 50 Hz.

Experiment 2

Figs. 3.3, 3.4 show the experimental results. When both the vibrators were vibrating at the same phase at 30 Hz, the detection threshold was almost the same as the detection
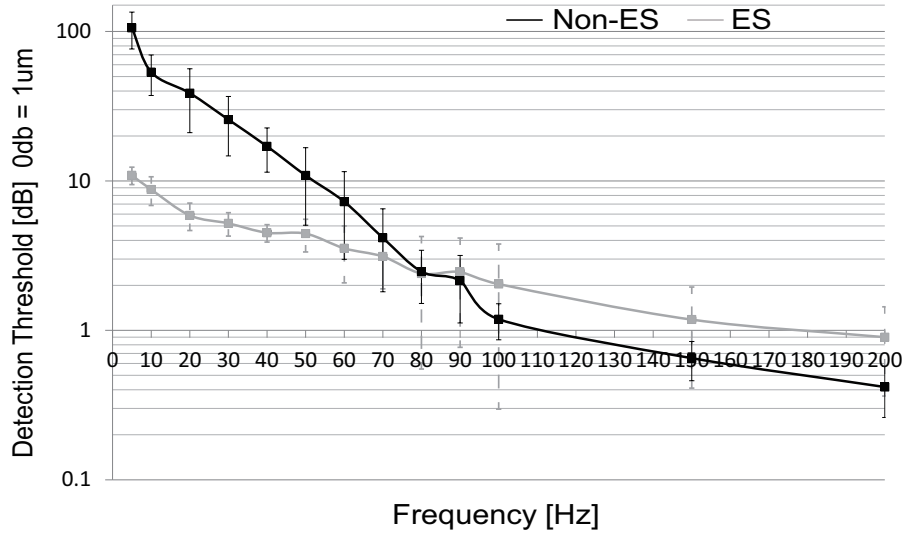
Fig. 3.2: Detection thresholds as a function of frequency. Black and gray line indicates the average detection thresholds for non-ES and ES condition respectively. Error bars indicate standard deviation.

threshold in Fig. 3.2 under the non-ES condition. At 5 Hz, the vibrators were not able to provide sufficient amplitudes for all subjects when both vibrators were in the same phase. Negative correlation was observed between the detection thresholds and phase deviation.

Experiment 3

Figs. 3.5, 3.6 show the experimental result. Smaller the gap distances decreases, the lower the detection threshold became. ES method was therefore effective when the gap distance was small for both frequencies. The feedback from the subjects indicated that the tactile sensation also differed at gaps of more than 3 mm at 30 Hz and 1 mm at 5 Hz: a sharp cutaneous sensation turned into a blunt shaking sensation.

3.1.2 Two Lines Discrimination

Two lines discrimination for ES line was examined in this experiment. This experiment is conducted to figure out how close the tactile lines by ES method can be placed without confusing them as a single line.

3.1.2.1 Method

Fig. 3.7 shows the experimental conditions of ES two lines and real two lines. Under condition of ES two lines, the central vibrator vibrates in opposite phase against the
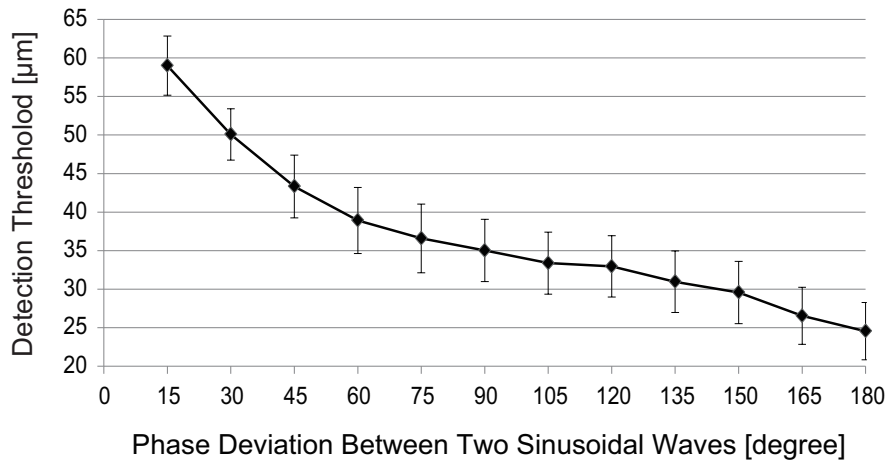
Fig. 3.3: Detection thresholds curve correspond to the phase deviation between two sinusoidal waves at 5 Hz. Error bars indicate standard deviation.
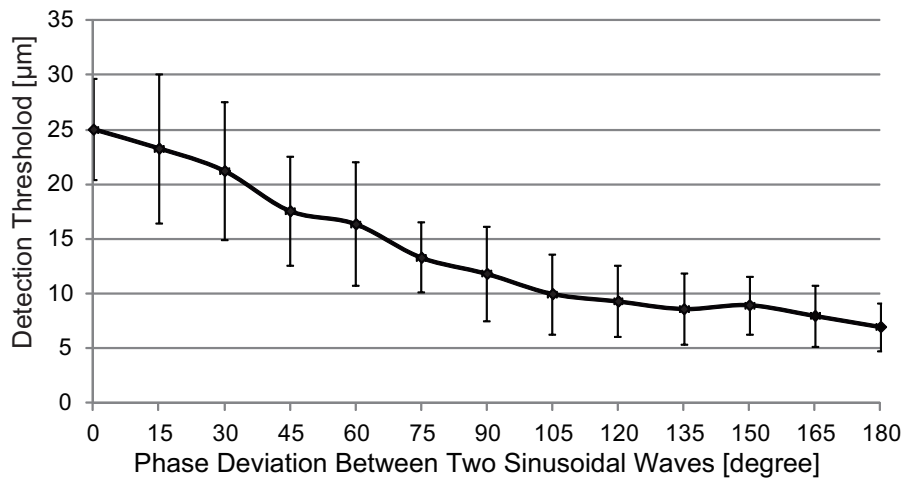
Fig. 3.4: Detection thresholds curve correspond to the phase deviation between two sinusoidal waves at 30 Hz. Error bars indicate standard deviation.
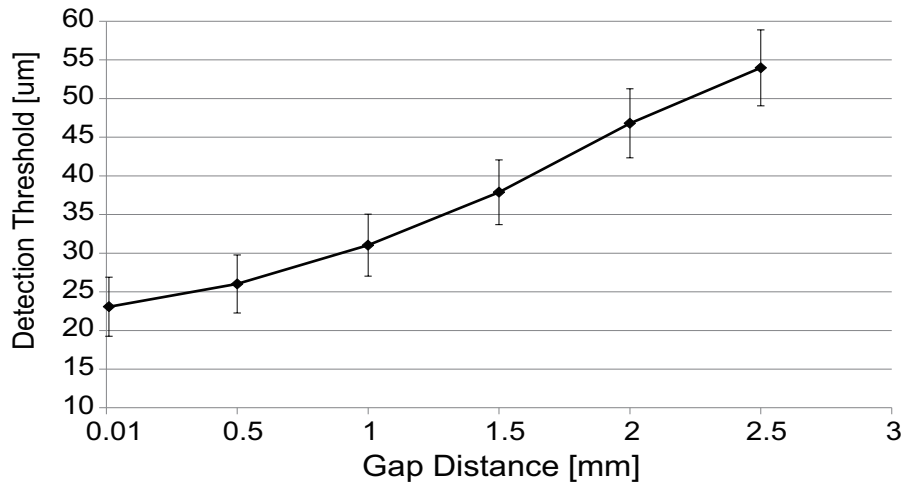
Fig. 3.5: Detection thresholds at each gap distance at 5 Hz. Error bars indicate standard deviation.
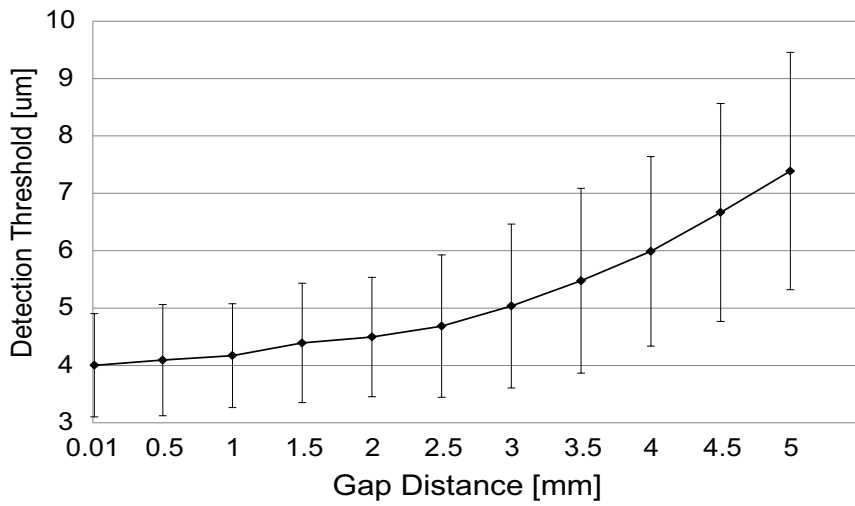
Fig. 3.6: Detection thresholds at each gap distance at 30 Hz. Error bars indicate standard deviation.
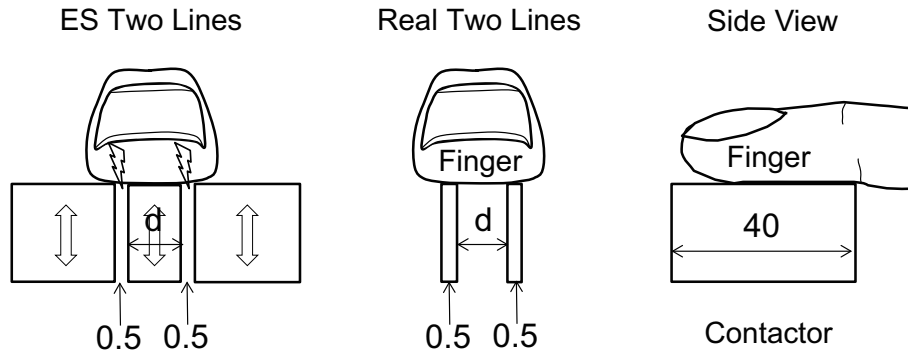
Fig. 3.7: Conditions of ES two lines (left) and real two lines (right). Contactor was large enough to cover a fingertip (Side View).

vibrator besides and two tactile line sensation were presented. Vibrotactile stimuli were the same as previous tests. The frequency was 30 Hz and the amplitude was set to 3 dB larger (5.8 μm) than detection threshold in Fig. 3.6 that is sufficiently perceivable. Eight subjects (all right-handed males age 21-24) wore eye mask and touch the ES lines with indentation force of 1 N. Experimenter guided to make sure that the index finger covers both ES lines. Then the subjects were asked to answer the perceived tactile lines were one or two. After this procedure, we changed the central vibrator's contactor size and repeated this procedure. At each trial, the gap distances were set to 0.5 mm by adjusting the mechanical stage jog. The contactor size in Fig. 3.7 "d" were 1, 2, 3, 4, and 5 mm and exchanged in random order. The real two lines discrimination was also conducted for the reference.

3.1.2.2 Result

Fig. 3.8 shows the average answer ratings and fitted curves (cumulative distribution function, right μ=3.78, σ=0.68. left μ=1.91, σ=0.87.). The 75 % discrimination distance for ES method was about 4.2 mm and for real lines it was about 2.5 mm. Participants reported that the ES lines were felt to be bold single line when the distance was small. The phantom sensation was not reported in this experiment.

3.1.3　Investigation on Width of Vibration Spread

This experiment is designed to verify how sharp the tactile sensation by ES method is by comparing tactile image widths under three conditions; a single pin vibrator, pin-array vibrator and flat vibrator. The tactile image width means the perceived spreading vibration area along the skin.
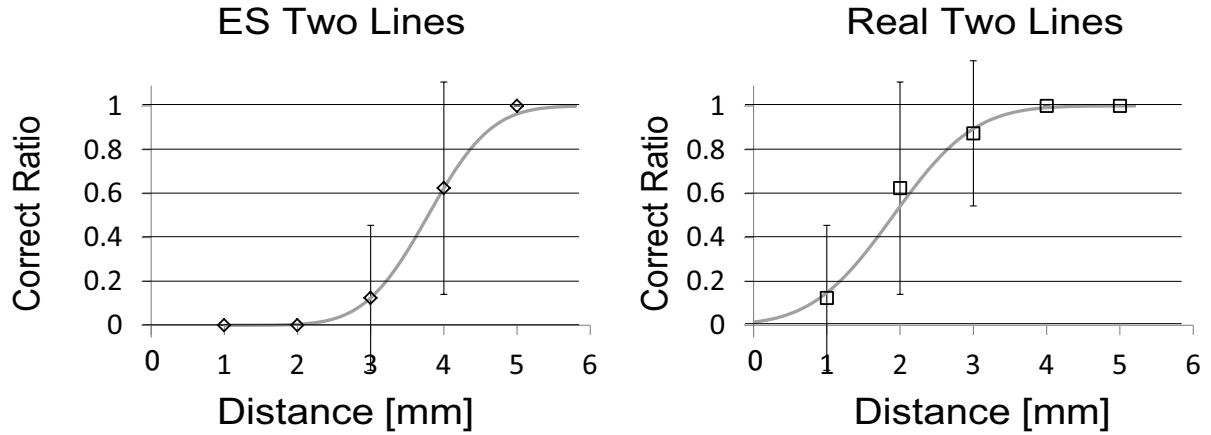
Fig. 3.8: Correct ratio of ES two line and real two line discrimination test. Error bars indicate standard deviation.

Table. 3.1: Conditions of vibrations

	1.ES	2.Pin	3.Pin-array	4.Non-ES
Equation	eq.1 & eq.2	eq.1	eq.1	eq.1
Frequency	30Hz	30Hz	30Hz	30Hz
Detection Threshold	$4.1\mu m$	$23\mu m$	$18.7\mu m$	$25.7\mu m$
Amplitude	$5.8\mu m$	$32.5\mu m$	$26.4\mu m$	$36.3\mu m$

(3 dB from detection threshold)

3.1.3.1   Apparatus Conditions

The experimental setup is identical to the previous experiment (Fig. 3.1). In particular, in this experiment, contactors were attached on the vibrators in order to change the vibration conditions, as shown in Fig. 3.9. Condition 1 is the ES method with 0.5 mm gap. Under condition 2, a pin-shaped contactor with a width of 0.5 mm were attached to one vibrator of the apparatus. Under condition 3, pin-shaped guides were placed besides the pin-shaped contactor of condition 2. Each pins' size were 0.5 mm and the gaps were set to 2 mm. This condition represented the general pin-array type tactile devices with a pins located in two point discrimination at finger tip (2 mm). Under condition 4, subjects touched the flat area of a single vibrator of condition 1. Contactors had a length of 10 mm (Fig. 3.9 side view).

3.1.3.2   Procedures and Tasks

Subjects touched the contactors under each condition with an indentation force of 1 N. The indentation force of this experiment was observed by electronic balance below the
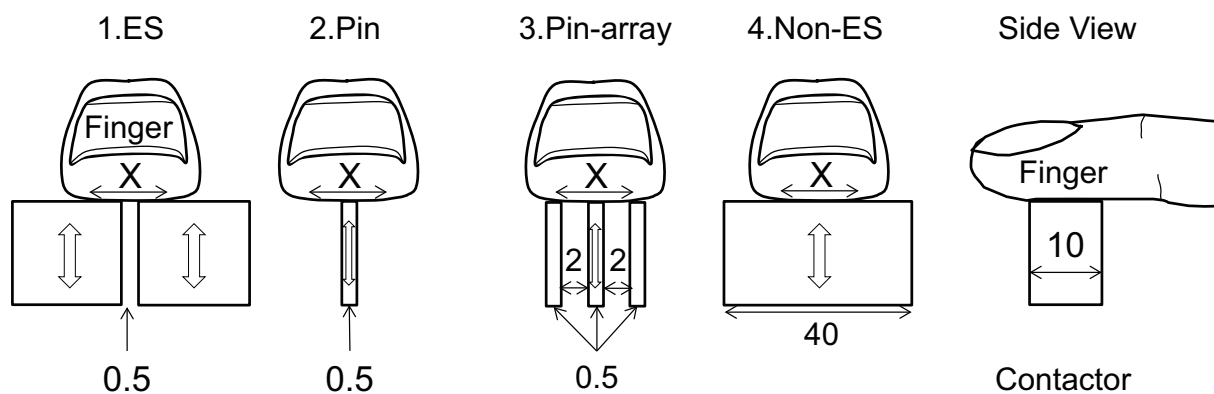
Fig. 3.9: Conditions of vibration presentation methods. Subjects answer the perceived tactile image width x. 1. ES method: Two vibratory surfaces vibrate in opposite phases with a gap of 0.5 mm. 2. Pin: A single 0.5 mm pin vibrator. 3. Pin-array: A single 0.5 mm pin vibrator with two static pins besides in 2 mm gap. 4. Non-ES: Flat vibrator with sufficient size to cover a finger.

apparatus. The forearm was fixed by using an armrest and subjects were only able to move the wrist and fingers. The stimuli conditions are shown in Table. 3.1. Amplitude was set to 3 dB larger than the detection thresholds of each condition. For conditions 1 and 4, the detection thresholds were taken from previous tests. For conditions 2 and 3, the detection thresholds were determined as an average of five subjects in preliminary experiment. After presenting the stimuli for 1 s, subjects were asked to answer the width of tactile images (Fig. 3.9 width: x mm) comparing to a length gage. The stimuli presentation was repeated as many times as the subjects were able to respond. The eleven subjects were all right-handed males of ages 21-28.

3.1.3.3 Result

The result is shown in Fig. 3.10. All subjects responded with significantly wider tactile images under condition 1 than under other conditions. There was no significant difference between conditions 2 and 3 ($p=0.14$). This result indicated that the ES methods produced significantly sharper tactile images than the other methods, though the tactile image (approximately 1-2 mm) was still wider than actual gap distance (0.5 mm); this may affect the two-line discrimination, which was larger than the real two lines condition.
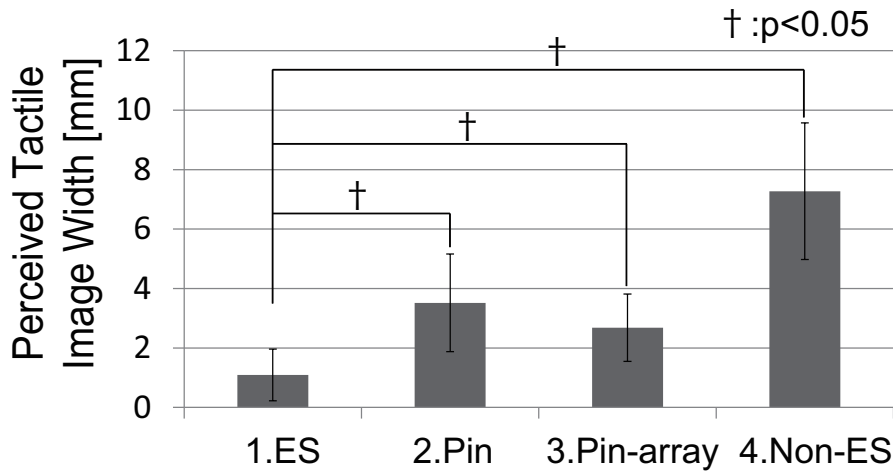
Fig. 3.10: Perceived tactile image width for each vibrotactile stimulation method.

3.2 Analysis on ES method with Multiple Vibrations

This section includes two topics to be investigated. Firstly, the mechanism why one feels sharper tactile sensation under ES condition than that produced by a single vibrator is investigated. Several analysis were conducted to observe the spatial distribution of the strain under ES condition inside a skin model. 1.the spread in width direction affects the tactile image extension and 2.the spread in height direction affects the types of mechanoreceptors. The spread in width direction contributes to the lateral extension of tactile image that results in blurriness of sensation. As for the latter, if the skin deformation reaches to the deep layer where the FA II exist, the tactile image gets blurred due to the wide receptive field.

Secondly, the parameters that change the effects of ES non-linear filtering effect is investigated. In section 2.3, we demonstrated under ES condition, not only the growth of SED absolute value by stress concentration at the edge but also increase in SED frequency by ES non-linear filtering effect. The existence of non-linearity of contact has already been implied, though positive application for a tactile stimulation have not been invented and the effects of arising high frequency deformation on tactile sensation has also not been clearly explained. For further understanding of this phenomenon, we conduct a serious of parameter studies with FE finger model viscosity of the skin and frequency of multiple vibrations.
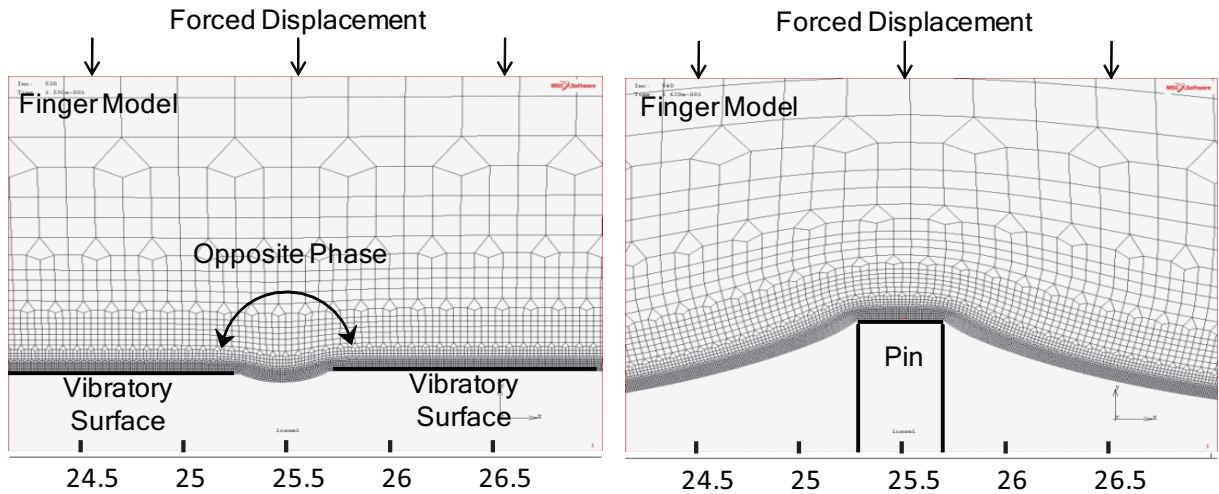
Fig. 3.11: Finger model and other mechanical conditions. (a) Left: Vibration overlap method (0.5 mm gap). (b)Right: Pin-shaped vibrator (0.5 mm diameter).

3.2.1 Investigation on the Spatial Distributions of Deformation Inside Finger Model

Investigation was conducted separately in two subsections, 1. Spread in width direction and 2. Spread in Height Direction.

1. Spread in Width Direction

In this subsection, we discuss the deformation analysis that we conducted on a finger model to observe the spatial distribution of the SED. By analyzing the spatial distribution of the SED and the spatial distribution of the frequencies of the SED, we investigated the effects of the mechanical structure and stimuli conditions on the tactile image width. The analysis solver was Marc Mentat.

3.2.1.1 Model and Method

Fig. 3.11 shows the finger model and vibrator conditions simulated in our study. The mechanical properties (layered structure, Young's modulus, Poisson's ratio and Density) and the sizes were identical to the previous analysis in section 2.3. In this study, we used vibratory stimuli of about 30 Hz, to which Meissner's disk is most sensitive. Since Meissner's disk exists in the boundary between the epidermis and the dermis, we observed the SED at a depth of 0.05 mm below the surface of the skin. There were two rigid surfaces of 30mm each under the contacting finger model as shown in Fig. 3.11 (a), both of which were vibratory surfaces with forced displacement. Both surfaces were in friction contact

Table. 3.2: Conditions of vibrations

	Condition 1 ES method	Condition 2 pin vibrator	Condition 3 ES method
Equation	eq. 3.1 & eq. 3.2	eq. 3.1	eq. 3.1 & eq. 3.2
Frequency	30 Hz	60 Hz	30 Hz
Amplitude	10 μm	10 μm	5 μ
—	same as condition 2	detection threshold level	

with the finger model and the former was able to peel off from the latter. The gap between the two surfaces was set to 0.5 mm, which was the same as in previous works that investigated the tactile image width. The pin vibrator, shown in Fig. 3.11 (b), had rigid rectangular surfaces and the narrow side was set to 0.5 mm. There was also a rigid surface on the top of the model, glued to the finger by a zero fixed displacement and representing the rigid bone of the finger. In the dynamic analysis, the vibratory surfaces moved according to the same sinusoidal equations in section 2.3.

Table. 3.2 shows the vibratory conditions used in this analysis. Condition 1 corresponds to the ES condition with the vibratory surfaces in opposite phase at 30 Hz. The amplitude was the same as that of the pin vibrator. Condition 2 corresponds to the pin vibrator with a frequency of 60 Hz. The amplitude was set to the detection threshold level of 10 μm. Condition 3 also corresponds to the ES condition but with the amplitude set to the detection threshold level of 5 μm. The analysis time was 0.5 s, with 10000 increments. The rigid bone moved down by 0.8 mm, which is equivalent to a 1 N pressure force. The rigid bone moved during the initial 0.1 s and the vibration started at 0.15 s. The analysis time was long enough for the stability of the dynamic analysis.

3.2.1.2 Result: Spatial Distributions of SED in Width Direction

Fig. 3.12 shows the spatial distributions of the SED at $\pi/2$ and $3\pi/2$. Under condition 1, the SED peaked in both cases at the edge of the vibratory surfaces. Under condition 2, the SED peaked at the edge of the pin corner at $\pi/2$; this was the highest absolute value of the SED and was due to the stress concentration at the edge. Compared SED peak to Condition 1, though amplitude is the same, the peak is three times larger. Although the absolute value of the SED under condition 3 was lower than that under condition 1, other spatial tendencies were almost the same in both cases.
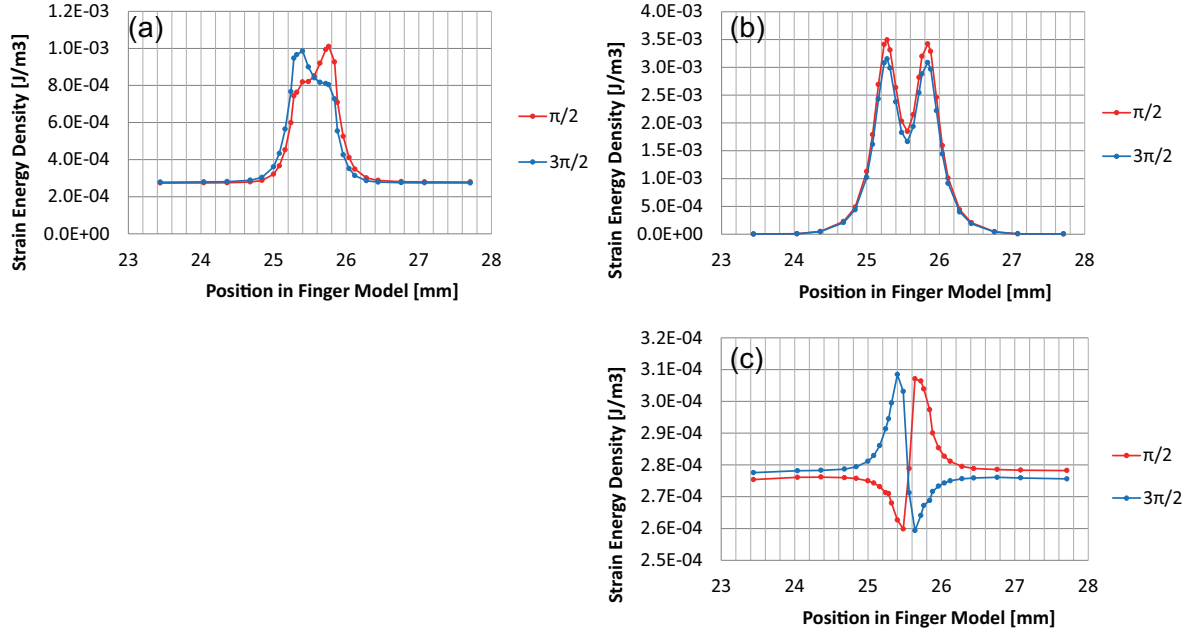
Fig. 3.12: Analysis results of spatial distributions of SED. (a). Condition 1. ES method (0.5 mm gap,10 μm). (b). Condition 2. Pin-shaped vibrator (0.5 mm diameter, 10 μm). (c). Condition 3. ES method (5 μm).

3.2.1.3   Estimation on Perceptual Area

According to the deformation analysis results, the absolute value of SED was highest under condition 2. However, the important information is the amplitude of the change in SED (difference between the maximum and minimum) rather than the absolute value of SED, because the deformation is caused by the vibration stimuli. Therefore, the SED amplitude was a better candidate for comparing the deformations caused by vibratory stimuli. Thus, we used the SED amplitude as an index to compare deformations. We calculated the SED amplitude by subtracting the maximum SED from the minimum SED selected from the direction of the time axis at every horizontal sample point. The results are shown in Figs. 3.13(a1), (b1) and (c1). Comparison of the curves of the SED amplitudes revealed that the pin condition had the widest base width, which means that the deformation of the vibratory stimuli spread. Under condition 1, the SED amplitude spread was still smaller than that in condition 2, which means that even the amplitude of the vibration was the same; the SED amplitude spatial distribution was localized significantly with the ES method. Under condition 3, the SED amplitude is more localized than any other conditions.

We also conducted the spectral analysis in order to investigate the frequency of deformation. We observed the frequency component of the change in SED at each sample
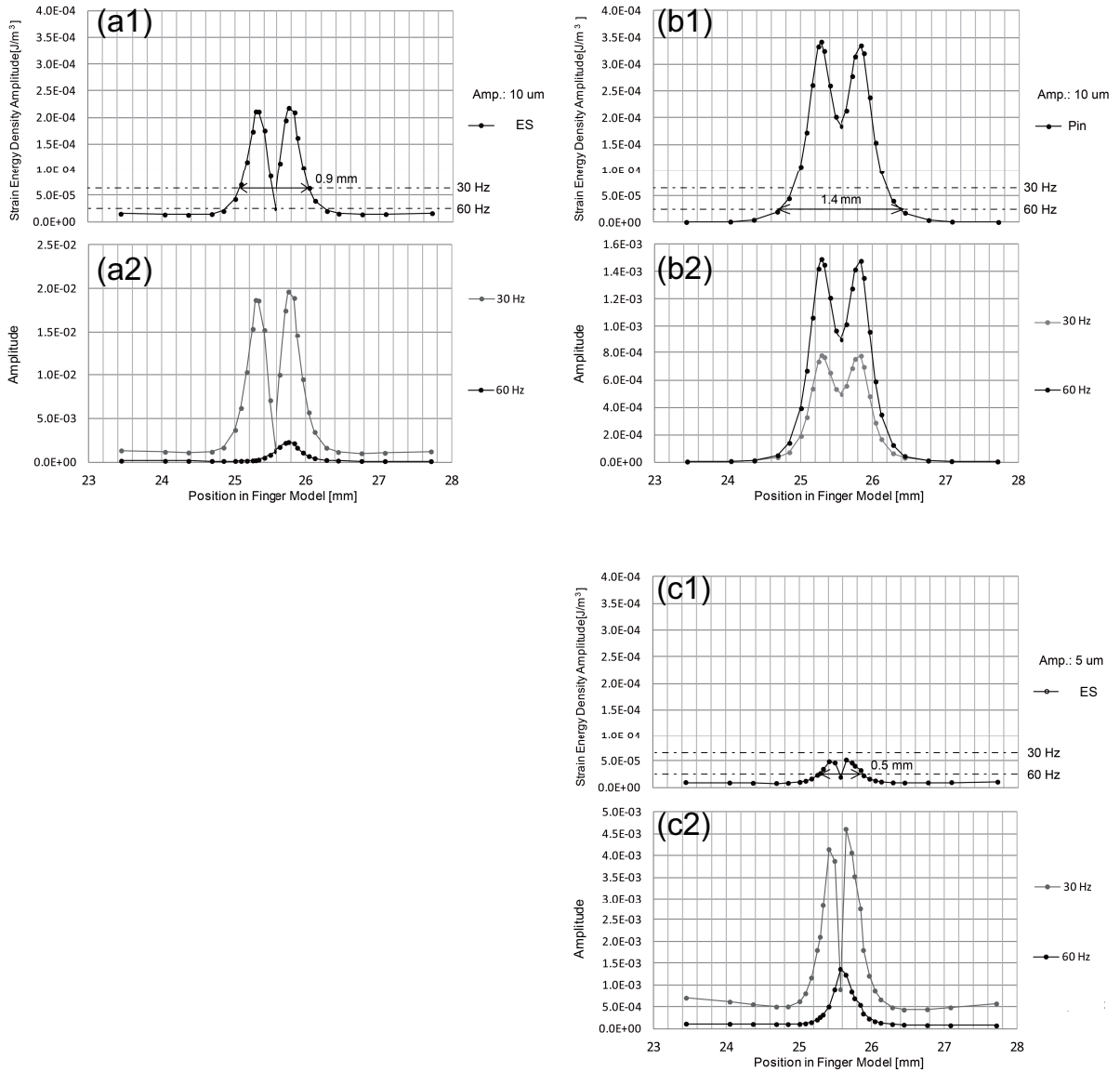
Fig. 3.13: Analysis results. (a1). Condition 1: Spatial distributions of SED amplitude. (a2). Condition 1: Spectral analysis result. (b1). Condition 2: Spatial distributions of SED amplitude. (b2). Condition 2: Spectral analysis result. (c1). Condition 3: Spatial distributions of SED amplitude. (c2). Condition 3: Spectral analysis result.

58
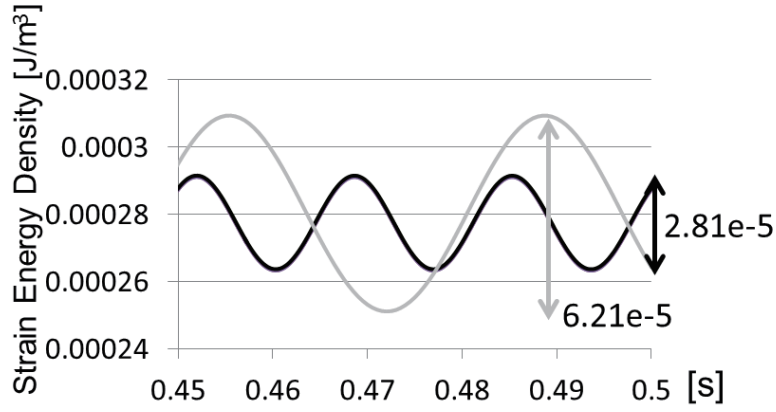
Fig. 3.14: SED Amplitude thresholds for a flat contactor at 30 Hz and 60 Hz. The threshold was 6.21×10^{-5} J/m^3 for 30 Hz and 2.81×10^{-5} J/m^3 for 60 Hz.

point. We categorized the frequency component into two parts: frequencies around linear components (30 Hz) of the stimuli and those at doubled frequency (60 Hz). Figs. 3.13 (a2), (b2) and (c2) show the spectral analysis results. Under condition 1, in almost every position, the linear component was dominant. At the very center of the gap, the amplitude of the doubled frequency component was almost the same as that of the linear component. This was due to the vibration overlap of the two opposite-phased vibrations, and evidence for the possibility of generating high frequencies using multiple vibrations in different phases. Under condition 2, the doubled frequency component was dominant at all positions since pin vibrator vibrates in 60 Hz and the shape of the curve is M-shape. Under condition 3, the amplitude of the doubled frequency component was typically more dominant than that of the linear component at the gap. Comparing the amplitudes of doubled frequency component of condition 2 and 3 in Figs. 3.13 (b2) and (c2), the shapes of spatial distribution of doubled frequency components are significantly localized under condition 3 which means, by overlapping small vibrations, the shape of the spatial distribution of doubled frequency can be typically shaped as a unimodal-shape and this distribution pattern cannot be achieved by a single pin-type vibrator. Pin vibrator with even detection threshold level vibration generates wider spatial distribution of the doubled frequency components than ES method.

Here, we discuss how we estimated the perceptual area and determined the tactile image width considering the analysis results. We determined the threshold of the SED amplitude for perception and compared it with the deformation analysis results.

In order to determine the SED amplitude threshold, we analyzed the basic mechanical

59

condition for presenting vibration stimuli: applying vibratory stimuli with a flat surface vibrator. In this analysis, an 80 mm rigid surface was brought in contact with the FE finger model and vibrated at 30 and 60 Hz. The rigid surface was large enough to cover the entire area of the bottom of the finger model for the entire analysis time. Vibratory stimuli were generated according to eq. 1. The amplitude was set to each detection threshold level: 30 μm for 30 Hz and 10 μm for 60 Hz. The other analysis conditions were the same as those of the previous analysis in this study. Fig. 3.14 shows the SED behavior average of each sample point for 30 and 60 Hz when the vibration of SED became stable. The SED amplitude threshold was $6.21e^{-5}$ J/m^3 for the 30 Hz vibration and $2.81e^{-5}$ J/m^3 for the 60 Hz vibration. These thresholds are drawn as dashed lines in Figs. 3.13(a1), (b1) and (c1). We then adopted amplitude thresholds (30 or 60 Hz) corresponding to which frequency component was dominant at each position in the model. The SED amplitude thresholds and SED amplitude for each condition were compared to estimate the tactile image width. Under condition 1, the SED amplitude was beyond the 30 Hz threshold, and the linear component was dominant in the spectral analysis result; thus, the tactile image width was 0.9 mm. Humans may perceive a 30 Hz vibration when the ES method is used with a large amplitude. Under condition 2, the SED amplitude was beyond the 60 Hz threshold, so the tactile image width was 1.4 mm, which is larger than that for the ES method with the same amplitude (10 μm). Under condition 3, the SED amplitude was smaller than the 30 Hz threshold; SED amplitudes beyond the 60 Hz threshold can be perceived. According to the spectral analysis, the doubled frequency component emerged at the gap, so the tactile image width was 0.5 mm. The tactile image was much smaller than that obtained using the pin vibrator. Human may perceive only the local doubled frequency vibration when using the ES method with an amplitude at the detection threshold level. The comparison of the 60 Hz component strain spatial distribution for each condition is shown in Fig. 3.15. Even 10 μm ES stimuli generates more localized strain spatial distribution.

Deformation analysis on a FE finger model to observe the SED spatial distribution revealed that the SED spread is more localized with the vibration overlap method than with the thin pole (0.5 mm diameter) pin vibrator even if the amplitudes are the same. When using ES method with the amplitude of the detection threshold level, the peak and width of the SED curve became significantly smaller than those obtained from pin-vibrator. Spectral analysis indicated that the high-frequency vibration is generated above the very center of the gap between vibrations in opposite phases. The spatial distribution
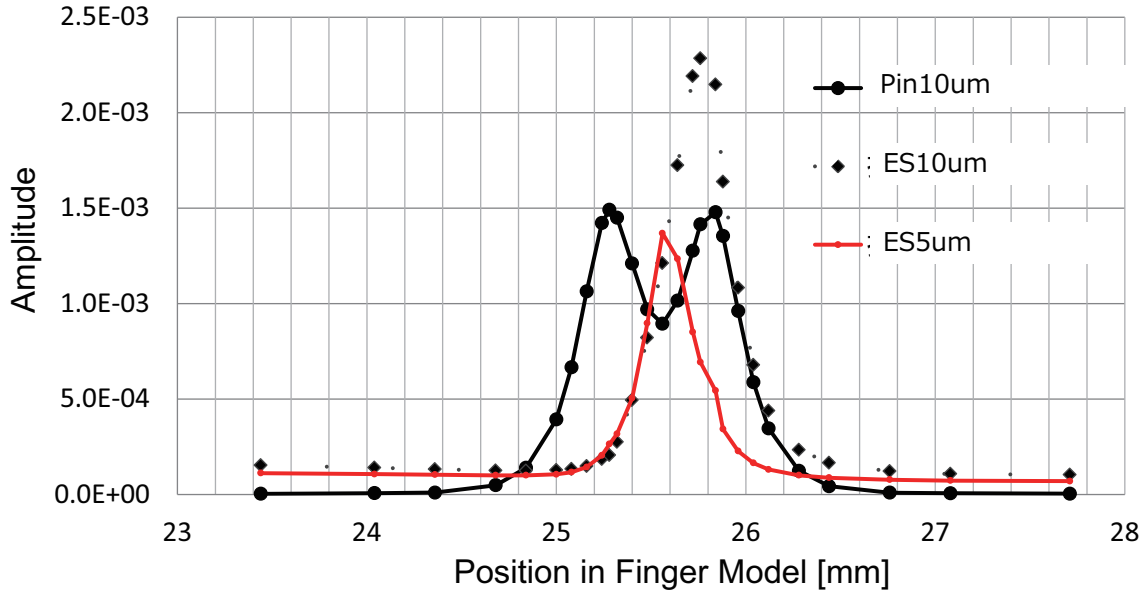
Fig. 3.15: The comparison of 60 Hz component strain spatial distribution between ES and pin-vibrator conditions.

of the high-frequency component was localized significantly using the ES method, and that localized unimodal-shape distribution pattern cannot be obtained by a single pin vibrator. The results of tactile image estimation suggested that with the ES method, human perceive tactile sensation only in a localized area that high-frequency component exists and the area is much smaller than one produced by a single pin-vibrator.

2. Spread in Height Direction

The SED spatial distributions especially for the height direction were analyzed. By comparing the SED of shallow layer and deep layer between ES and non-ES conditions, we investigate whether the ES method has the characteristic of selective stimulation for mechanoreceptors in shallow layer as described in Fig. 1.10 [14] in chapter 1. From this section, we have changed the FE analysis solver from Marc Mentat to Ansys Mechanical Workbench, and the FE models to be more realistic. Hence, we do not compare the absolute value of SED to previous FE analyze; we mention about qualitative tendencies.

3.2.1.4   Model and Method

Fig. 3.16 shows the finger model and vibrator conditions renewed in this study. The mechanical properties (layered structure, Young's modulus, Poisson's ratio and Density) and the sizes were identical to the previous analysis in section 2.3. In this study, we used vibratory stimuli of about 5 Hz. We observed shallow (1 mm from surface) and deep
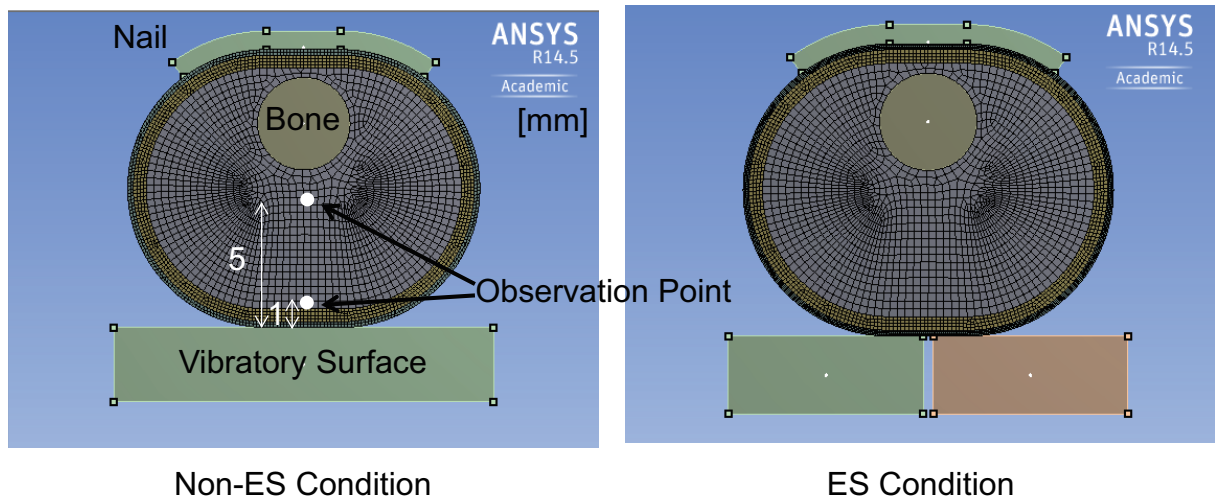
Fig. 3.16: Renewed FE models on ANSYS and their observation points of shallow (1 mm from surface) and deep (5 mm from surface) layer. Left. Non-ES condition. Right. ES condition.

(5 mm from surface) layer at the center of the models. Both surfaces were in friction contact with the finger model and the former was able to peel off from the latter. The vibratory surfaces moved according to the same sinusoidal equations in section 2.3. Other conditions were the same as previous analysis above.

3.2.1.5 Result: Spatial Distributions of SED in Height Direction

Fig. 3.17 shows the SED change for each non-ES and ES conditions. The SED peak emerges at the edge of the vibratory surfaces of the ES condition. Though the peak SED remains at the shallow layer in contrast to the SED distribution of the non-ES condition.

Fig. 3.18 shows the spectral of shallow layer and deep layer at observation points in Fig. 3.16.

At the very center of the model, doubled frequency 10 Hz was observed in ES conditions that did not contradict to the analysis above. The SED values in shallow layer were almost the same, while SED of ES condition for deep layer was much smaller, almost 1/4. Then, the stimuli of ES condition is effective for mechanoreceptors in shallow layer.

3.2.2 Effects on Several Mechanical Parameters for the Generation of Doubled Frequency

In this subsection, the effects of 1. viscosity of the model and 2. frequency on the generation of doubled frequency were investigated under ES condition.
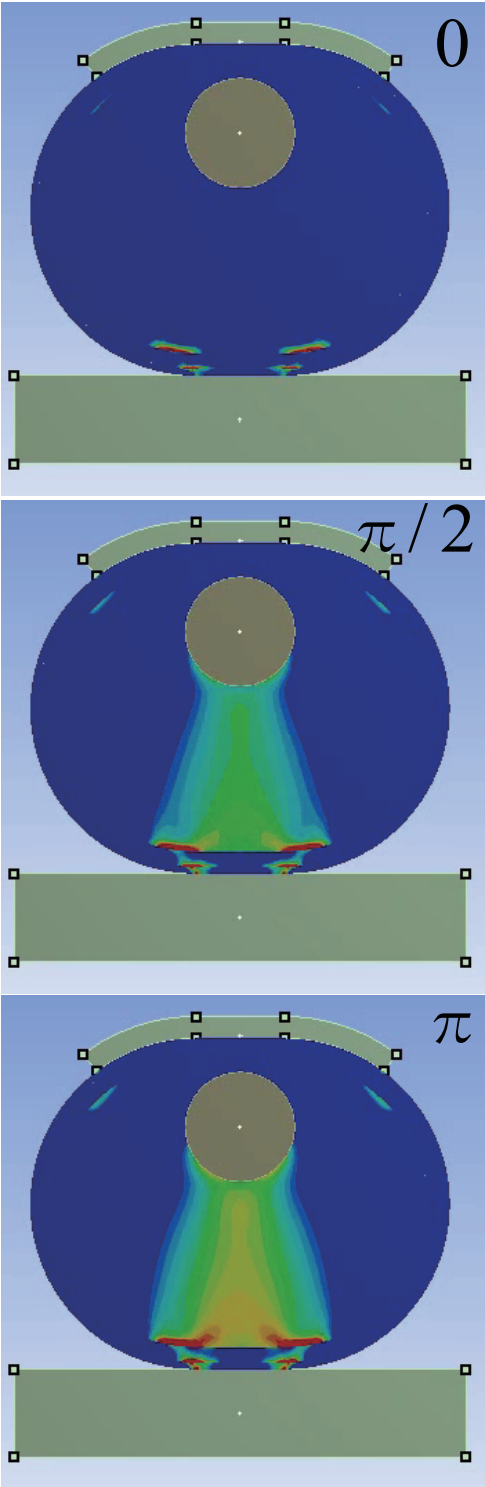
non-ES method   ES method
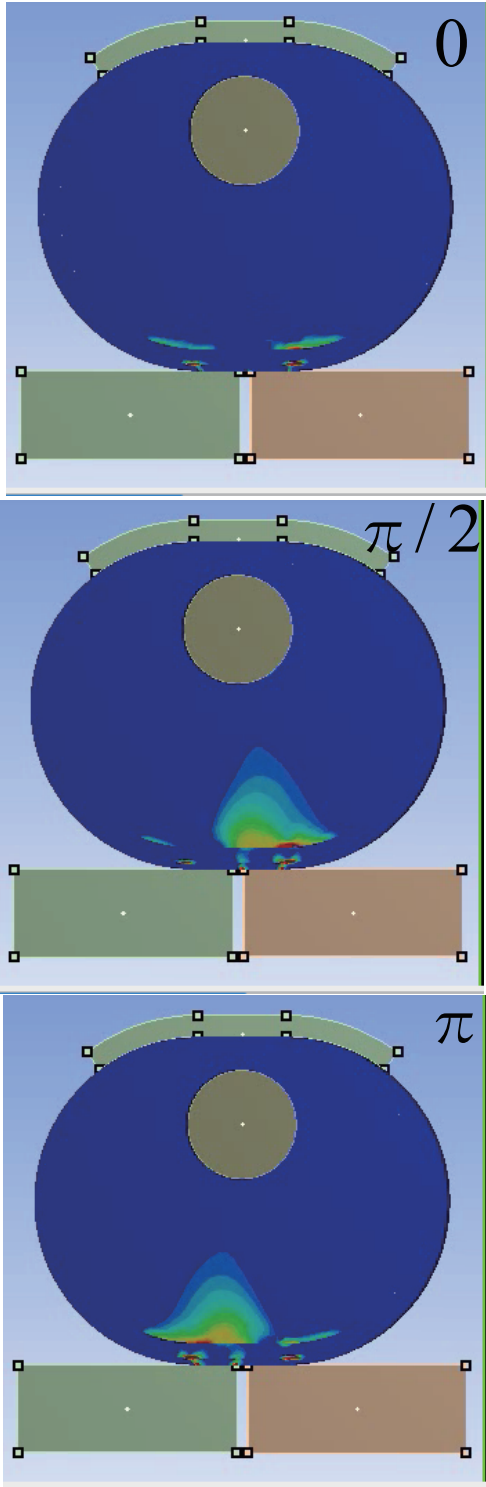
Fig. 3.17: The analysis results for SED distribution for height directions in time chart.
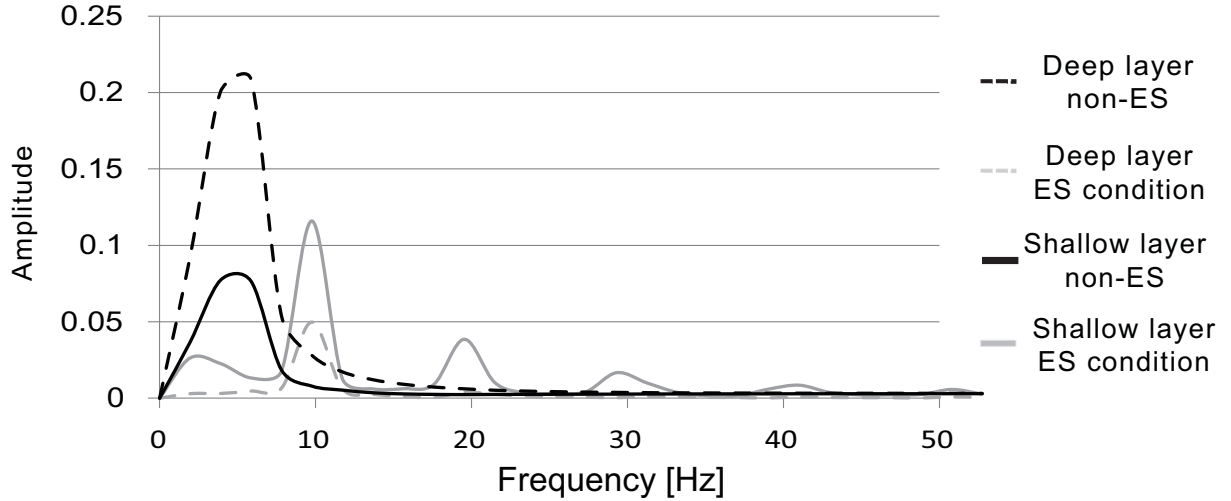
Fig. 3.18: The analysis results for SED distribution for height directions. Dashed lines show the deep layer results. Solid lines show the shallow layer results. Gray lines are ES condition and black lines are non-ES condition.

3.2.2.1   Model and Method

The FE model and analysis conditions are the same as previous analysis. β attenuation coefficient and frequency were varied while either of them were fixed. We changed β attenuation coefficient from 0.01, 0.02 and 0.04 (0.02 is referred from [33]) and frequency was 5 Hz. Frequency was varied for 5, 30 and 300 Hz and β attenuation coefficient was 0.02.

3.2.2.2   Result

Fig. 3.19 shows the spectral amplitude of SED for three viscosity conditions. When the viscosity increased, the doubled frequency component became small. Fig. 3.20 shows the spectral amplitude of SED for three indention conditions. When the frequency increased, the doubled frequency component became small.

3.2.2.3   Discussion

We have found out that the increase of either viscosity or frequency decreases the power of doubled frequency. These parameters may affect the non-linear filtering effect of ES method which suggested in section 2.3. Fig. 3.21 shows the schematic of the parameter effect on doubled frequency. Even if the input frequency is doubled at the center of the gap, the viscoelasticity of the skin low-passed it and the skin's doubled frequency component becomes small. When the vibrator rises, the skin follows the input displacement. When the vibrator goes down, the skin starts free fall. If the skin's time constant is

64
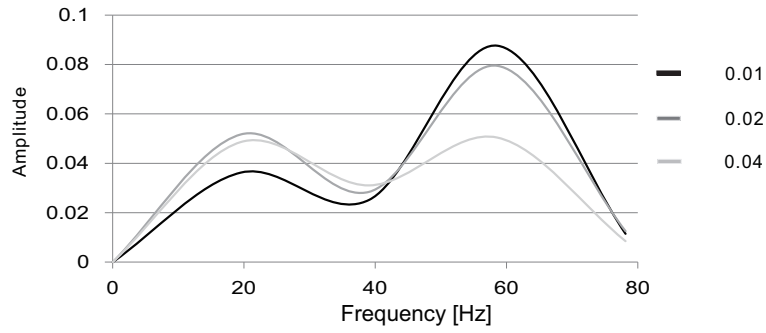
Fig. 3.19: The analysis results. SED spectral of three viscosity conditions.
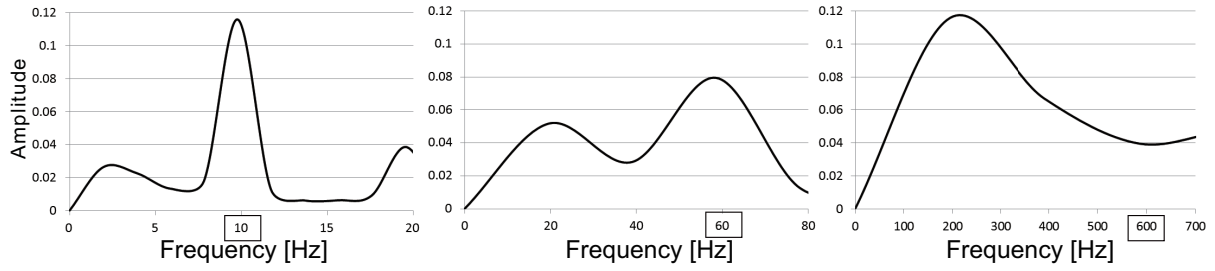
Fig. 3.20: The analysis results. SED spectral of three frequency conditions.

small, the skin follows the vibrator going down, while the skin peels off from the vibrator if the time constant is large; this is the main effect for viscosity. If the input frequency increases, the skin has less time to free fall and the doubled frequency amplitude becomes small which is the same phenomenon as contact envelope detection; this is the main effect for frequency.

65
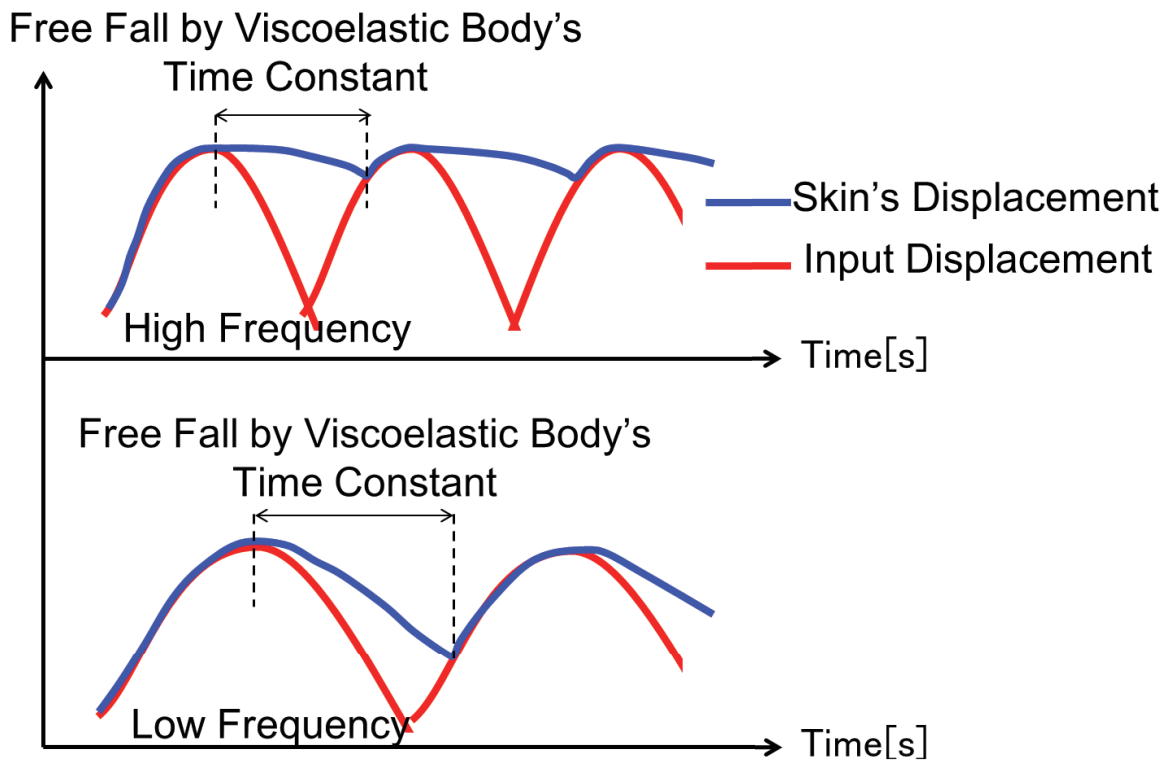
Fig. 3.21: The schematic of the parameter effect on doubled frequency. The input displacement is low-passed through the contact non-linearity under ES method.

Chapter 4

Verification on Doubled Frequency

4.1 Measurement on ES method Using Finger Sensor

In this chapter, to verify the generation of the high frequency strain, we develop two sensors embedding strain gages spatially distributed. The first sensor was a prototype skin model sensor which has a simple rectangular layer structure. The purpose for the first skin model sensor was to examine whether we could observe doubled frequency with the urethane resin and strain sensors. This skin model sensor has horizontally distributed strain gages. The second sensor has a finger model structure and has vertically distributed strain gages. We modified the development method for this finger model sensor; we customized the urethane resin mold and sensor embedding method, which made the sensor fabricated more precise.

A measuring system was developed representing ES condition using two independent vibratory surfaces. We measure the spatio-temporal strain behavior inside the skin under ES condition using these skin sensors. Also 3D finite element deformation analysis is conducted to observe the detail skin deformation and the changes of skin-surface boundary conditions around the gap.

4.1.1 Skin Model Sensor

A skin sensor needs to have soft tissue layer structure and capable for measuring the spatio-temporal distribution of skin strain. Our skin sensor consists of three layers; the first layer represents epidermis/dermis (0.0-1.0 mm deep), the second layer represents subcutis (1.0-8.0 mm), and the last layer (8.0-12.0 mm) represented the bone. The first layer was created by urethane resin (Exseal Hitohada gel) which was elastic modulus of 5.2 kgf/cm ^{2} and the second layer was 1.2 kgf/cm ^{2}. The last layer was rigid acrylic
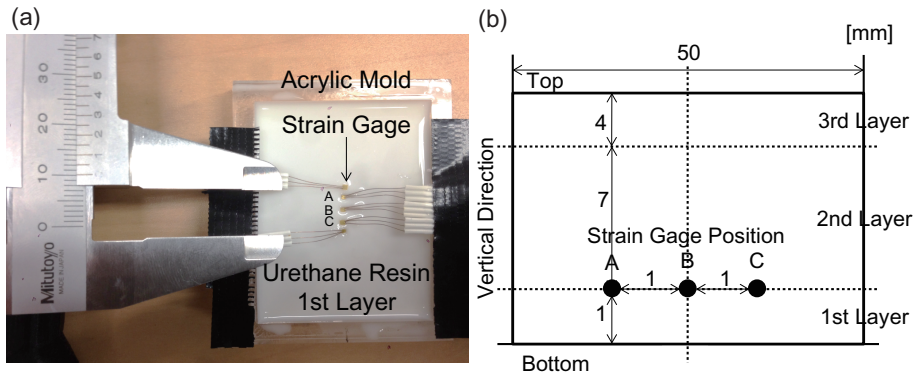
Fig. 4.1: Skin sensor. (a). Horizontal location of strain gages. (b). Cross section sketch of the skin sensor.

plate representing a bone. The structure, the material properties and the method of the construction of the sensor were referenced from Maeno's study that analyzed the spatial distribution inside a finger sliding on a plate [33]. Fig. 4.1 (a), (b) shows the horizontal and vertical location of the strain gages. Five strain gages were embedded between the first and the second layers where the FA I and SA I receptors exist. The gages were attached on the membrane of the first layer and measured the spatial distribution of skin strain in 1.0 mm resolution. The output signals of the sensor were amped by an amplifier (San.ei STRAIN AMPLIFIER 6M82).

4.1.2   Measurement

The objective of this measurement is to observe the spatio-temporal behavior of strain inside the skin. We expect high frequency component of strain, the non-linear frequency component, is observed at the gap.

4.1.2.1   Experimental Setup

Fig. 4.2 (a), (b)shows the experimental setup. A mechanical stage with a precision of 0.1 mm and a rigid stage were located on a base with sufficient area and weight. Two piezoelectric actuators (TOKIN, AHB850C851FPOL-1F) were placed on these stages. These vibrators can provide amplitudes of more than 85 μ m, and the response frequency is greater than 400 Hz. By tuning a jog of the mechanical stage, the gap distance and the height can be easily changed. Then skin sensor was placed on the center of two vibrators' contactors with 100 g weight representing 1 N indentation force.
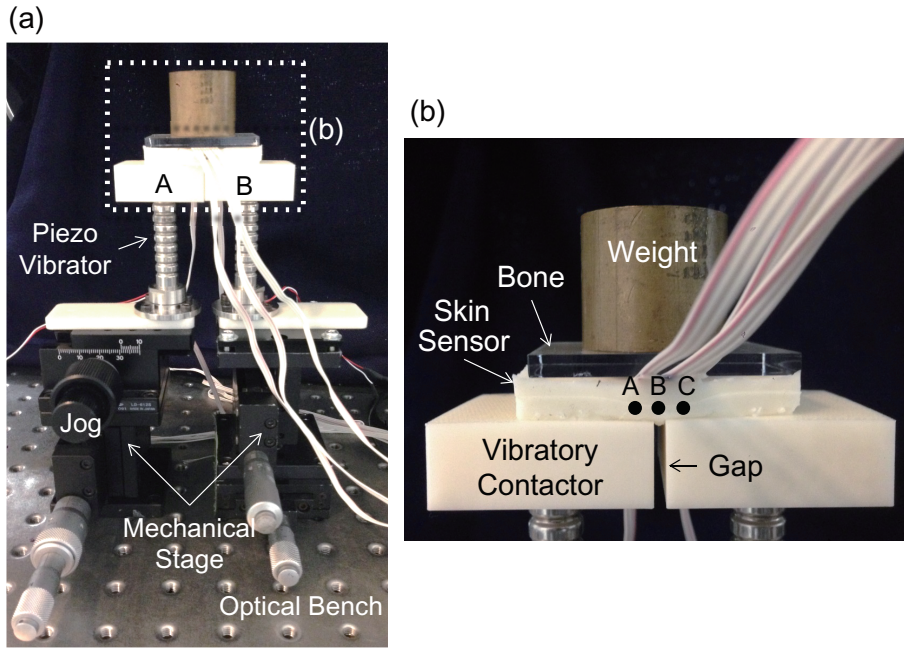
Fig. 4.2: Skin model sensor. (a). Whole experimental system. (b). Conditions around the skin sensor.
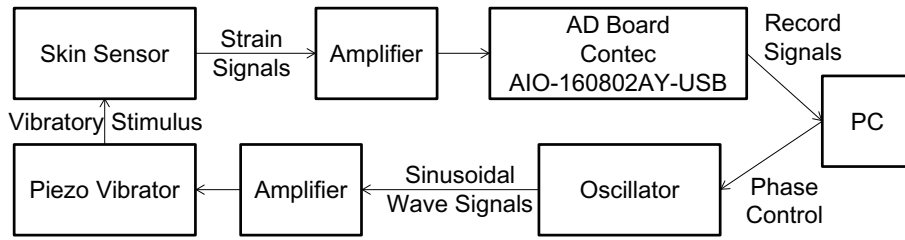
Fig. 4.3: System of the measurement.

4.1.2.2 Method

The vibrators were actuated by the following equation:

$$Vibrator A : f(t) = A\sin(2\pi ft) \tag{4.1}$$

$$Vibrator B : g(t) = A\sin(2\pi ft + \pi) \tag{4.2}$$

where $f(t)$ and $g(t)$ are the displacement [μm], A is the amplitude [μm] and f is the frequency [Hz]. Frequency was set to 10 Hz and amplitudes to 20 μm and the gap distance was set to 0.5 mm. The system of measurement is shown in Fig. 4.3.

4.1.2.3 Result

Fig. 4.4 shows the sensor output signals and the result of their spectral analysis. According to Fig. 4.4 (a), skin sensor's outputs followed the vibrator displacement at position A

69
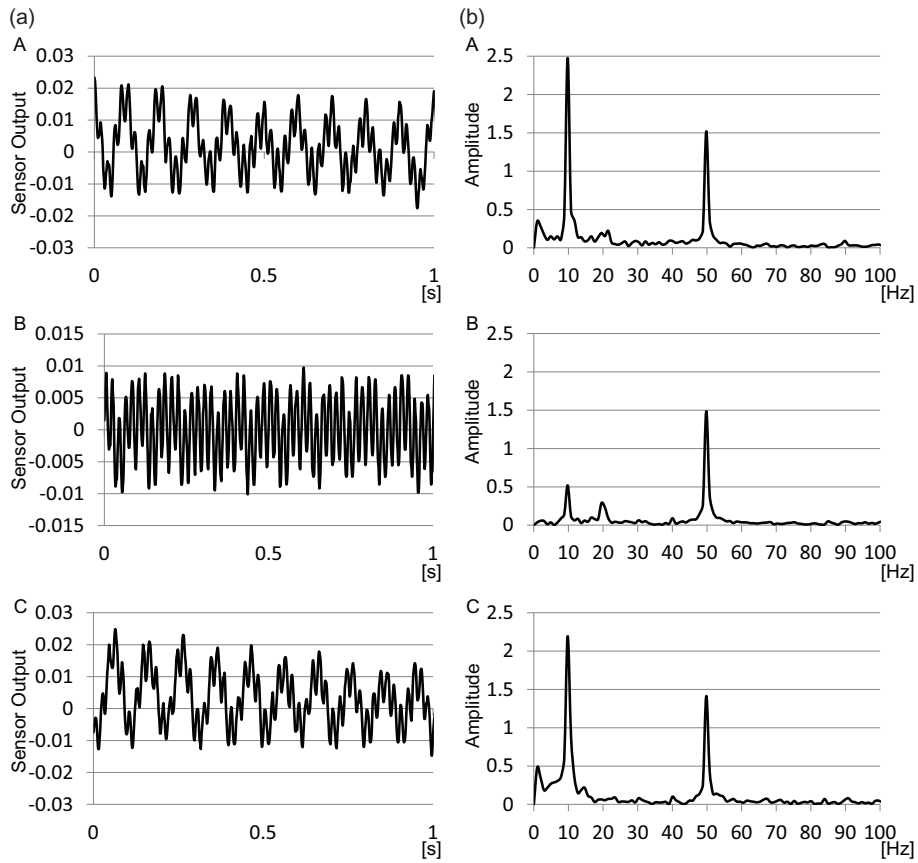
Fig. 4.4: Experimental results. (a). Skin sensor output at each strain gage position. (b). Spectral amplitude of each signal.

and C in Fig. 4.1 (b) while the strain behavior at position B did not. At position B, the amplitude of main frequency 10 Hz was weaken and the high frequency 20 Hz accounted for a large percentage compared to position A and C. However an obvious increase in high frequency that we expected to occur was not observed on this skin sensor. Position A and C, the signals had only linear frequency component and the spectral amplitude peak at 50 Hz were hum noise.

We have succeeded in observing the major behavior of the strain using the strain gages embedded into the urethane resin. However the strain gages position were slightly moved from the supposed position when molding, thus the outputs could be different from the ideal data. We modified this for the next sensor.

4.1.3 Finger Model Sensor

Fig. 4.5 shows the sensor size and its finite element model. Fig. 4.6 shows the developed sensor. Basic components were the same as the skin model sensor. This finger sensor consists of two layers and bone; the first layer represents epidermis/dermis (0.0-2.0 mm
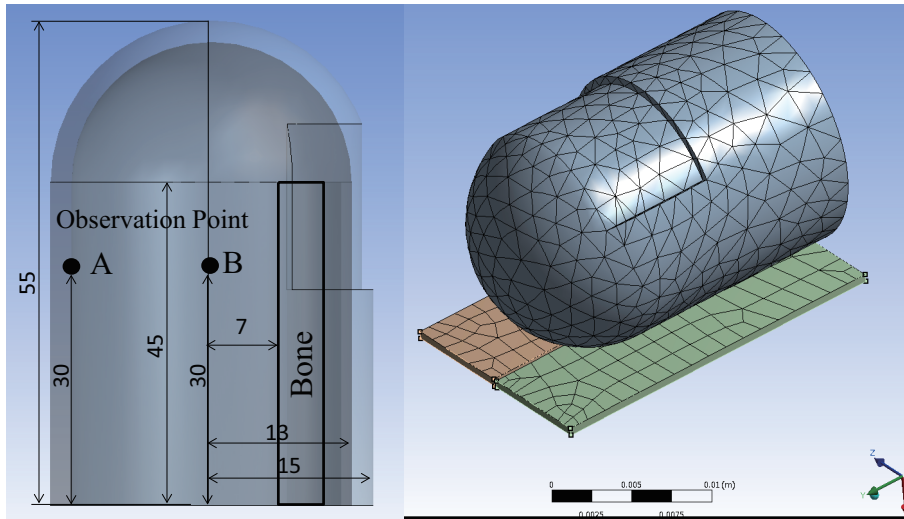
Fig. 4.5: Finger model sensor FE model. Left. Cross-section view. A and B indicate the positions of the strain gages. Right. Whole sensor shape.
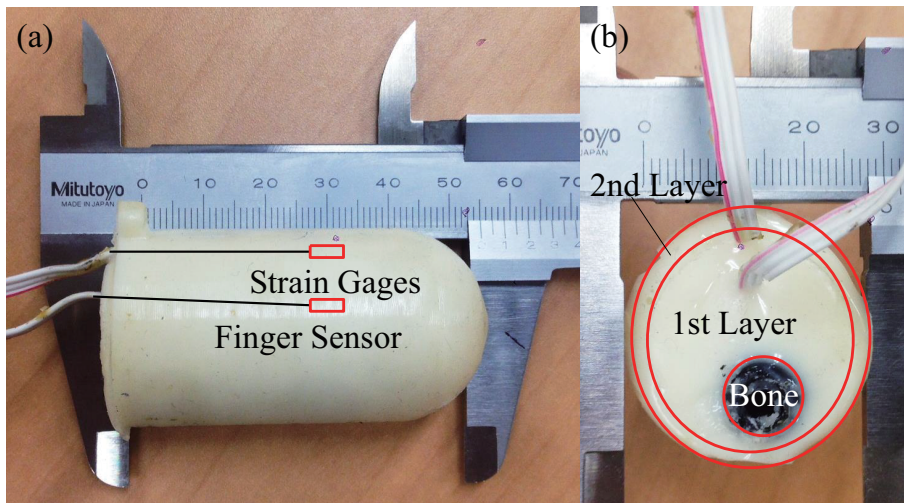
Fig. 4.6: Overview of developed finger model sensor. (a). Side view. (b). Back view.

deep), the second layer represents subcutis (2.0- mm), and the bone (22.0-27.0 mm). The first layer was created by urethane resin (Exseal Hitohada gel) which was elastic modulus of 5.2 kgf/cm ^{2} and the second layer was 1.2 kgf/cm ^{2}. The bone was rigid ABS resin of 3-D printer (Cube-X Cubify). Two strain gages were embedded between the first and the second layers (Fig. 4.5 position A) and at the center (Fig. 4.5 position B) where the FA II exist.

4.1.4 Measurement

The strain behaviors of shallow layer are observed for three frequencies conditions in this measurement. The effect of the frequency toward the high frequency generation is

71
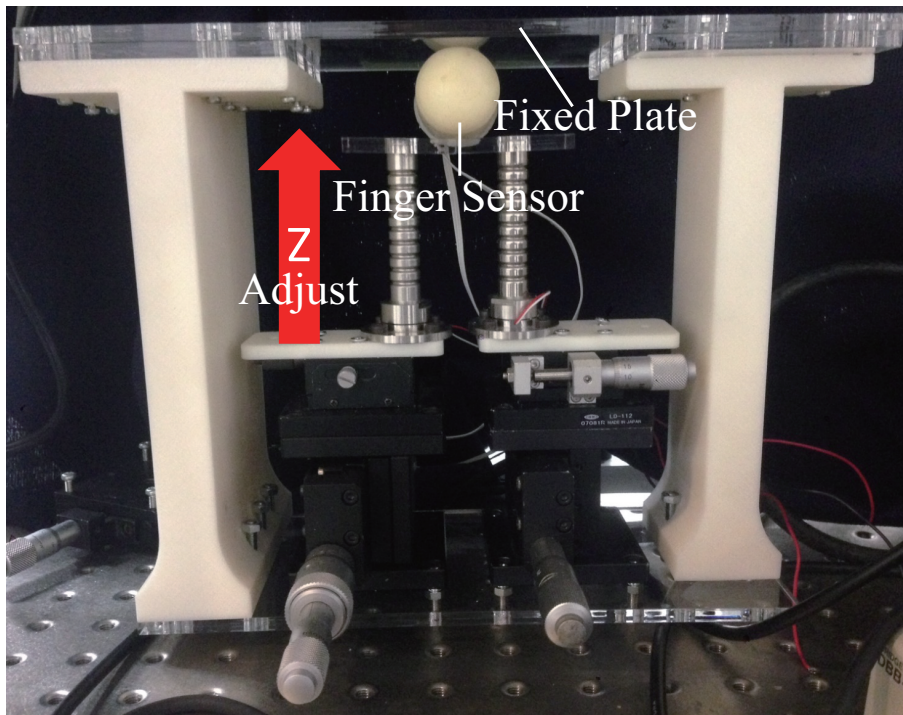
Fig. 4.7: Experimental setup. The way of fixing the sensor was changed to sand with fixed plate.

investigated.

4.1.4.1 Experimental Setup

Fig. 4.7 shows the experimental setup. The measurement system was mainly the same as the previous experiment, though the way of fixing the sensor was changed. The previous setup has problem; the weight was shaking when the vibrators vibrated that is not happen during actual touch. We placed fixed plane on the top and the sensor was sand 1 mm by the fixed plate and vibratory surfaces. Then skin sensor was placed on the center of two vibrators' contactors.

4.1.4.2 Method

The vibration and other method was the same as the previous experiment of the skin sensor. We used three frequency conditions; 5 Hz with 40 μm, 30 Hz with 9 μm, and 200 Hz with 5 μm. The amplitude was the detection threshold for ES condition which estimated and taken from section 3.1. The background noise was shown in Fig. 4.8; 50 Hz peak was hum noise.
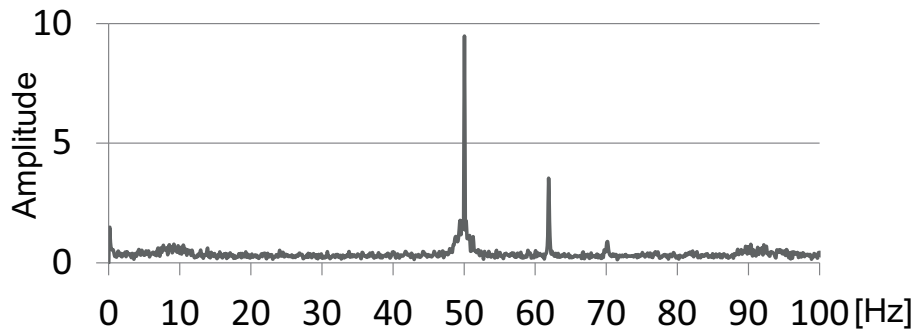
Fig. 4.8: Background noise of the sensor.

4.1.4.3 Result

Fig. 4.9 shows the sensor output signals for shallow layer at position A in Fig. 4.5. According to Fig. 4.9, 5 Hz and 30 Hz had doubled high frequency while 200 Hz did not. The occupied ratio of doubled frequency was the largest at 5 Hz. Hence, the non-linear filtering effect of ES method are significant when the frequency was low. Eijkman reported that the skin would not respond to the vibratory stimuli by a piston over a frequency of 15 Hz due to the viscoelasticity of the skin[88]. The skin under ES condition also might not respond completely to the vibratory surface when the frequency was 30 Hz and 200 Hz.
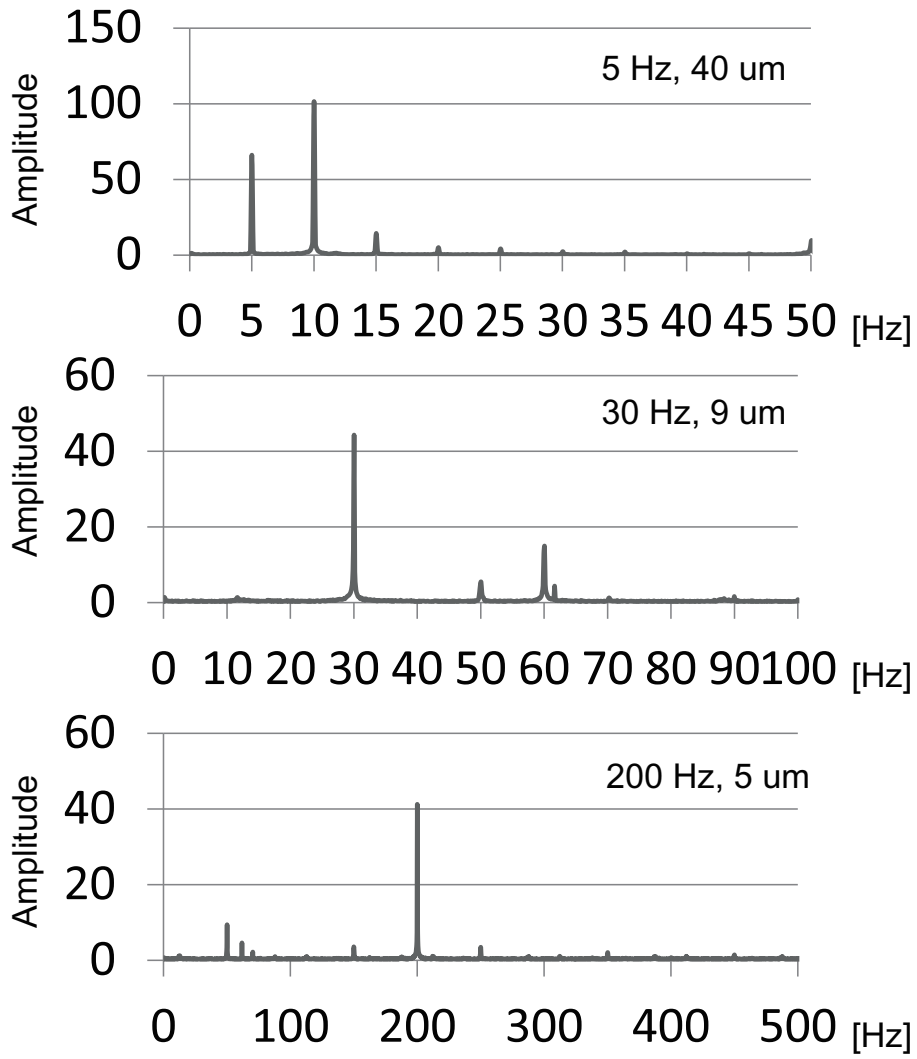
Fig. 4.9: Spectral results for each frequency and amplitude condition at the shallow layer of the finger model sensor.

74

Chapter 5

Development of Edge Stimulation Device for Fine Vibrotactile Line Presentation

5.1 Concept of Shape Presentation with ES method

From this section and next section, the possible arrangements of ES method for tactile shape presentation and the tactile devices are described.

5.1.1 Shape Presentation Using Continuous Line Sensation

As mentioned in section 2.1 Fig. 2.2, we consider to utilize ES method on the vibrator array and vibrate them individually to make shape. Fig. 5.1 shows the concept of the line presentation using ES method. We use 1. vertical line and 2. horizontal line for the tactile line primitives. These lines are done by ES method using opposite phased vibrations. By combining the tactile line primitives of the vertical and/or horizontal line, a tactile shape sensation is created as a continuous line.

5.1.2 Freedom Line Control: Problems

Chapter 3 demonstrated that there emerges line sensation not only between vibrations in opposite phases but also between stationary and vibratory surfaces, and this disturb from presenting freedom lines. For example, in Fig. 5.2 indicates that a single line element cannot be achieved by existing ES methods.

Tactile Line Primitives

1.Vertical Line
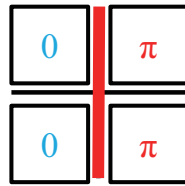
2.Horizontal Line
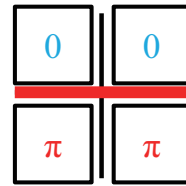
Apply to Large Array
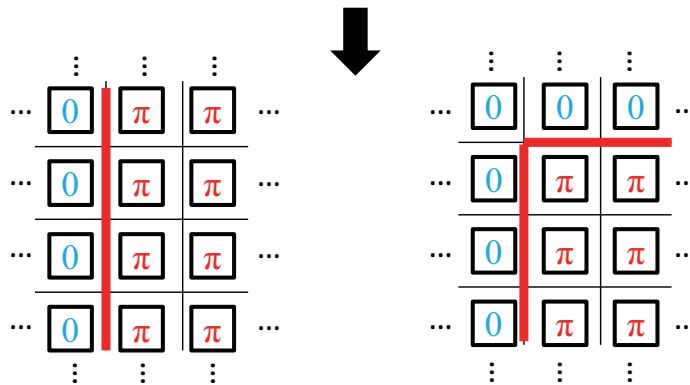
Fig. 5.1: Schematic of a tactile line presentation. Red lines show the perceived tactile line. Symbols on the vibrators indicate the phases of the vibrations. Upper: An image of the tactile line primitives of a vertical line and a horizontal line. Line primitives emerge between the vibrators in opposite phases. Lower: An image of large array using ES method.

Goal: Single Line Element
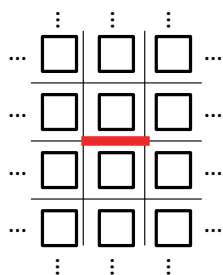
ES methods for example…

Multiple Vibration
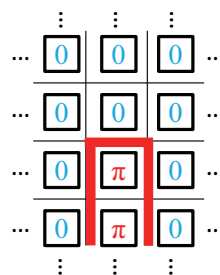
Stationary Surface
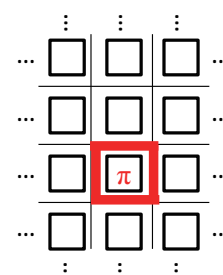
Fig. 5.2: Schematic of the problem with making a single line. Red lines show the perceived tactile line. Symbols on the vibrators indicate the phases of the vibrations. Left: Our goal of single line element. Right: Failed examples with ES methods.
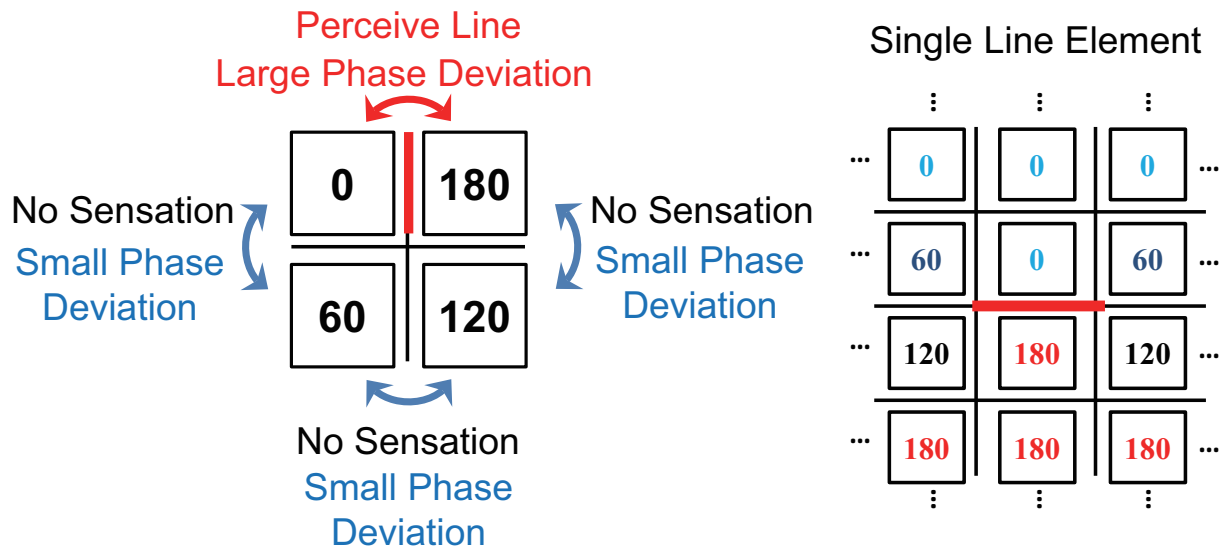
Fig. 5.3: Interrupted line can be presented by changing four vibrators phases step by step. Human cannot perceive any vibration between the boundaries when the phase deviations are small. Vibration can be perceived only where the phase deviation is large.

5.1.3 Freedom Line Control: Stimulus Intensity Controlling by Phase Shift

In section 3.1, Fig. 3.4 shows that the detection threshold can be coordinated by changing the phase deviation of two vibrators. Therefore, the stimulus intensity can be controlled as an inverse function of this approximate line of detection thresholds. According to this result, by using 10 μm vibrations, any vibration when the phase deviation is $\pi/3$ can be perceived; on the other hand, when the phase deviation is π, vibrations above the boundary can be perceived. Therefore, it is possible to interrupt the line sensation using the method shown in Fig.5.3. Here we show the examples of presenting alphabets by the combination of selective tactile lines by phase shift. The phases are denoted on the vibrator and one is able to feel tactile lines on the gap that has phase deviation over $\pi/3$.

5.1.4 Selective Line Control Using Phase Shift

To verify the validity of selective line control method, a tactile device equipped four vibrators is developed and psychophysical experiment is conducted with the device.

120	120	120	120
120	0	0	120
120	240	240	120
180	180	180	180

Fig. 5.4: a

120	120	120	120
120	0	0	120
120	240	240	120
120	120	120	120

Fig. 5.5: b

180	180	180	120
180	0	0	60
180	0	0	60
180	180	180	120

Fig. 5.6: c

180	180	180	180
180	0	180	180
180	0	180	180
180	180	180	180

Fig. 5.7: d

120	120	180	120
120	0	60	120
120	240	180	120
120	120	60	120

Fig. 5.8: e

120	120	120	120
120	0	60	120
120	240	180	120
120	180	180	120

Fig. 5.9: f

300	300	0	60
300	120	180	120
240	60	0	180
240	240	180	180

Fig. 5.10: g

120	60	60	120
120	0	0	120
120	240	240	120
120	180	180	120

Fig. 5.11: h

60	60	120	120
60	0	180	120
60	0	180	120
60	60	120	120

Fig. 5.12: i

120	120	120	120
60	0	240	180
120	0	240	180
120	120	180	180

Fig. 5.13: j

120	60	0	60
120	0	120	120
120	240	120	120
120	180	240	180

Fig. 5.14: k

120	60	0	0
180	0	0	0
180	0	0	60
180	180	180	120

Fig. 5.15: l

120	120	120	120
120	0	240	120
180	60	180	60
120	120	120	120

Fig. 5.16: m

180	180	180	180
180	0	0	180
180	0	0	180
120	60	60	120

Fig. 5.17: n

180	180	180	180
180	0	0	180
180	0	0	180
180	180	180	180

Fig. 5.18: o

240	240	240	240
240	0	0	240
240	120	120	180
180	180	180	180

Fig. 5.19: p

240	240	240	180
240	0	0	120
240	0	120	0
240	240	240	240

Fig. 5.20: q

120	120	120	120
120	0	0	120
120	240	120	180
180	180	240	180

Fig. 5.21: r

Fig. 5.22: s

Fig. 5.23: t

Fig. 5.24: u

Fig. 5.25: v

Fig. 5.26: w

Fig. 5.27: x

Fig. 5.28: y

Fig. 5.29: z

Fig. 5.30: The overview of the tactile line presentation device system. The overview of the developed device system

5.1.4.1 Tactile Line Presentation System

Fig. 5.30 left shows the whole device system. Four channel waves are generated by PC audio and transferred to a USB audio interface (Roland UA-101). The parallel output signals are amped with audio amps and actuate the four voice coils (VISATON FRWS 5 SC) individually. Fig. 5.30 right shows the tactile display. Acrylic plates are mounted on voice coil cones and we can vibrate them individually controlling their phases, amplitudes, and frequencies. One can feel a sharp tactile line sensation along the gaps of the vibrators in different phases. The cones are of low rigidity and they drop for about 0.5 mm against the 1 N indentation force of touch. We can then present sufficient vibrotactile sensation by using amplitudes of more than 9 μm according to the previous experiment result.

5.1.4.2 Evaluation of the Tactile Line Presentation Display

We evaluate whether the voice coil actuated surfaces are able to achieve the ES methods. Here, we conduct a psychophysical experiment to investigate the detection threshold with the use of the developed tactile device. If the developed device reflects the ES effects, the detection threshold should be much lower than that obtained by simply touching a vibratory surface. Also, the detection threshold behavior toward the phase deviation of two vibrations should reflect the tendency of the ES method.

Method

Subjects touched the vibratory surfaces 3 and 4 in Fig. 5.30 right with an indentation force of 1 N. While subjects touching to the surfaces, the vibratory surfaces were vibrated
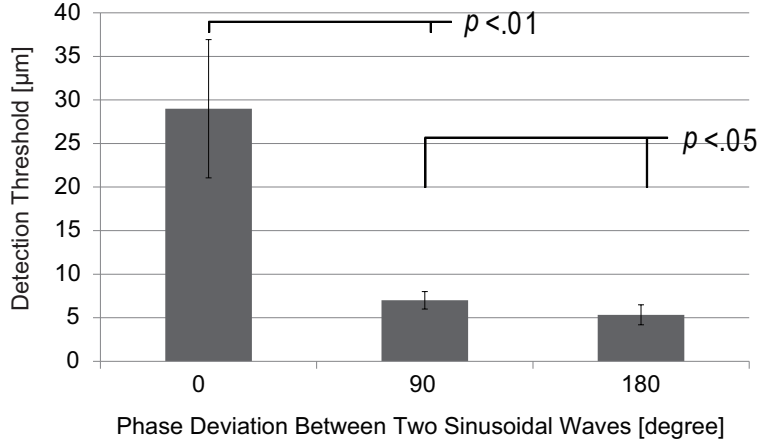
Fig. 5.31: Results of psychophysical experiments. Detection thresholds under each phase deviation.

according to the following equation:

$$f(t) = A\sin(2\pi f t) \tag{5.1}$$

$$g(t) = A\sin(2\pi f t + \phi) \tag{5.2}$$

where $f(t)$, $g(t)$ are the input displacement [μm], A is the amplitude [μm], f is the frequency [Hz] and ϕ is the phase deviation between two surfaces. We used three conditions of phase deviation 0, $\pi/2$, π. We determined the detection thresholds using the method of limits for each condition. The gap distance between surfaces 3 and 4 was 0.1 mm. Subjects wore headphones that played pink noise so that they would not perceive any environmental changes. The three subjects were all right-handed males and a female, all of ages 21-32. All subjects had no known medical condition or disorders affecting their tactile sense.

Result

Fig. 5.31 shows the detection thresholds under each of the phase conditions. When both surfaces were vibrated in the same phase, there were no ES effects and the detection threshold was the same as simply touching a single vibratory surface. The detection threshold fell as the phase deviation became large. This tendency and threshold values did not contradict previous information on ES effects in section 3.1. The ES effects were sufficiently obtained by using vibratory surfaces with low rigidity voice coil motors.
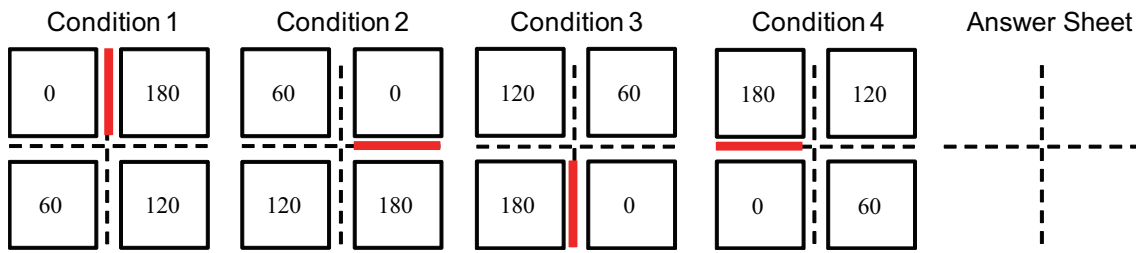
Fig. 5.32: Conditions of four tactile images and answer sheet. Subjects will perceive vibration only above boundary of contactors with large phase deviation.

5.1.5 Evaluation of Selective Line Control Method

In this experiment, psychophysical experiments were conducted to verify the validity of the selective line control method with the developed tactile line presentation display.

5.1.5.1 Procedures and Tasks

Four patterns of tactile images were presented in random order. Fig. 3.4 shows the four patterns-Up, Right, Down, and Left. Each vibrator vibrated at 10 μm, and the phase deviation was set to $\pi/3$. The stimuli had been presented previously, and the subjects touched the contactors for 2 s before removing their fingers. The subjects touched four contactors with their thumb with an indentation force of 1 N. This process was repeated as many times as the subjects satisfactorily recognized the tactile image. The subjects were then asked to sketch the perceived tactile image on the answer sheet shown in Fig. 5.32; they were not told the four correct patterns of tactile images and to simply write the perceived lines along the dashed line on the answer sheet. Two finger positions were drawn on the contactors (Fig. 3.1, vertical and horizontal positions) in order to consider the effects of the finger contact area because the finger position could affect the rate of correct judgments. Each condition of the tactile images was presented thrice randomly and repeated twice for finger positions for a total of $4\times3\times2$=24 times for each individual. In order to ensure that they would not perceive any environmental changes, the subjects wore headphones that played white noise to them and also wore an eye mask. The seven subjects were all right-handed males of ages 19-25.

5.1.5.2 Experimental Results

Table. 5.1 lists the correct rates for each subject under each condition. Almost all the subjects answered correctly in more than 80% trials while subject G's score was 67%. Fig. 5.33 shows the representative wrong patterns observed in all the subjects and

Table. 5.1: Correct rate of each subject

Subject	Up	Right	Down	Left	Total
A	4/6	5/6	6/6	5/6	20/24
B	5/6	5/6	5/6	5/6	20/24
C	5/6	5/6	5/6	6/6	21/24
D	6/6	5/6	5/6	6/6	22/24
E	6/6	6/6	4/6	5/6	21/24
F	5/6	4/6	5/6	6/6	20/24
G	3/6	5/6	3/6	5/6	16/24
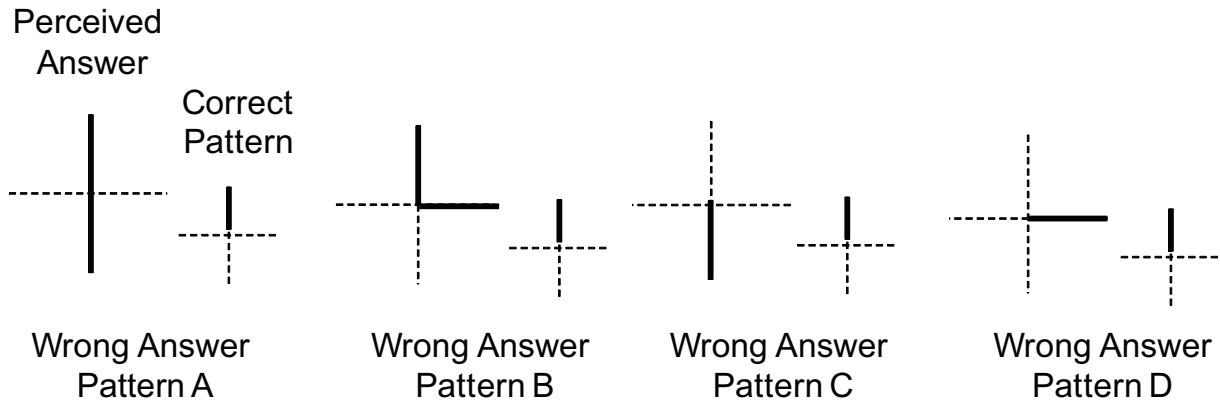
Fig. 5.33: Wrong patterns observed in the answer sheet and clarified them into four patterns.

divided them into four patterns A, B, C, and D. The wrong pattern A includes correct and wrong lines in the same direction; the wrong pattern B includes correct and wrong lines in different directions; wrong pattern C does not have correct line but the wrong line is in the same direction as the correct line; and wrong pattern D has the wrong line as totally different from the correct line. There were a total of 30 wrong answers in all the trials, and the rate for each pattern was A = 12/30, B = 10/30, C = 3/30, and D = 5/30. According to this result, more than 70% of wrong answers included the correct line.

5.2 Line Presentation with ES Device

We have developed ES line presentation device that has nine vibrators in a 3×3 array. Fig. 5.34 shows the entire system of the device. A PC controls each phase of the vibrators. An Arduino MEGA 2560 generates nine-channel pulse width modulated signals; an
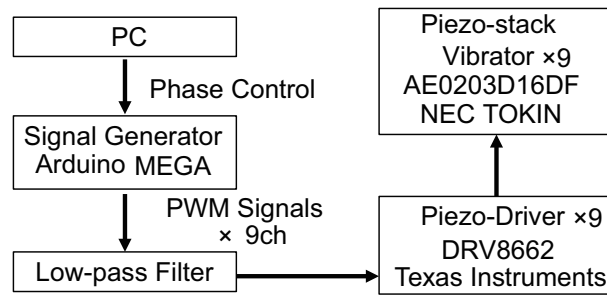
Fig. 5.34: Overview of tactile line presentation device system.
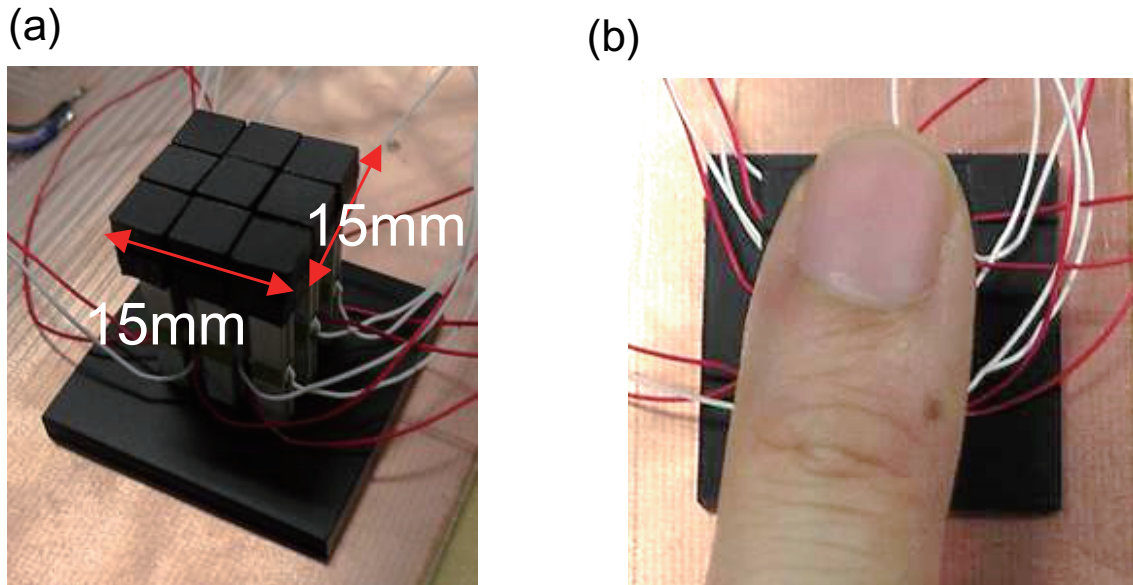
Fig. 5.35: Overview of developed haptic display: (a) square-shaped vibrators in array vibrate in different phases; (b) entire display is smaller than fingertip of index finger.

analog low-pass filter turns them into sinusoidal waves. Piezo drivers (Texas Instruments DRV8662) amplify the signals at a maximum of 40 dB to 200 V. We used piezo-stack type actuators (NEC TOKIN AE0203D16DF; $2\times3\times20$ mm) owing to their rigidity against the indentation normal force. They show a 17.4 μm displacement at a maximum voltage of 150 V and normal force of 200 N; these are sufficient for human touch (several newtons). The 5 mm square acrylic plates are attached on the top of the vibrators to make the display surface a 15-mm-square flat plane (see Fig. 5.35(a)). The entire display is less than the area of a human index finger, as shown in Fig. 5.35(b). The length of the gap between two surfaces were fabricated to be less than 0.1 mm. Vibratory surfaces vibrate in a normal direction, and they do not interfere with each other.

5.2.1 ES Device Evaluation Experiment

We evaluated the developed ES device through a psychophysical experiment to validate the feasibility of ES method for 3×3 arrays. Detection thresholds were investigated under several different conditions where nine vibrators were vibrated in the same and opposite phases. If the device achieves ES method properly, the detection threshold of the former will be larger than that of the latter.

5.2.1.1 Method

Fig. 5.36 shows the experimental overview. Participants touched the display shown in Fig. 5.35 with the tip of their index fingers and with an indentation force of 1 N. As the participants were touching the surfaces, the vibratory surfaces were vibrated according to the following equation:

$$A : f(t) = A\sin(2\pi ft) \tag{5.3}$$

$$B : g(t) = A\sin(2\pi ft + \phi) \tag{5.4}$$

where $f(t)$ and $g(t)$ are the displacement [μm], A is the amplitude [μm], f is the frequency [Hz] and ϕ is the phase deviation between two surfaces A and B. We used two phase deviation conditions: 0, π and the frequency was set to 30 Hz. Three conditions were presented, (a)left, (b)up and (c)all were in the same phases, which were set as shown in Fig. 5.37.

As the participants were touching the vibrator contactor, we repeatedly changed the vibrators' input voltage by 2 V. After each increase, the participants were asked whether they perceived a vibratory stimulus. The input was increased from 0 V to 150 V, and the threshold amplitude was recorded. Next, the input was decreased in steps of 2 V from a well-defined input, and the threshold amplitude at which the participant could not perceive the vibratory stimulus was recorded. The method of limits was then used to calculate the detection threshold for vibration. For condition(c), 17.4 μm amplitude that is the maximal amplitude of the device, when the participants were not able to perceive a 17.4 μm amplitude, we instead used large displacement type piezoelectric actuator (TOKIN, AHB850C851FPOL-1F) with a 15 mm square acrylic plate on top and repeated the same task. This process was repeated three times at each condition for a total of nine times for each individual. Participants wore headphones playing white noise so that they would not perceive any environmental changes. The seven participants

86
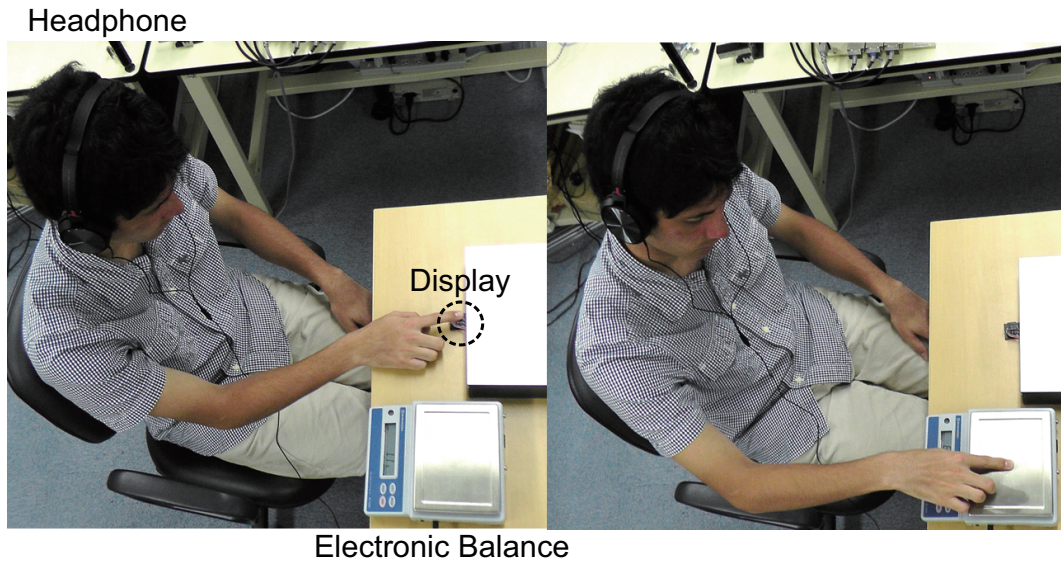
Fig. 5.36: Experimental setup.
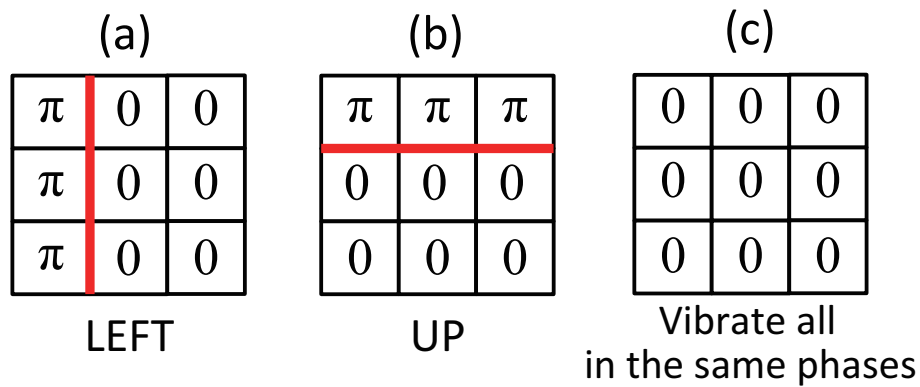
Fig. 5.37: Pattern conditions: (a) left line, (b) up line, (c) vibrate all in same phase (no lines).

were all right-handed males, aged 21-32. None of the participants had any known medical conditions or disorders affecting their tactile senses.

5.2.1.2 Result

Fig. 5.38 shows the detection thresholds under each conditions. Under conditions (a) and (b), the average detection thresholds were about 5 μm, which did not contradict previous information on ES effects in section 3.1. When all vibrators were vibrated in the same phase, only one participant reported that he felt no vibration under 17.4 μm with the ES device. This may be due to the displacement difference of each vibrator to the input voltage; the difference may be felt as a vibratory sensation. After the vibrators were changed to large-displacement ones, the average detection threshold was 28 μm.
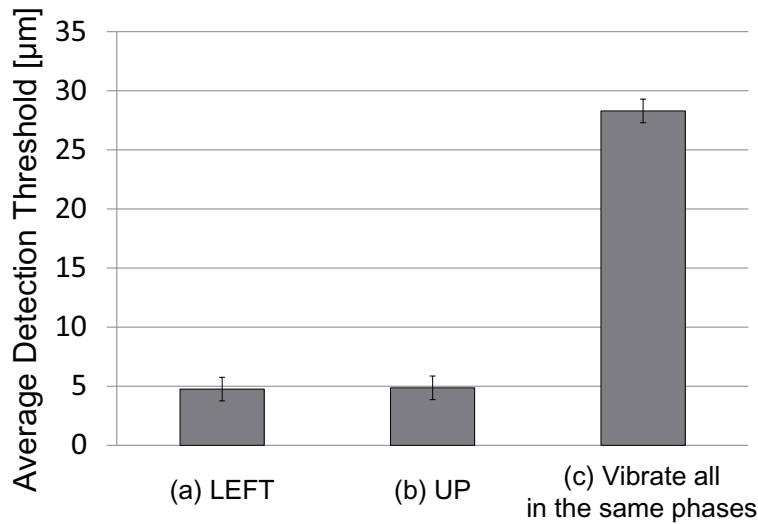
Fig. 5.38: The result of the psychophysical experiment. Error bars indicate standard deviation.

5.2.1.3 Discussion

In the detection threshold studies of Verrillo and others [25, 83, 84], it is about 10 μm for condition under touching both circular vibrator and rigid surroundings with hole and about 30 μm for vibrator only that is similar to the results of under conditions (a) and (b), condition (c), respectively. Based on the results, the developed ES device achieved the ES effects, and a line sensation could be generated; for example, at 10 μm, the lines between surfaces in the same phases could not be perceived, while those between surfaces in opposite phases could be selectively perceived. The vibratory sensation was sufficiently strong when the amplitude was 10 μm; the piezo-stack type vibrator can be made thinner and replaced for a 10 mm height.

5.2.2 Line Recognition Experiment

This experiment was designed to examine the validity of the proposed line presentation by the ES method. Here we presented several tactile line patterns and investigated whether the subjects were able to distinguish the line orientation or the numbers of lines through a psychophysical experiment.

5.2.2.1 Method

Fig. 5.39 shows the experimental overview. Eight patterns of tactile images, including two conditions with no tactile sensations, were presented in random order. Fig. 5.40 shows six line patterns–left, right, up, bottom, double vertical lines, and double horizontal lines–

Table. 5.2: Correct recognition ratio

Participant	(a)LEFT	(b)RIGHT	(c)UP	(d)BOTTOM	(e)Double VERTICAL	(f)Double HORIZONTAL	LINE TOTAL
A	10/10	10/10	10/10	10/10	9/10	10/10	59/60
B	10/10	10/10	10/10	10/10	10/10	10/10	60/60
C	10/10	6/10	8/10	10/10	8/10	9/10	51/60
D	10/10	10/10	10/10	10/10	7/10	10/10	57/60
E	10/10	9/10	9/10	10/10	9/10	9/10	57/60
F	10/10	10/10	10/10	8/10	10/10	10/10	58/60
RATE	1.0	0.92	0.95	0.97	0.92	0.97	**0.95**

Participant	(g)Vibrate ALL	(h)Vibrate NONE	TOTAL
A	10/10	10/10	79/80
B	10/10	10/10	80/80
C	10/10	10/10	71/80
D	10/10	10/10	77/80
E	10/10	10/10	77/80
F	10/10	10/10	78/80
RATE	1.0	1.0	**0.96**

and two conditions with no line sensations–vibrate all and vibrate none. The stimuli were presented previously, and the participants knew the stimuli sets described above. The participants touched the display and ensured that their index finger covered the entire display with an indentation force of 1 N. Participants practiced touching with a force of 1 N by touching an electronic balance. The stimuli were presented for 2 s before the participants removed their fingers. After each trial, the participants were asked to sketch the perceived tactile image on the answer sheet by drawing lines. If the participants sensed no lines, they did not provide an answer. Each condition of tactile lines was presented 10 times for a total of 10×8 = 80 trials by each individual. Participants wore headphones that played white noise to ensure that they did not perceive any environmental changes. The six participants were all right-handed males between 20-28 years of age. Vibratory stimuli were generated according to eqs. 1 and 2 in the first test. We used two phase conditions of 0 and π, a frequency of 30 Hz and an amplitude of 10 μm which is sufficiently perceptible at the gap for the ES method, while not perceptible on the vibrators surfaces.

5.2.2.2 Result

Table. 5.2 shows the results of the recognition test. The participants were able to discriminate lines at a rate of 95%, and the total correct answer rate was 96%. When presented with the (g) or (h) condition, all participants skipped the answer sheet correctly. Reports from the participants after the tests showed that they were not able to discriminate the (g) from (h) conditions. This indicates that the amplitude of 10 μm was sufficiently lower than the detection threshold for all the subjects, and they certainly perceived vibratory
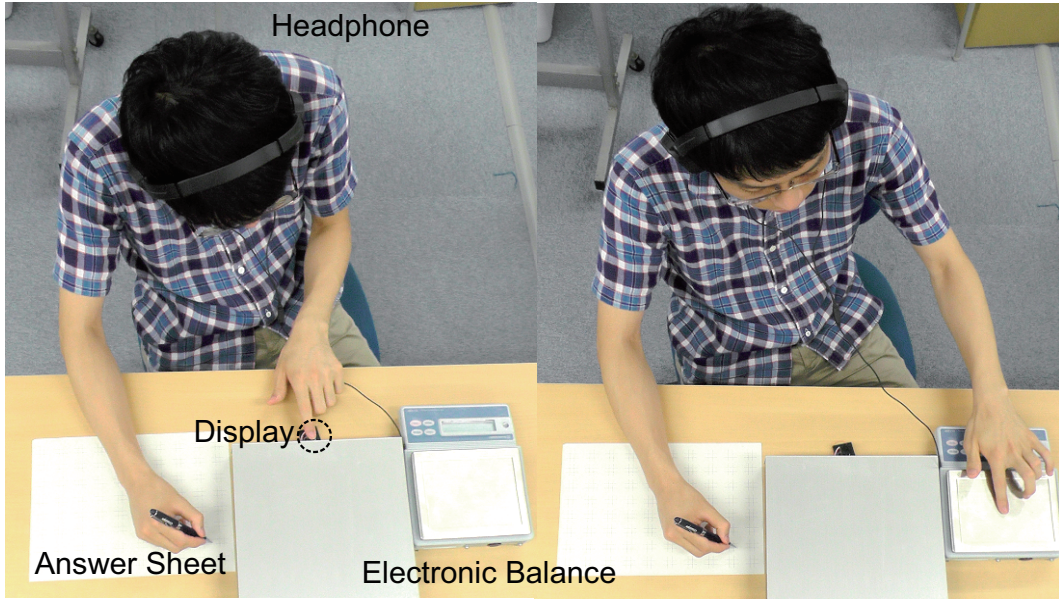
Fig. 5.39: Experimental setup. Indentation force was adjusted by electronic balance for each trail.
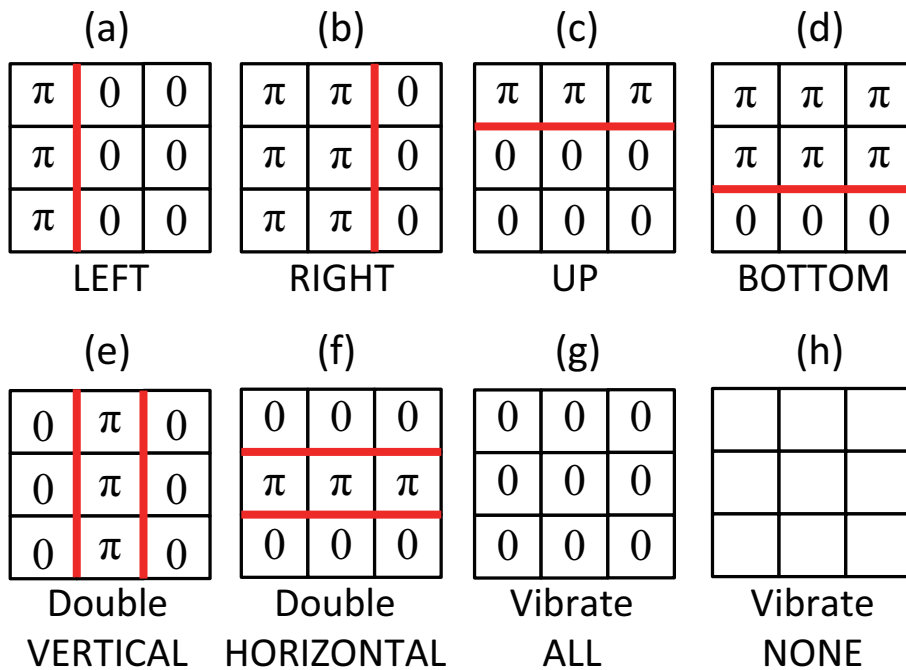
Fig. 5.40: Eight tactile image patterns. Line sensations only arise above the edges between surfaces in different phases.

sensations at the gap for conditions (a)-(f). Most mistakes were made under condition (e), where double vertical lines were mistaken for a vertical line in either the (a) or (b) condition.

Chapter 6

Conclusions and Future Perspectives

This chapter addresses the contribution and future perspectives of each topics.

section 2.1

The edge stimulation (ES) method was proposed in this chapter. Simultaneous touch to a vibratory surface and a stationary surface or multiple vibratory surfaces in different phases provides strong tactile sensation along the edge. ES method provides sharp and localized tactile sensations that is suitable for designing tactile shape presentation.

section 2.2

The performance of ES method for several mechanical parameters on vibrotactile stimuli intensities were investigated. Psychophysical experiments revealed that ES method is effective for lower frequencies (5, 30 Hz) and human vibratory detection threshold become about 1/2 (110 μm to 40μ) for 5 Hz and 1/4 (35 μm to 8μ) for 30 Hz compared to simply touching to a vibrator. ES method was also affected by the gap distance and height deviation between the surfaces; either gap distance or height deviation became large, the vibrotactile stimulus intensities became small. This means that if the gap distance is fabricated close to zero and surfaces are to be flat, ES method exhibits the best performance that is ideal characteristic for the vibrator array device.

section 2.3

Deformation analysis was conducted on finite element (FE) skin model under the condition of ES method with a stationary and a vibratory surface. Static analysis demonstrated the increase in strain energy density (SED) peak at the edge, although the tendency for gap distance obtained in psychophysical experiment could

not be explained only by the SED peak. Dynamic analysis revealed that the SED frequency is also increased between the boundaries of the surfaces under ES condition and the tendencies did not contradict to the psychophysical result. Verification psychophysical experiments indicated that the subjects feels about 50 Hz sensation against 30 Hz vibration under ES condition. Both increase in peak and frequency of SED could affects the human vibratory detection threshold.

The discovery of the generation of a non-linear frequency component due to the time variant contact condition has impact on haptic science field, since general apparatus used for the investigation on vibratory detection threshold has the mechanical structure to arise other frequency component and the result could be different.

section 3.1

The performance of ES method using multiple vibrations was investigated. Overlapping vibrations in different phases supposes the use of ES method in vibrator array device. This is also affected by gap distance and additionally, by phase deviation of two vibrations; the opposite phased vibrations presents the strongest tactile stimuli intensities.

The sharpness of tactile images (vibratory sensation width in index finger) by ES method is examined comparing to a tactile image by a single-pin vibrator, a pin array vibrator, and a flat vibrator The result demonstrated the sharpness of tactile image by ES method; a tactile image by ES method with 0.5 mm gap provides approximately 1 mm tactile image while 0.5 mm width pin-vibrator provides approximately 3 mm tactile image. The two-line discrimination test was conducted, and the discrimination distance was 4.2 mm for the ES method, while the real two-line discrimination distance was 2.5 mm.

section 3.2

The FE deformation analyze were conducted to investigate the mechanism for sharp and localize tactile sensation under ES condition. SED was both horizontally and vertically concentrated under ES conditions compared to a pin-vibrator. Deformation spread in horizontal affects the numbers of mechanoreceptors and that in vertical affects the types of mechanoreceptors (wide receptive field FA II are at deep layer).

section 4.1

Measurement of the strain behavior inside the skin was conducted. A finger model

sensor was developed and the output signals were observed under stimulating with ES method. Three frequencies were examined and the doubled frequency was observed under the conditions of 5 Hz and 30 Hz while 200 Hz was not.

section 5.1

The concepts for applying ES method to shape presentation is proposed. For the further variations of achieving tactile patterns, we developed a selective line control method by changing the phases of vibrators. We developed 2×2 array ES device with four voice coil vibrators for an verification experiment of the method and psychophysical experiments demonstrated correct rate for 4 tactile line directions was more than 80 % using selective line control method.

section 5.2

A 3×3 array ES device using piezo-electoric vibrators was developed and presentation experiments of tactile patterns were conducted. The display size became smaller compared to previous 2×2 array ES device, within the cover of an index fingertip. Rigidity of actuates and precise phase control were also improved. The discrimination experiments for 8 tactile patterns resulted in 96 % correct rate.

Overall Conclusions

We have developed a vibrotactile stimulation method called edge stimulation (ES) method throughout this thesis. Considering from a view of vibrotactile stimulation method, ES method is useful since it quires considerably small amplitude with low frequency that cannot be accomplished in previous works. Using the ES method, the piezo-electric vibrators that have high rigidity but can provide small amplitude, can be applied to these tactile displays without using displacement magnification mechanism such as levers. These characteristics contribute to a low power actuation and miniaturization of the tactile displays. The ES method enables to fabricate the tactile display surface to be flat, which enables to project images on the tactile surfaces while previous tactile displays had bumps and dents.

Furthermore, the tactile image obtained by the ES method has different features compared to that obtained by previous vibrotactile stimulation methods, since the stimulation area is formed by the gap between two surfaces, and is applicable for representing virtual lines, areas, and shapes as a combination of lines. Through-

out the psychophysical experiments and deformation analysis, the ES method succeeded in suppressing the vibration spread and selectively stimulate high resolution cutaneous mechanoreceptors in shallow layer that leads to a highly localized vibrotactile stimulation. We have found that not only strain peak but also strain frequency was enhanced at the gap under ES condition and found its importance of the frequency enhancement on tactile intensity since the increase in frequency has much more improvement in human vibrotactile sensitivity. For the next step to utilize ES method onto actual line presentation, we developed a 3×3 vibrator-array ES tactile display that was considered two-lines discrimination when fabricating the array size. The tactile line pattern recognition test was conducted; the recognition ratio was 95%, which supports the validity of tactile line presentation using the ES method. Though the tactile vibrator array display succeeded in presenting several tactile patterns, the presentation of alphabets and other shapes have not been accomplished. Then, we demonstrated a possibility for extensibility to larger array solving the problems that the current ES method has limitation in presenting freedom combinations of line, by developing a selective line control method. By slightly shifting each phase of the vibrator, we have succeeded in presenting variant patterns; the possibility for applying ES lines into the shapes of alphabet were theoretically demonstrated. The development of large array display and the presentation of tactile alphabets are our future works.

Appendix A

Possible Arrangements of ES Method

Purpose

Having demonstrated the effectiveness of ES enhancement, we now investigated other possible arrangements of ES focusing on the ES produced line sensation for developing practical devices. Based on the psychophysical results and FEM analyses, ES requires skin impact against the stationary surface edge. To get a larger contact area with the edges, we suggest the circular stationary contactor shown in Fig. A.1. The inner vibrator is covered with a finger. This shape has advantages in terms of the edge-contact ratio, total device size, and structural strength. Thus, we suggested that ES produced line sensation can be perceived along the gap of any forms between stationary surface and vibratory surface with passive touch. In this experiment, we changed the forms of the gap shown in Fig. A.1 and investigated how the ES produced line sensation changes, hollow circle sensation along the gap or just a solid circle sensation above the contactor.

To investigate the possible arrangement suggested above, we conducted psychophysical experiments to determine the detection threshold for the following four conditions, as shown in Fig. A.2:

- Condition 1: Small circular vibrator (Diameter: 12 mm)
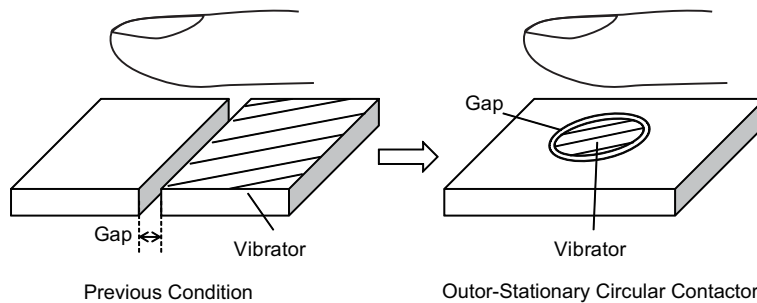
Fig. A.1: Arrangement of ES method.
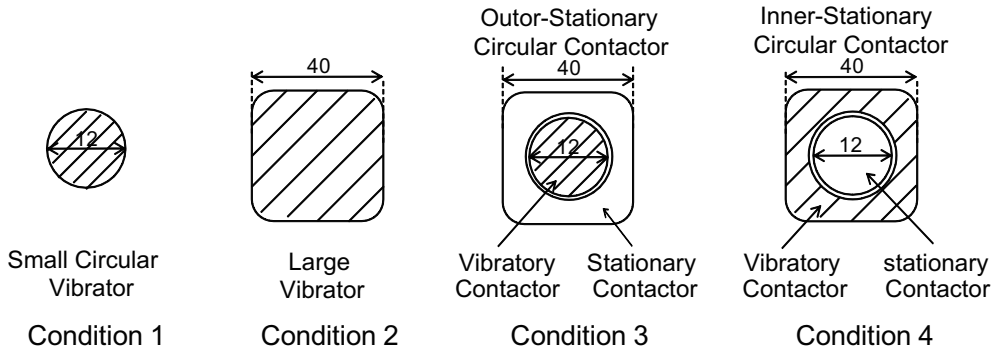
Fig. A.2: Contactor conditions: Condition 3,4 are our suggested arrangements that contacting with the circle-shaped stationary surface in the gap distance of 0.5 mm

- Condition 2: Large vibrator (Diameter: 40 mm)

- Condition 3: Outer-stationary circular contactor (Diameter of the vibratory contactor: 12 mm, Gap: 0.5 mm)

- Condition 4: Inner-stationary circular contactor (Diameter of the stationary contactor: 12 mm, Gap: 0.5 mm)

Method

Subjects wore headphones playing pink noise so that they would not perceive any environmental changes. Under Conditions 1 and 2, subjects touched the center of the vibrator contactor with an index finger. Under Conditions 3 and 4, subjects touched both the vibrator and stationary contactors with an index finger using an indentation force of 1 N. In this experiment, the frequency was set to 30 Hz. We made sure that all subjects covered the entire 1.2 mm diameter contactor with the surface of the index finger. The detection threshold for vibration under each condition was then calculated by the method of limits for a total of 12 trials per subject. For Condition 3, after the trial, we presented a vibration with an amplitude around each subject's threshold and asked two questions: "Where do you feel the vibration?" and "Which contactor do you feel vibrating?" We asked this question to investigate how the subjects perceive the ES produced line sensation of circular gap form. The five subjects were all right-handed males aged 21-25.
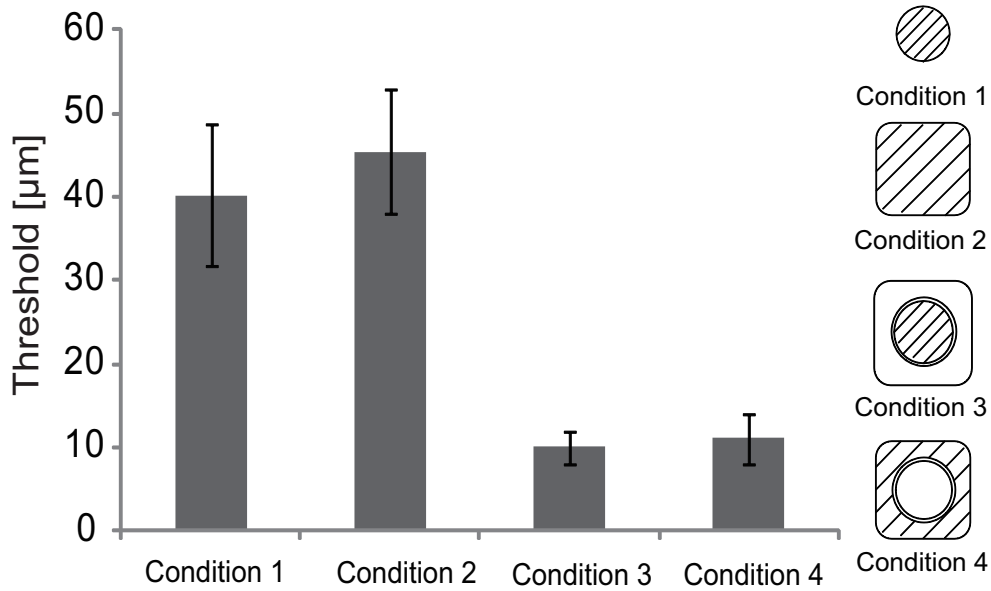
Fig. A.3: detection threshold of all subjects in each conditions

Results

Fig. A.3 shows the detection threshold under each condition for each subject. The detection threshold was lower under Condition 1 than under Condition 2 for all subjects. Under Condition 1, when touching the circular contactor, subjects covered the entire edge of contactor surface; in contrast, no edges existed for Condition 2. These results do not contradict previous studies showing that edges at the contactor surface enhances the vibrotactile sensitivity[25].

Conditions 3 and 4 are the suggested arrangements. Under both conditions, the detection threshold is about one-fourth lower than that under Conditions 1 and 2. This confirms the effectiveness of the suggested arrangements.

For the questions "Where do you feel the vibration?" and "Which contactor do you feel vibrating?", all subjects answered "I felt the vibration along above the gap" and "I could not discriminate which is vibrating." Hence the ES produced line sensation can be applied to circular gap form.

Reference

[1] C. Darwin: "The expression of the emotions in man and animals," Oxford University Press, 1998.

[2] B. M. DePaulo: "Nonverbal behavior and self-presentation," Psychological Bulletin, Vol. 111, Issue 2, pp. 203-243, 1992.

[3] S. E. Jones and C. D. LeBaron: "Research on the Relationship Between Verbal and Nonverbal Communication: Emerging Integrations," Journal of Communication, Vol. 52, Issue 3, pp. 499-521, 2002.

[4] J. K. S. Teh, A. D. Cheok, R. L. Peiris, Y. Choi, V. Thuong and S. Lai: "Huggy Pajama: a mobile parent and child hugging communication system." Proceedings of the 7th international conference on Interaction design and children. ACM, 2008.

[5] N. Wiener: " Cybernetics or Control and Communication in the Animal and the Machine," Vol. 25. MIT press, 1965.

[6] K. Johnson: "Neural basis of haptic perception," In S. Yantis(Ed): Stevens handbook of experimental psychology (third edition). Vol.1: Sensation and perception, John Wiley & Sons., pp.537-583, 2002.

[7] R. S. Johansson, U. Landstro and R. Lundstro: "Sensitivity to Edges of Mechanoreceptive Afferent Units Innervating the Glabrous Skin of the Human Hand," Brain Research Vol.244, Issue 1 , pp. 27-32, 1982.

[8] A. B. Vallbo and R. S. Johansson: "Properties of cutaneous mechanoreceptors in the human hand related to touch sensation," Hum Neurobiol 3.1, 1984.

[9] R. S. Johansson and A. B. Vallbo: "Tactile sensory coding in the glabrous skin of the human hand ," Trends in Neurosciences, Vol. 6, pp. 27-32, 1983.

[10] K. Sato and S. Tachi: Transmission System of Spatially Distributed Tactile Information using Finger-shaped GelForce and Electrotactile Display, Trans. of the Human Interface Society of Japan, Vol.12, No.2, pp.55-62, 2010.

[11] H. Kajimoto, N. Kawakami, and S. Tachi: "Smarttouch: Electric skin to touch the untouchable," IEEE Computer Graphics & Applications Magazine, vol. Jan.-Feb., pp. 36-43, 2004.

[12] M. Konyo, A. Yoshida, S. Tadokoro, and N. Saiwaki: "A tactile synthesis method using multiple frequency vibration for representing virtual touch," Proceedings of the 2005 IEEE/RSJ International Conference on Intelligent Robots and Systems, pp. 3965-3971, 2005.

[13] M. Pare, A. M. Smith and F. L. Rice: "Distribution and terminal arborizations of cutaneous mechanoreceptors in the glabrous finger pads of the monkey," J. Comp. Neur., Vol. 445, pp/347-59, 2002.

[14] N. Asamura, N. Yokoyama, and H. Shinoda: "Selectively stimulating skin receptors for tactile display," Computer Graphics and Applications, IEEE Vol.18, Issue 6, pp. 32-37, 1998.

[15] M. Shimojo: "Mechanical filtering effect of elastic cover for tactile sensor," IEEE Transactions on Robotics and Automation, Vol.13, Issue 1, pp. 128-132, 1997.

[16] J. C. Eccles, R. M. Eccles and A. Lundberg: "Synaptic actions on motoneurones caused by impulses in Golgi tendon organ afferents," The Journal of Physiology, Vol. 138, Issue. 2, pp. 227-252, 1957.

[17] B. David, K. E. Hagbarth, L. Lofstedt and B. G. Wallin: "The responses of human muscle spindle endings to vibration during isometric contraction," The Journal of Physiology. Vol. 261, Issue. 3, pp. 695-711, 1976.

[18] T. H. Massie and J. K. Salisbury: "The phantom haptic interface: A device for probing virtual objects," Proceedings of the ASME winter annual meeting, symposium on haptic interfaces for virtual environment and teleoperator systems, Vol. 55, No. 1, 1994.

[19] S. Saga, N. Kawakami and S. Tachi: "Haptic teaching using opposite force presentation," Poster presentation (CD proceedings) World Haptics Conference. 2005.

[20] G. Chris, M. Hutchins, D. Stevenson, M. Adcock and P. Youngblood: "Using collaborative haptics in remote surgical training." World Haptics Conference. IEEE Computer Society, 2005.

[21] J. Luk, J. Pasquero, S. Little, K. E. MacLean, V. Levesque and V. A. Hayward: "Role for Haptics in Mobile Interaction: Initial Design Using a Handheld Tactile Display Prototype," Proc. of the ACM 2006 Conference on Human Factors in Computing Systems, CHI 2006, pp.171-180, 2006.

[22] H. Y. Jeong, M. Higashimori and M. Kaneko: "Improvement of Vibration Sensitivity by Tangential Vibration," Journal of Robotics and Mechatronics, Vol.21, No.4, pp.554-562, 2009.

[23] W. Liu, Lewis A. Lipsitz, M. Montero-Odasso, J. Bean, D. C. Kerrigan and J. J. Collins: "Noise-Enhanced Vibrotactile Sensitivity in Older Adults, Patients With Stroke, and Patients With Diabetic Neuropathy," Arch Phys Med Rehabil 2002 by the American Congress of Rehabilitation Medicine and the American Academy of Physical Medicine and Rehabilitation, 83, pp.171-6, 2002.

[24] T. D. Neel, N. B. James, D. H. Jason, A. L. Lewis and J. J. Collins: "Enhancing tactile sensation in older adults with electrical noise stimulation," somatosensory systems, January 2002.

[25] R. T. Verrillo: "Effect of Spatial Parameters on the Vibrotactile Threshold," Journal of Experimental Psychology Vol.71, Issue 4, pp. 570-575, 1966.

[26] G. A. Gescheider, S. J. Bolanowski, and K. R. Hardick: "The Frequency Selectivity of Information-Processing Channels in the Tactile Sensory System," Somatosens Motor Res, Vol.18, No.3 , pp.191-201, 2001.

[27] V. B. Mountcastle, R. H. LaMotte and G. Carli: "Detection Thresholds for Stimuli in Humans and Monkeys: Comparison With Threshold Events in Mechanoreceptive Afferent Nerve Fibers Innervating the Monkey Hand," Journal of Neurophysiology, Vol.35, Issue 1, pp. 122-136, 1972.

[28] S. M. Barlow: "Mechanical Frequency Detection Thresholds in the Human Face," Experimental Neurology, Vol.96, Issue 2, pp. 253-261, 1987.

[29] R. T. Verrillo: "Investigation of Some Parameters of the Cutaneous Threshold for Vibration," J. Acoust. Soc. Am, Vol.34, Issue 11, pp. 1768-1773, 1962.

[30] G. A. Gescheider, A. J. Capraro, R. D. Frisina, R. D. Hamer and R. T. Verrillo: "The effects of a surround on vibrotactile thresholds," Sens Processes, Vol.2, No.2, pp. 99-115, 1978.

[31] H. Shinoda, N. Asamura and N. Tomori: "A tactile feeling display based on selective stimulation to skin receptors," Proc. IEEE ICRA, pp.435-441, 1998.

[32] M. A. Srinivasan and K. Dandekar: "An Investigation of the Mechanics of Tactile Sense Using Two-Dimensional Models of the Primate Fingertip" Trans. ASME, J. Biomech. Eng, Vol.118, pp. 48-55, 1996.

[33] T. Maeno and K. Kobayashi: "Relationship between the Structure of Finger Tissue and the Location of Tactile Receptors (3rd Report, Results of Contact Analysis between a Finger and a Rough Plate)," Trans. of the Japan Society of Mechanical Engineers, Series C, Vol.65, No.636, pp. 3321-3327, 1999.

[34] A. W. Goodwin, K. T. John and I. D. Smith: "Skin profiles during sinusoidal vibration of the fingerpad," Experimental Brain Research, Vol. 77, Issue 1, pp. 79-86, 1989.

[35] O. Franzen and J. Nordmark: "Vibrotactile frequency discrimination," Perception and Psychophysics, Vol.17, pp.480-4, 1975.

[36] T. Imai, S. Kamping, C. Breitenstein, C. Pantev, B. L. Tkenhoner and S. Knecht: "Learning of Tactile Frequency Discrimination in Humans," Human Brain Mapping. Vol.18, pp.260-71, 2003.

[37] D. A. Mahns, N. M. Perkins, V. Sahai, L. Robinson and M. J. Rowe: "Vibrotactile Frequency Discrimination in Human Hairy Skin," J Neurophysiol, Vol.95, pp.1442-50, 2006.

[38] Y. L. Hegner, Y. Lee, W. Grodd and C. Braun: "Comparing Tactile Pattern and Vibrotactile Frequency Discrimination: A Human fMRI Study," J Neurophysiol Vol.103, pp.3115-22, 2010.

[39] E. Eijkman and A. J. H. Vendrik: "Dynamics of the Vibration Sense at Low Frequency," J. Acoust. Soc. Am. Volume 32, Issue 9, pp. 1134-1139 1960.

[40] J. C. Stevens and K. K. Choo: "Spatial acuity of the body surface over the life span," Somatosensory and Motor Research, p.p.153-166, 1996.

[41] V. V. Fernando and H. Moustapha: "Graphical Tactile Displays for Visually-Impaired People," Journal of Neural Systems and Rehabilita, Vol.15, Issue 1, pp. 119-130, 2007.

[42] W. Schweikhardt and Kloper: "Rechnerunterstutzte aufbereitung von bildshirmtext-grafiken in eine tastbare darstellung Institut fur Informatik" Universitat Stuttgart, Institutsbericht, pp. 1-16, 1984.

[43] Library helps the blind enjoy graphics Apr. 23, 2002 [Online]. Available: http://www.japantimes.co.jp/news/2002/04/23/national/library-helps-the-blind-enjoy-graphics/

[44] M. Shimojo, M. Shinohara, M. Tanii and Y. Shimizu: "An approach for direct manipulation by tactile modality for blind computer users: Principle and practice of detecting information generated by touch action," in ICCHP 2004. New York: Springer-Verlag, Vol. 3116, Lecture Notes Computer Science, pp. 753-760.

[45] [Online].Available: http://www.abtim.com ABTIM. Wuppertal, Germany.

[46] [Online]. Available: http://www.nist.gov/public_affairs/factsheet/ visualdisplay.cfm National Institute of Standards and Technology. Gaithersburg, MD

[47] S. Mitic, H. B. Kim and A. Vujanic: "Development of a graphical tactile display based on electromagnetic actuators," in Proc. 24th Int. Conf. Microelectronics (MIEL 2004), Serbia and Montenegro, 2004, Vol. 1, pp. 223-226.

[48] M. Shinohara, Y. Shimizu and A. Mochizuki: "Three-dimensional tactile display for the blind," IEEE Trans. Rehabil. Eng., Vol. 6, no. 3, pp. 249-255, Sep. 1998.

[49] Y. Kawai and F. Tomita: "Interactive tactile display system," in Proc. 2nd Int. ACM/SIGCAPH Conf. Assistive Technol. ASSETS '96, Vancouver, BC, Canada, 1996, pp. 45-50.

[50] R. Velazquez, E. Pissaloux, M. Hafez and J. Szewczyk: "A low-cost highly-portable tactile display based on shape memory alloy microactuators," in Proc. IEEE Int. Conf. Virtual Environ., Human-Comput. Interfaces, Measurement Syst. VECIMS 2005, Giardini Naxos, Italy, pp. 121-126, 2005.

[51] Y. Haga, M. Mizushima, T. Matsunaga and M. Esashi: "Medical and welfare applications of shape memory allow microcoils actuators," Smart Materials Structures, Vol. 14, pp. S266-S272, 2005.

[52] P. M. Taylor, D. M. Pollet, A. Hosseini-Sianaki, and C. J. Varley: "Advances in an electrorheological fluid based tactile display," Displays, Vol. 18, pp. 135-141, 1998.

[53] A. Iggo: "Sensory receptors in the skin of mammals and their sensory functions," Rev. Neurol., 141, Issue 10, pp. 599-613, 1985.

[54] H. Kajimoto, N. Kawakami and S. Tachi: "Electro-tactile display with tactile primary color approach," Int. Conf. on Intelligent Robots and Systems(IROS), 2004.

[55] M. Konyo, M. Nakamoto, T. Maeno and S. Tadokoro: "Reflective grasp force control of humans induced by distributed vibration stimuli on finger skin with ICPF actuators,"Japan VirtualRealityconference, Vol.11(1), pp. 3-10, 2005.

[56] S. Tsuchiya, M. Konyo, H. Yamada, T. Yamauchi, S. Okamoto and S. Tadokoro: "Virtual Active Touch II: Vibrotactile Representation of Friction and a New Approach to Surface Shape Display," Proc. IEEE/RSJ International Conference on Intelligent Robots and Systems (IROS), pp.3184-3189, St. Louis, 2009.

[57] K. Minamizawa, M. Nakatani, Y. Kakehi, S. Mihara and S. Tachi: "TECHTILE toolkit," IEEE Haptics Symposium 2012, Hands-on-demos, Vancouver, Canada, 2012.

[58] G. L. Aiello: "Multidimensional Electrocutaneous Stimulation," IEEE Trans. Rehabil., Vol.6, No. 1, pp. 95-101, 1998.

[59] A. B. Anani, K. Ikeda and L. M. Korner: "Human ability to discriminate various parameters in afferent electrical nerve stimulation with particular reference to prostheses sensory feedback," Med. Biol. Eng. Compt., pp. 363-372, 1977.

[60] P. J. Blamey and G. M. Clark: "Psychophysical studies relevant to the design of a digital electrotactile speech processor," J. Acoust. Soc. Am, pp. 116-125, 1987.

[61] J. G. Linvill and J. C. Bliss: "A direct translation reading aid for the blind," Proc. IEEE, Vol. 54, pp. 40-50, 1966.

[62] Y. Ikei, K. Wakamatsu and S. Fukuda: "Vibratory tactile display of image-based textures," IEEE Comput. Graph. Appl., Vol. 17, no. 6, pp. 53-61, 1997.

[63] I. R. Summers, C. M. Chanter, A. L. Southall and A. C. Brady: "Results from a tactile array on the fingertip," in Proc. EUROHAPTICS, Birmingham, U.K., 2001, pp. 26-28, 2001.

[64] K. U. Kyung, M. Ahn, D. S. Kwon and M. A. Srinivasan: "A compact broadband tactile display and its effectiveness in the display of tactile form," in Proc. IEEE 1st Joint Eurohaptics Conf. Symp. Haptic Interfaces Virtual Environment Teleoperator Syst. WHC, pp. 600-601, 2005.

[65] P. Kammermeier and G. Schmidt "Application-specific evaluation of tactile array displays for the human fingertip," in Proc. 2002 IEEE/RSJ Int. Conf. Intelligent Robots Syst., Lausanne, Switzerland, pp. 2937-2942, 2002.

[66] T. Maucher, K. Meier, and J. Schemmel "An interactive tactile graphics display," in Proc. 6th Int. Symp. Signal Process. Its Appl. ISSPA 2001, Kuala Lumpur, Malaysia, pp. 190-193, 2001.

[67] J. Pasquero and V. Hayward: "STReSS: A practical tactile display system with one millimeter spatial resolution and 700 Hz refresh rate," in Proc. Eurohaptics 2003, Dublin, Ireland, pp. 94-110, 2003.

[68] C. J. Hasser: "HAPTAC: A Haptic Tactile Display for the Presentation of Two-Dimensional Virtual or Remote Environments Armstrong Laboratory, Wright-Patterson Air Force Base," Interim Report for the Period June 1993 to March 1995.

[69] C. J. Hasser and M. R. Roark: "Tactile Graphics Display," U.S. Patent 5 736 978, Apr. 7, 1998.

[70] P. M. Taylor, A.Moser and A. Creed: "A sixty-four element tactile display using shape memory alloy wires," Displays, Vol. 18, pp. 163-168, 1998.

[71] R. D. Howe, D. A. Kontarinis and W. J. Peine: "Shape memory alloy actuator controller design for tactile displays," in Proc. 34th IEEE Conf. Decision Control, New Orleans, LA, Vol. 4, pp. 3540-3544, 1995.

[72] P. S.Wellman, W. J. Peine, G. E. Favalora and R. D. Howe: "Mechanical design and control of a high-bandwidth shape memory alloy tactile display," in Lecture Notes

in Control and Information Sciences. Berlin, Germany: Springer-Verlag, Vol. 232, pp. 56-66, 1997.

[73] F. Vidal-Verdu and R. Navas-Gonzalez: "A thermopneumatic approach for tactile displays," in Proc. IEEE Conf. Mechatronics Robotics, Aachen, Germany, Vol. I, pp. 395-399, 2004.

[74] G. Moy, C. Wagner and R. S. Fearing: "A compliant tactile display for teletaction," in Proc. IEEE Int. Conf. Robotics Automation, San Francisco, CA, pp. 3409-3415, 2000.

[75] Y. Makino, N. Asamura, and H. Shinoda: "A cutaneous feeling display using suctions pressure," in Proc. SICE Annu. Conf., Fukui, Japan, pp. 2931-2934, 2003.

[76] P. Kammermeier, M. Buss and G. Schmidt: "Dynamic display of distributed tactile shape information by a prototypical actuator array," in Proc. IEEE/RSJ Int. Conf. Intelligent Robots Syst., Vol. 2, pp. 1119-1124, 2000.

[77] D. T. V. Pawluk, C. P. van Buskirk, J. H. Killebrew, S. S. Hsiao and K. O. Johnson: "Control and pattern specification for a high density tactile display," in Pro. 7th Haptics Symp. ASME IMECE, Anaheim, CA, 1998, Vol. DSC-64, pp. 97-102.

[78] M. B. Khoudja, M. Hafez, J. M. Alexandre and A. Kheddar: "Electromagnetically driven high-density tactile interface based on a multilayer approach," in Int. Symp. Micromechatronics Human Sci., Nagoya, Japan, pp. 147-152, 2003.

[79] C. R.Wagner, S. J. Lederman and R. D. Howe: "A tactile shape display using RC servomotors," in Proc. 10th Symp. Haptic Interfaces Virtual Envir. Teleoperator Syst. HAPTICS ' 02, pp. 354-355, 2002.

[80] M. V. Ottermo, O. Stavdahl and T. A. Johansen: "Electromechanical design of a miniature tactile shape display for minimally invasive surgery," in Proc. IEEE 1st Joint Eurohaptics Conf. Symp. Haptic Interfaces Virtual Environment Teleoperator Syst. WHC, pp. 561-562, 2005.

[81] I. Sarakoglou, N. Tsagarakis and D. G. Caldwell: "A portable fingertip tactile feedback array-transmission system reliability and modelling," in Proc. 1st Joint Eurohaptics Conf. Symp. Haptic Interfaces for Virtual Environ. Teleoperator Syst., pp. 519-520, 2005.

[82] S. M. Labs, G. A. Gescheider, R. R. Fay and C. H. Lyons: "Psychophysical tuning curves in vibrotaction," Sensory Processes. Vol.2, pp.231-247, 1978.

[83] G. A. Gescheider, A. J. Capraro, R. D. Frisina, R. D. Hamer and R. T. Verrillo: "The effects of a surround on vibrotactile thresholds," Sens Processes, Vol.2, No.2, pp.99-115, 1978.

[84] P. J. Lamore and C. J. Keemink: "Evidence for different types of mechanoreceptors from measurements of the psychophysical threshold for vibrations under different stimulation conditions," The Journal of the Acoustical Society of America, Vol.83, pp.2339-51, 1988.

[85] C. L. V. Doren: "The effects of a surround on vibrotactile thresholds: Evidence for spatial and temporal independence in the non-Pacinian I (NP I) channel," The Journal of the Acoustical Society of America, Vol.87, pp.2655-61, 1990.

[86] A. K. Goble, A. A. Collins and R. W. Cholewiak: "Vibrotactile threshold in young and old observers: The effects of spatial summation and the presence of a rigid surround," The Journal of the Acoustical Society of America, Vol.99, pp.2256-69, 1996.

[87] V. B. Mountcastle and T. P. S. Powell: "Neural mechanisms subserving cutaneous sensitibility, with special reference to the role of afferent inhibition in sensory perception and discrimination," Bull. Johns Hopk. Hosp., pp. 201-232, 1960.

[88] E. Eijkman and A. J. H. Vendrik: "Dynamics of the Vibration Sense at Low Frequency", The Journal of the Acoustical Society of America, Vol. 32, pp. 1134, 1960.

[89] カラー基本生理学

[90] 佐藤 誠, 一色 正晴, 林 理平, 赤羽 克仁: "Open Source Interface, Spidar-mouse について," 2009 年度 HCG シンポジウム（電子情報通信学会, No.HCG2009-C6-2, 2009.

[91] 菅一十　視覚障害者と点字　福祉図書出版　1988.

[92] 厚生労働省　平成 18 年度身体障害児者実態調査結果

[93] 下條 誠, 前野 隆司, 篠田 裕之, 佐野 明人 編, 触覚認識メカニズムと応用技術 -触覚センサ・触覚ディスプレイ-, サイエンス& テクノロジー株式会社, 2010.

[94] 串山久美子: "Thermo Drawing: 冷温提示による小型触覚ディスプレイを使用した温度描画システムの開発." Interaction 2012.

[95] T. Maeno: "Tactile Sensation of Humans Mechanical Dynamics, Analogy and Illusion", 電気学会センサマイクロマシン部門誌 2002 年 10 月号特集解説電, Vol. 122-E, No. 10, pp.469-473, 2002.

Related Papers

[1] T. Sakurai, M. Konyo, and H. Shinoda: "Sharp Tactile Line Presentation Using Edge Stimulation Method," IEEE Transaction on Haptics, submitted.

[2] K. Hasegawa, T. Sakurai, Y. Makino, and H. Shinoda: "Transmitting full set of alphabet letters to human hand via writing motion with 5-minute training," Proc. IEEE World Haptics Conference (WHC'15), submitted.

[3] T. Sakurai and H. Shinoda: "Sharp Tactile Line Display using Superposition of Vibtotactile stimuli," SICE annual conference, pp. 1631-1634, Sapporo, 2014.

[4] T. Sakurai and H. Shinoda: "Sharp Tactile Line Presentation Array using Edge Stimulation Method," Proc. IEEE Haptics Symposium, pp. 271-275 , Huston, 2014.

[5] T. Sakurai, H. Shinoda, and M. Konyo: "Sharp Tactile Sensation using Superposition of Vibrotactile Stimuli in Different Phases," Proc. IEEE World Haptics Conference (WHC'13), pp. 235-240, Daejon, 2013.
(IEEE the Best Poster Award)

[6] T. Sakurai, H. Shinoda, and M. Konyo: "Sharp Tactile Lines by Multiple Vibrations," Proc. IEEE World Haptics Conference (WHC'13), demo paper, Daejon, 2013.

[7] T. Sakurai and H. Shinoda: "Sharp Tactile Line Display using Superposition of Vibtotactile stimuli", SICE annual conference, pp. 2035-2040, Osaka, 2013.

[8] T. Sakurai, M. Konyo, and S. Tadokoro: "Presenting Sharp Surface Shapes Using Overlapped Vibrotactile Stimuli," Proc IEEE/RSJ International Conference on Intelligent Robots and Systems (IROS'12), pp. 3300-3307, Faro, 2011.

[9] M. Konyo, T. Sakurai, A. Higuchi, L. B. Porquis, and S. Tadokoro, "Vib-Touch: Virtual Active Touch through a Pointing-Stick on Handheld Devices," IEEE World Haptics Conference (WHC'11), Fr.D22. Istanbul, Turkey, 2011.

[10] T.Sakurai, M.Konyo, and S.Tadokoro: "Enhancement of Vibrotactile Sensitivity: Effects of Stationary Boundary Contacts," Proc IEEE/RSJ International Conference on Intelligent Robots and Systems (IROS'11), pp. 3494 - 3500, San Francisco, 2011. (2011 IEEE Robotics and Automation Society (RAS) Japan Chapter Young Award)

[11] T. Sakurai, M. Konyo, S. Okamoto, and S. Tadokoro: "The Research of Conditions of Stimulus for Inducing Grasping Force Control Reflex," Proceedings of the 2010 IEEE/SICE International Symposium on System Integration (SII'10), pp.408-413, Sendai, 2010.

Domestic Presentations

[12] 櫻井 達馬, 牧野 泰才, 篠田 裕之, "ヒト指型センサを用いたヒト指内部の非線形ひずみ挙動の計測," 第 31 回センシングフォーラム 計測部門大会, 2A3-3, 佐賀, 2014. (測自動制御学会 学術奨励賞受賞)

[13] 櫻井 達馬, 篠田 裕之, "エッジ刺激法による剛体平面上での精細触覚パターン提示 第 2 報 : エッジ刺激デバイスの性能評価," 第 14 回計測自動制御学会システムインテグレーション部門講演会, 1I4-5, 神戸, 2013.

[14] 櫻井 達馬, 篠田 裕之, "エッジ刺激法による剛体平面上での精細触覚パターン提示," 第 18 回日本バーチャルリアリティ学会大会, 2C3-6, 大阪, 2013.

[15] 櫻井 達馬, 篠田 裕之, "複数振動刺激の重畳を用いた触覚提示," 日本機械学会 ロボティクス・メカトロニクス講演会 2013, 講演会 CD-ROM, 1A1-E10, 福岡, 2013.

[16] 櫻井 達馬, 篠田 裕之, 昆陽 雅司, "振動刺激の重畳を用いた鮮明な触刺激に関する研究," 第 13 回計測自動制御学会システムインテグレーション部門講演会, 1D3-4, 福岡, 2012.

[17] 櫻井達馬, 昆陽雅司, 田所諭, "静止面と振動面の同時接触がヒトの振動知覚を向上するメカニズムの解明," 第 16 回日本バーチャルリアリティ学会大会, 11C-6, 函館, 2011, Sep. (バーチャルリアリティ学会大会 学術奨励賞受賞)

[18] 櫻井達馬, 昆陽雅司, 田所諭, "振動刺激の重畳を用いた表面形状呈示," 第 12 回計測自動制御学会システムインテグレーション部門講演会, 1I3, 京都, 2011. (測自動制御学会 優秀講演賞受賞)

[19] 櫻井達馬, 昆陽雅司, 岡本正吾, 田所諭, ”把持力調整反射の誘発手法に関する研究,” 第 11 回計測自動制御学会システムインテグレーション部門講演会, 2C3-6, 仙台, 2010, Dec.

[20] 櫻井達馬, 昆陽雅司, 岡本正吾, 田所諭, ”把持力調整反射を誘発する触刺激条件に関する研究,” 第 15 回日本バーチャルリアリティ学会大会, 1A3-2, 金沢, 2010, Sep.

[21] 櫻井達馬, 昆陽雅司, 岡本正吾, 田所諭, ”把持力調整反射を誘発する皮膚刺激の解明,” 日本機械学会 ロボティクス・メカトロニクス講演会 2010, 講演会 CD-ROM, 1A2-D21, 旭川, 2010, Jun.

[22] 櫻井達馬, 昆陽雅司, 田所諭, ”静止面と振動面の同時接触によるヒトの振動知覚向上に関する研究,” 日本機械学会 ロボティクス・メカトロニクス講演会 2011, 講演会 CD-ROM, 2A2-O10, 岡山, 2011, Jun.

[23] 大竹達也, 荒川尚吾, 樋口篤史, 櫻井 達馬, Porquis Lope Ben, 昆陽雅司, 田所諭, ”Vib-Touch: 指先による仮想能動触を利用した触力覚インタラクション,” 日本機械学会 ロボティクス・メカトロニクス講演会 2011, 講演会 CD-ROM, 2P1-P03, 岡山, 2011, Jun.

[24] 樋口篤史, 櫻井達馬, 土屋翔, 石井優希, Porquis Lope Ben, 昆陽雅司, 田所諭, ”Vib-Touch: 仮想能動触を利用した直感的操作,” 第 15 回日本バーチャルリアリティ学会大会, T17, 金沢, 2010, Sep.

謝辞

数多くの皆様の応援と支えにより、博士課程の3年間、研究に邁進し、本論文を完成することが出来ました。指導教官である篠田裕之教授には、研究を進めるにあたってのアドバイスを頂き、現象の本質を捉える考え方を学びました。また、ディスカッションの際はご多忙の中、私が理解できるまで丁寧に教えて頂きました。研究テーマは以前の研究室のものから引き継いだものにも関わらず、自由に研究させて頂けたことにも大変感謝しています。安藤繁教授、石川正俊教授、山本晃生准教授、奈良高明准教授には博士審査を通じて、研究に関する貴重なご助言を頂き、より研究に対する考察が深まりました。牧野泰才講師には研究の方向性や、研究目的の絞り込みなど、大変貴重なご意見を頂きました。また専門に関する深い考察や議論を通して、新しい研究テーマへの発想に繋がりました。門内靖明特任助教には研究の内容だけでなく、研究生活や将来の対する考え方、良い研究をするための、健康な身体の維持方法等のアドバイスを頂きました。野田聡人特任助教には公私ともに多くの鋭い意見を頂きました。装置や道具の正しい使い方、研究環境の維持方法、投資に至るまで、幅広い分野で議論を交わしました。長谷川圭介特任研究員は、一つ上の先輩であったこともあり、研究や日常生活で苦しい時に親身になって相談に乗って頂きました。また、共同研究では様々な困難を突破する、前向きさと胆力を学びました。同期の藤原正浩君からは、研究に対する姿勢を学び、忌憚なき意見を交わしあいました。藤原君とはトルコの国際学会で出会いましたが、その後、篠田研究室に移り右も左も分からない時期から、構内やシステムの案内等、懇切丁寧に教えてくれました。大変感謝しております。研究、学会、就活と多くの苦楽を共に過ごしましたが、就職先も同じようなので、これからもよろしくお願い致します。井上碩君、小林鉱石君、森下和哉君は一つ下の後輩ですが、気さくかつ非常に優秀で研究能力が高く、いつも良い刺激を受けていました。博士生活を明るく過ごせたのは彼らのおかげです。ここに名前を挙げた方以外にも、多くの方々に支えて頂き、数々のアドバイスやアイディアを頂きました。大変感謝しております。ありがとうございました。